UNIVERSIDADE FEDERAL DE PERNAMBUCO
CENTRO DE TECNOLOGIA E GEOCIÊNCIA
DEPARTAMENTO DE ENERGIA NUCLEAR
PROGRAMA DE PÓS-GRADUAÇÃO EM TECNOLOGIAS ENERGÉTICAS E NUCLEARES

TAQMEEM HUSSAIN

SYNTHESIS OF $BaSO_4$ DOPED WITH RARE EARTH IONS AND CHARACTERIZATION OF ITS LUMINESCENT RESPONSE

Recife
2020

TAQMEEM HUSSAIN

SYNTHESIS OF $BaSO_4$ DOPED WITH RARE EARTH IONS AND CHARACTERIZATION OF ITS LUMINESCENT RESPONSE

Tese apresentada ao Programa de Pós-Graduação em Tecnologias Energéticas e Nucleares da Universidade Federal de Pernambuco, como requisito parcial para a obtenção do título de Doutor em Ciências.

Área de Concentração: Dosimetria e Instrumentação Nuclear.

Orientadora: Profa. Dra. Helen Jamil Khoury.

Coorientador: Prof. Dr. Walter Mendes de Azevedo.

Recife

2020

Catalogação na fonte
Bibliotecária Margareth Malta, CRB-4 / 1198

H972s Hussain, Taqmeem.
Synthesis of $BaSO_4$ doped with rare earth ions and characterization of its luminescent response / Taqmeem Hussain. - 2020.
97 folhas, il., gráfs., tabs.

Orientadora: Profa. Dra. Helen Jamil Khoury.
Coorientador: Prof. Dr. Walter Mendes de Azevedo.
Tese (Doutorado) – Universidade Federal de Pernambuco. CTG. Programa de Pós-Graduação em Tecnologias Energéticas e Nucleares, 2020.
Inclui Referências.
Texto em inglês.

1. Energia Nuclear. 2. TL. 3. OSL. 4. Sulfato de bário. 5. Radiações ionizantes. 6. Termoluminescência de fototransferência. I. Khoury, Helen Jamil (Orientadora). II. Azevedo, Walter Mendes de (Coorientador). III. Título

UFPE

612.01448 CDD (22. ed.) BCTG/2020-240

TAQMEEM HUSSAIN

SYNTHESIS OF $BaSO_4$ DOPED WITH RARE EARTH IONS AND CHARACTERIZATION OF ITS LUMINESCENT RESPONSE

Tese apresentada ao Programa de Pós-Graduação em Tecnologias Energéticas e Nucleares da Universidade Federal de Pernambuco, como requisito parcial para a obtenção do título de Doutor em Ciências.

Aprovada em: 10/03/2020.

BANCA EXAMINADORA

_____

Profa. Dra. Helen Khoury (Orientadora)

Universidade Federal de Pernambuco

_____

Prof. Dr. Pedro Luiz Guzzo

Universidade Federal de Pernambuco

_____

Prof. Dr. Vinicius Saito Monteiro de Barros (Examinador Interno)

Universidade Federal de Pernambuco

_____

Profa. Dra. Carmen Cecilia Bueno (Examinadora Externa)

Instituto de Pesquisas Energéticas e Nucleares

_____

Prof. Dr. Henry Lavalle Sullasi (Examinador Interno)

Universidade Federal de Pernambuco

ACKNOWLEDGMENTS

All praises to my Lord, the Almighty **ALLAH** (*Subhaana-wa-ta'aala*) for providing me the opportunity, ability and strength, for guiding me the right path and for honoring me the ultimate success.

Countless "Salaat-o-Salaam" on my beloved Holy Prophet **MUHAMMAD** (*Peace be upon him*) who is merciful to all mankind.

I am deeply indebted to my supervisor Prof. Dr. Helen Jamil Khoury owing to her wonderful personality, extremely professional persona, thoroughly gentle and kind attitude and skillful scientific behavior, which consequently has left an everlasting impression in my life. I would like to express my heartiest gratitude for her consistent and incredible support, encouragement, motivation, dedication, precious time, kind attention, constructive suggestion, directional efforts, helpful guidelines and positive criticism which were proved to be decisive in the quality and the completion of this work and without which this milestone could not have been achieved. I have benefited greatly from many fruitful discussions with her, which groomed my personality in scientific world.

Special thanks to my Co-supervisor Prof. Dr. Walter Mendes de Azevedo, for his help throughout the course of my doctoral degree.

I really acknowledge Prof. Dr. Vinícius Saito Monteiro de Barros for his sincere, scholastic and professional comments when and where needed to complete this work. Prof. Dr. Viviane Asfora Khoury who really proved to be a great and honest helping hand to achieve this milestone, I will never forget her cooperation for the rest of life.

I am really very thankful to all the non-teaching staff members, who were and are part of GDOIN & LMRI-DEN/UFPE, Ana Dayse, André, Charles, Clemanzy, Égita, Elias, Janeide, Itaiana, Péricles, Bruno Nobre, Kalina, and Taislanne, who somehow contributed and helped with the development and progress of this work.

I am thankful to the friends: Bois, William, Robson, Thalita, Renata, Danial, Caio, Max, Regina, Edielly, Moema, Wladimer, Charles, Jorge and Yellina who through conversations and discussions contributed to maintaining the study and research environment at a high level of knowledge.

To FACEPE for the financial grant and timely support.

I am deeply indebted to the most precious gift of Lord to me, yes, my father and mother. I am really speechless, words are unable to express my humble feelings in order to thank and acknowledge them for what they have done for me, within their limited resources and tough circumstances, for their willingness to relief my stress of life through education. Especially my mother, who is one of the greatest motivators and for being present at all times of my journey with her blessed prayers. They are all-time motivational Figures throughout my life, who explored my potential and pursued my dreams. I have the best parents in the world who advised me to speak truth and to stay positive always in each step of life. I am thankful to my brothers, Abid Hussain, Kaleem Hussain, Rashid Hussain and Wajid Hussain for their consistent moral and ethical support throughout my study-career, for their undue favors to me in domestic and outdoor assignments, for their understanding and affection, especially in the most essential and difficult days. I must thank my caring and lovely family members.

Time to thank my ideal, a motivator, a teacher, a real hero, a brother and a friend, Muhammad Shahbaz who supported me to get higher education.

I would also like to thank all the researchers on both side of the Atlantic for their services in Science and Technology.

I would like to say thanks to Recife, its beaches, palms, heat, and unexpected rain. I will always miss you Recife. Eu te amo Recife.

Last but not least, I want to thank my wife, my soulmate, Kanwal Younas, who stood by me in every moment with love and care to help me unconditionally. She gave me support and help, discussed ideas and prevented me several wrong turns. Such a sincere friend, such a solid personality. I was lucky to have you with me. Thanks a lot for everything you did for me.

ABSTRACT

In this work the luminescent properties of $BaSO_4$ phosphor (doped with Eu, Tm, Dy, Ce and Pr), synthesized by the solid state combustion technique, were analyzed. Studies of the emission spectrum of $BaSO_4$ pellets doped with rare earths ions, as well as the TL and OSL response for gamma radiation, X-rays and beta radiation were performed. TL readings were performed using Harshaw 3500 reader with a heating rate of 2°C/s. For OSL response we used the Lexsyg Smart OSL reader equipped with excitation LEDs in the blue and infrared region. The results showed that the highest sensitivity in the TL response was obtained with Eu dopant concentration of 0.02 mol%. This concentration was used to prepare $BaSO_4$ pellets doped with Eu, Tm and Dy and to characterize their luminescent response. The results showed that the pellets prepared with Eu have a TL response that is around 20 times greater than that obtained with the Dy and Tm dopants. On the other hand, the OSL response of the pellets, stimulated by blue light (BSL), were practically similar. The pellets prepared with Ce and Pr did not show BSL response and the pellet with all dopants did not show any response after infrared excitation. The study of the TL glow curve obtained after the BSL reading i.e., the residual TL, showed that for $BaSO_4$:Eu pellets the peak remained the same, indicating that the recombination centers for OSL are not the same for TL. While whereas for the $BaSO_4$:Tm and $BaSO_4$:Dy pellets, the TL peak around 100°C decreased after the BSL reading and there was an increase in the peak area at high temperature. This fact suggests that the phototransference phenomenon may be occurring in this case. The calibration curve of $BaSO_4$:Eu irradiated with gamma radiation beam from the ^{137}Cs showed a linear response and the minimum detection limit is 17.9 μGy, while this limit is 0.59mGy for the BSL response. These results show that the TL sensitivity is greater than the BSL. The results obtained show the potential for the use of this phosphor for the dosimetry of ionizing radiation.

Keywords: TL. OSL. Barium sulphate. Ionizing radiations. Phototransfer thermoluminescence.

RESUMO

Neste trabalho foram analisadas as propriedades luminescentes do fósforo BaSO4 (dopado com Eu, Tm, Dy, Ce e Pr), sintetizado pela técnica de combustão de estado sólido. Foram realizados estudos do espectro de emissão de pastilhas de BaSO4 dopado com os terras raras, bem como a resposta TL e OSL para radiação gama e raios-X e para radiação beta. As leituras de TL foram realizadas usando a leitora Harshaw 3500 com taxa de aquecimetno de 2°C/s. Para resposta OSL, usamos a leitora Lexsyg Smart equipada com LEDs de excitação na região do azul e do infravermelho. Os resultados mostraram que a maior sensibilidade na resposta TL foi obtida com concentração de dopante de Eu de 0,02 mol%. Esta concentração foi utilizada para preparar pastilhas de BaSO4 dopadas com Eu, Tm e Dy para a caracterização da sua resposta luminescente. Os resultados mostraram que as pastilhas preparadas com Eu apresentam resposta TL cerca de 20 vezes maior do que obtido com os dopantes Dy e Tm. Por outro lado a resposta OSL das pastilhas, estimuladas por luz azul (BSL), foram praticamente similares. As pastilhas preparadas com Ce e Pr não apresentam resposta BSL e nenhuma pastilha apresenta resposta após excitação no infravermelho. O estudo da glow curve TL obtida após a leitora BSL, isto é a TL residual, mostrou que para as pastilhas de BaSO4:Eu o pico permaneceu o mesmo, indicando que os centros de recombinação para OSL não são os mesmos para o TL, enquanto que para os as pastilhas de BaSO4:Tm e BaSO4:Dy o pico TL em torno de 100°C diminuiu após a leitora BSL e houve um aumento na área do pico em alta temperatura. Este fato sugere que pode estar ocorrendo neste caso o fenômeno de fototransferência. A curva de calibração do BaSO4:Eu irradiado com feixe de radiação gama do 137Cs mostrou uma resposta linear e o limite minimo de detecção é de 17,9 µGy, enquanto que este limite é de 0,59 mGy para a resposta BSL. Estes resultados mostram que a sensibilidade TL é maior do que a BSL. Os resultados obtidos evidenciam o potencial para o uso deste fosforo para a dosimetria de radiação ionizante.

Palavras-chave: TL. OSL. Sulfato de bário. Radiações ionizantes. Termoluminescência de fototransferência.

LIST OF FIGURES

LIST OF TABLES

LIST OF ABBREVIATIONS AND ACRONYMS

BSL	Blue Light Stimulated Luminescence
CW-OSL	Continuous Wave Osl
DTA	Differential Thermal Analysis
E_f	Fermi Energy
E_g	Energy Band Gap
Gy	Gray
IAEA	International Atomic Energy Agency
IRSL	Infrared Stimulated Luminescence
LDL	Low Detection Limit
LED	Light Emitting Diode
LM-OSL	Linearly Modulated Osl
OSL	Optically Stimulated Luminescence
OSLD	Optically Stimulated Luminescence Dosimeters
PL	Photoluminescence
PMT	Photomultiplier Tube
POSL	Pulsed Optically Stimulated Luminescence
PSL	Photo Stimulated Luminescence
PTTL	Phototransfer Thermoluminescence
RE	Rare Earth
RPL	Radiophotoluminescence
SEM	Scanning Electron Microscopy
SSCT	Solid State Combustion Technique
TGA	Thermal Gravimetric Analysis
TL	Thermoluminescence
TLD	Thermoluminescent Dosimeter
UV	Ultra Violet
XRD	X-Ray Diffraction
T	Characteristic Lifetime

SUMMARY

1 INTRODUCTION

Nuclear techniques are widely used in a considerable number of industries, clinics, hospitals and research laboratories that use radioactive sources or X-ray equipment for the development of their activities. These applications require different types of dosimeters to be used for personnel, environment and accident dosimetry. There are many active devices like electronic personal dosimeters and area monitors that are often used within a facility, usually passive systems like thermoluminescent (TL) dosimeters and film badges. These are preferred for the purpose of personnel dosimetry because of their easy usage and minimal maintenance requirement. The properties and uses of many TL dosimeter materials have been discussed in detail (MCKEEVER et al., 1985).

Lithium fluoride doped with magnesium and titanium (LiF:Mg,Ti), known commercially as TLD-100, is still the most commonly used radiation dosimeter. It has become popular because of several properties, such as tissue equivalence, relatively low fading and the possibility of its manufacturing with acceptable reproducibility.

On the other hand, there are materials which over-respond due to their higher effective atomic number (Z_{eff}) but they have higher sensitivity and are characterized as non-tissue equivalent materials for example calcium sulfate ($CaSO_4$) and calcium fluoride (CaF_2) are used for environmental monitoring.

Highly sensitive with high effective atomic number (Z_{eff}) phosphors e.g., $BaSO_4$:Eu,P, $Ba_5SiO_4Br_6$:Eu^{2+}, $K_3Na(SO_4)_2$:Eu, $K_2Ca_2(SO_4)_3$:Eu, $BaSO_4$:Eu has already been documented for application as an X ray imaging and storage phosphors (SHINDE et al., 1996; MEIJERINK et al., 1989; SAHARE; MOHARIL 1990; OKAMOTO et al., 1986). High Z_{eff} phosphors, like BaFBr:Eu^{2+} are also used for spatial dose distribution of high energy photons in an irradiated phantom made of a tissue-equivalent material, like a human body (SEGGERN et al., 1988). BHATT et el., (2014) also evaluated the TL response of $BaSO_4$:Eu and described its applicability for relative dose measurements in radiation dosimetry similar to that of $CaSO_4$:Dy and LiF:Mg,Cu,P. For this reason, the interest in the development of high Z phosphors for radiation dosimetry is renewed. The TL response of $BaSO_4$:RE was largely evaluated for Eu and Dy dopants. In the literature there are few studies with other dopants.

Another luminescence phenomenon used for radiation detection is the Optically Stimulated Luminescence (OSL). It has first used as a dosimeter to

measure luminescence from quartz for dating sediments and artifacts from archeological samples exposed to background radiation for thousands of years (YUKIHARA; MCKEEVER, 2011).

The phenomenological description of the OSL and TL process are the same. Pure crystalline dielectric materials either contain or have added trace amounts of impurities or dopants that form crystal-lattice imperfections. These imperfections act as traps for electrons or holes and also can act as luminescence centers which emit light when electrons or holes recombine (YUKIHARA; MCKEEVER, 2011). After irradiation, free electrons and holes are generated that can be trapped. When the crystal is heated (in TL) or optically stimulated (in OSL), electrons can be ejected out of traps and result in the emission of light after recombination.

OSL has a number of operational advantages compared to thermoluminescent (TL) dosimetry, such as (a) simplicity of theoretical concepts and interpretation of signals; (b) optical readout and bleaching of dosimeters without heating and (c) compact, simple and rather inexpensive instrumentation (YUKIHARA et al., 2015). In spite of these advantages, there are few suitable materials, in comparison with TL, that can be used for radiation dosimetry. Today Al_2O_3:C and more recently BeO are practically commercial OSL dosimeters used for medical, environmental and personnel dosimetry.

There are few studies about the optically stimulated luminescent response of $BaSO_4$:RE and in these studies the materials were synthesized by methods such as re-crystallization, co-precipitation and solid-state diffusion at high-temperature sintering etc. (BHATT et al, 2014).

The research group of Instrumentation and Nuclear Dosimetry of Nuclear Energy Department of UFPE has been searching for alternative routes for the production of new dosimetric materials. In this direction, this project was developed to characterize the luminescent response (TL and OSL) of $BaSO_4$ doped with different rare earth ions using solid-state combustion technique.

1.1 OBJECTIVE

The general objective of this research is to synthesize pellets of $BaSO_4$ doped with different rare earth ions by solid-state combustion technique and to evaluate their luminescent response to be used as a dosimeter of ionizing radiation.

1.2 SPECIFIC OBJECTIVES

The specific objectives are:

a) To synthesize the pellets of $BaSO_4$ doped with rare earth ions (i.e., Eu, Dy, Tm, Ce and Pr), using the solid state combustion technique.
b) To evaluate the effect of different dopant ions and their concentrations in the TL, BSL and IRSL response of sample pellets of $BaSO_4$:RE.
c) To evaluate the TL response of $BaSO_4$:RE to identify and to optimize the best concentration of the dopant ion; to obtain high sensitivity for radiation doses and hence, to evaluate the TL dose response and energy dependence of $BaSO_4$:RE pellets.
d) To evaluate the OSL (BSL & IRSL) response of $BaSO_4$:RE irradiated with gamma and beta radiation.

2 REVIEW OF LITERATURE

2.1 LUMINESCENCE

Luminescence phenomenon can be understood in terms of the band theory of solids which describes the energy states of an electron moving in a solid. While in an atom, an electron can have discrete energy states, in a solid these energy states form energy bands. The highest filled energy band in the solid is referred to as the valence band. The first empty band above the valence band is called the conduction band. In between these two bands there is an energy gap. The classification of materials as electrical conductors, insulators and semiconductors can be easily understood based on the band theory; conductors easily allow for flow of electrical current, insulators resist the flow of electrical current and semiconductors possesses properties in between those of conductors and insulators (KNOLL, 2010). The degree to which a material will be able to conduct electricity will depend on the ability of electrons to move in the conduction band of the solid. In a conductor, the valence band and conduction band overlap, allowing electrons from the valance band to move freely between the valence and conduction bands. In a perfect insulator, the valence and conduction bands are separated by a big energy gap separation (BOTTER-JENSEN et al 2003). In the material used in luminescence dosimetry, impurities are added to an insulating material in order to create energy levels within the band gap of the materials. When a material is exposed to ionizing radiation, the radiation interacts with electrons in the valence band of the material causing them to move to the conduction band. When this occurs, a subsequent “hole” is created in the valence band. These electrons and holes can then move freely within their respective bands until either an electron recombines with a hole or they become trapped in one of the intermediate energy levels within the band gap referred to as trapped states (MCKEEVER et al., 1999). Electrical charges (either holes or electrons) can live trapped in these states for long periods of time unless the material is exposed to light or thermal stimulation.

Luminescence is the emission of visible light from a material following the initial absorption of energy from an external source, e.g., ultra-violet or high energy radiation (CHEN; MCKEEVER, 1997). In general, the transfer of energy from the excitation source to the electrons of the materials explains the luminescence of the material. The electrons are excited from lower energy states to higher excited states

and when they return to their ground states or recombine with holes, photons are emitted. If the energy of the emitted photons is in the visible range, it is called luminescence. As the valence band and the conduction band needs to be well separated for such kinds of phenomena to occur, it could occur only in insulating materials or wide band gap semiconductors. The materials which exhibit such phenomena are popularly known as ‘phosphors’. The emission can be categorized as either fluorescence or phosphorescence, depending upon the characteristic lifetime (τ) between absorption (excitation) and emission of the energy. For luminescence emission with $\tau < 10^{-8}$ s, the process is classified as “*fluorescence*”, whereas for $\tau > 10^{-8}$ s the process is called “*phosphorescence*”. Phosphorescent materials are known for their use in radar screens and glow-in-the-dark materials, whereas fluorescent materials are common in cathode ray tube (CRT), plasma video display screens, fluorescent lights, sensors and white LEDs. Phosphors are often transition-metal compounds or rare-earth compounds of various types.

The transfer of energy from radiation to the electrons of solid materials may explain luminescence emission and Figure 1 shows the process of exciting the electrons from a ground state to an excited state. Fluorescence is the emission of light that follows the excitation of an electron from *ground state* to *excited state* and its subsequent return back to ground state level (Figure 1a). Lifetime in the excited state may be very short or may be as long as a few milliseconds.

On the other hand, if this return to the ground state is delayed by a transition into and out of *metastable level*, then much longer delays between excitation and emission can result (Figure 1b) and in this case, the process is known as phosphorescence.

Thus, the delay observed in phosphorescence corresponds to the time the electron spends in the meta-stable state. The mean time (τ) spent in the trap at temperature *T* is given by the equation 1.

$$\tau = s^{-1} \exp\left(\frac{E}{kT}\right) \qquad (1)$$

where *s* is a constant, *E* is the energy difference between 'm' and 'e', called trap depth and *k* is Boltzmann's constant (MCKEEVER, 1985).

Figure 1 – (a) Fluorescence and (b) Phosphorescence, where ‘e’ is excited state, ‘g’ is ground state, ‘m’ is meta-stable level and ‘E’ is energy difference between ‘m’ and ‘e’

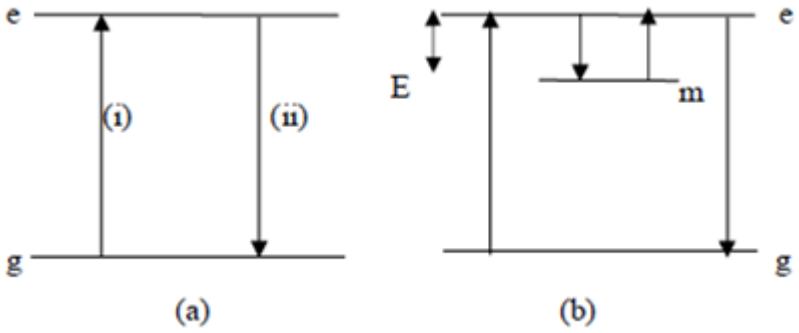

Fonte: McKeever (1988).

When the solid is thermally stimulated, the luminescence phenomenon is called thermoluminescence (TL). If the stimulation is by a light, the phenomenon is called optical stimulated luminescence (OSL). The principle of these two phenomenon are discussed below.

2.2 THERMOLUMINESCENCE

A thermoluminescent material is the material that during exposure to ionizing radiation absorbs some energy, which is stored, and it is released in the form of visible light when the material is heated. This phenomenon should not be confused with the light spontaneously emitted from a substance when it is heated to incandescence. At higher temperatures (say in excess of 200°C) a solid emits infrared radiation of which the intensity increases with increasing temperature. This is thermal or black body radiation. TL, however, is the thermally stimulated emission of light following the previous absorption of energy from radiation. From this description, the three essential ingredients necessary for the production of TL are: Firstly, the material must be an insulator or a semiconductor—metals do not exhibit luminescent properties. Secondly, the material must have absorbed energy during exposure to ionizing radiation. Thirdly, the luminescence emission is triggered by heating the material (MCKEEVER, 1985).

An explanation of the observed TL properties can be obtained from the energy band theory of solids. In an ideal crystalline semiconductor or insulator most of the electrons reside in the valence band. The next highest band that the electrons can

occupy is the conduction band, separated from the valence band by the so-called orbidden band gap. The energy difference between the two bands is E_g (Figure 2). However, whenever structural defects occur in a crystal, or if there are impurities within the lattice, there is a possibility for electrons to possess energies which are forbidden in the perfect crystal. In a simple TL model two levels are assumed, one situated below the bottom of the conduction band and the other situated above the top of the valence band (see Figure 2).

The highest level indicated by T in Figure 2 is situated above the equilibrium Fermi level (E_f) and thus empty in the equilibrium state, i.e., before the exposure to radiation and the creation of electrons and holes. It is referred to be an electron trap. The level (indicated by R) is referred to be a hole trap and can serve as a recombination center. The absorption of radiant energy with $h\nu > E_g$ results in ionization of valence electrons, producing energetic electrons and holes which will, after thermalization, produce free electrons in the conduction band and free holes in the valence band (transition a). The free charge carriers recombine with each other and if this center is a luminescence center then gives off luminescent response (BOS, 2006).

A certain percentage of the charge carriers can be trapped, for example, the electrons at T and the holes at R (transition b) (Figure 2). The probability per unit time of release of an electron from the trap is assumed to be described by the Arrhenius equation 2:

$$p = s \exp\left(-\frac{E}{kT}\right) \qquad (2)$$

where, “p” is the probability per unit time, the term “s” is called the frequency factor or attempt-to-escape factor. In the simple model, “s” is considered as a constant (not temperature dependent) with a value in the order of the lattice vibration frequency, namely 10^{12}-10^{14} s^{-1}. “E” is called the trap depth or activation energy, the energy needed to release an electron from the trap into the conduction band.

If the trap depth $E \geq kT_0$, with T_0 the temperature at irradiation, then any electron that becomes trapped will remain so for a long period of time, so that even after exposure to the radiation there will exist a substantial population of trapped electrons.

Figure 2 – Energy band model showing the electronic transitions in a TL material according to a simple two-level model: (a) generation of electrons and holes; (b) electron and hole trapping; (c) electron release due to thermal stimulation; (d) recombination. Solid circles are electrons and open circles are holes. Level T is an electron trap, level R is a recombination center, E_f is Fermi level, Eg is the energy band gap

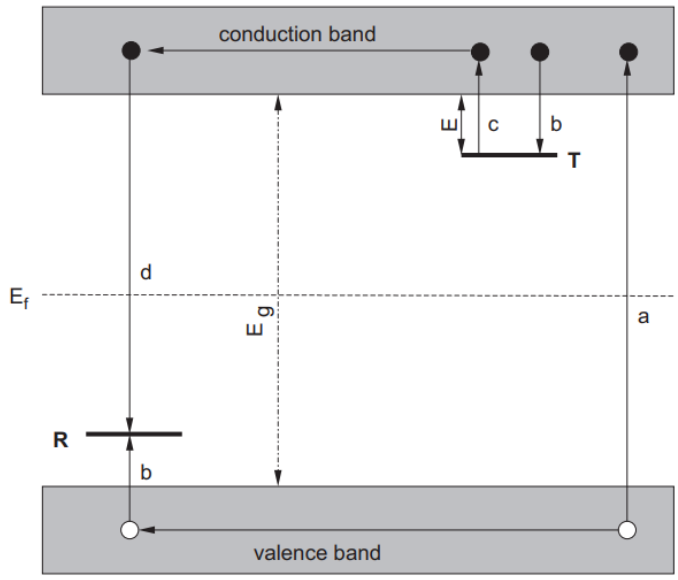

Source: Bos, 2006.

Raising the temperature of the material above T_0 will increase the probability of the electrons to move from the trap into the conduction band. The charge carrier migrates through the conduction band of the crystal until it undergoes recombination at recombination center R. In the simple model, this recombination center is a luminescent center where the recombination of the electron and hole leaves the center in one of the higher excited states. A return to the ground state is coupled with the emission of light quanta, i.e., thermoluminescence. The TL intensity I(t) in photons per second at any time t during heating is proportional to the rate of recombination of holes and electrons at R (BOS, 2007).

The glow curve corresponds to the graphic of the light intensity plotted as a function of temperature, or time, during which the temperature rises. Figure 3 shows the TL glow curve of the dosimeter LiF:Mg,Ti (TLD100) (MCKEEVER, 1985).

Figure 3 – TL Glow curve of LiF:Mg,Ti (TLD100)

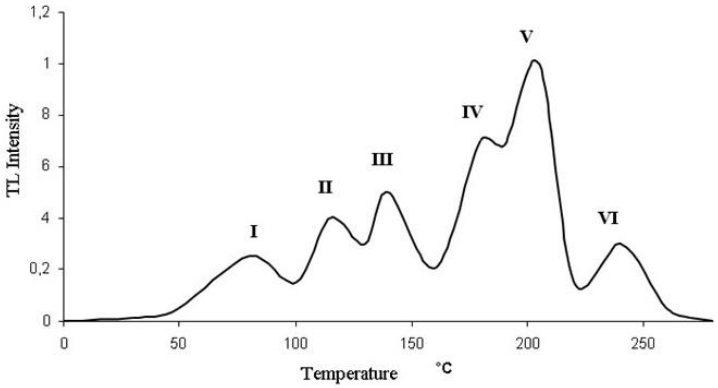

After: McKeever, 1985.

This curve is the best way to characterize a TL material and generally consists of several peaks. Each of them is associated with a certain trap (attributed to electrons or holes) of depth "E" and is characterized by the temperature where the maximum emission occurs. The shape of the glow curve depends on the types of traps and luminescence centers in the crystal, the heating rate and the detector used to measure the light emitted by the material. The presence of more than one peak in the curve reveals more than one type of traps. To estimate the absorbed dose received by the crystal, both the peak area and the peak height can be used. The heating rate should be uniform during the emission curve to avoid fluctuations in measurements.

2.3 OPTICALLY STIMULATED LUMINESCENCE (OSL)

The basis of the OSL process is the measurement of luminescence emitted by an irradiated sample from stimulation with a light beam. In this process, the transition from the trapped electrons to the conduction band is affected by the incidence of light. Some electrons may decay to the recombination centers releasing light whose intensity is proportional to the amount of recombination. These traps may or may not be the same as traps associated with TL peaks. Since the population of electrons in the traps is the result of irradiation of material, therefore, measured OSL intensity of a sample after irradiation can be related to the absorbed radiation dose (MCKEEVER, 2001).

This technique was proposed more than 60 years ago by ANTONOV-ROMANOVSKY et al (1955), but the widespread use of this technique has been greatly hindered due to the few number of suitable materials, in comparison with TL.

Today Al_2O_3:C and BeO are practically the only commercial OSL dosimeters used for medical, environmental and personnel dosimetry (AKSELROD et al., 1990; BØTTER-JENSEN et al., 2003; BULUR; GOEKSU, 1998). In recent years there has been an extensive search for novel materials for OSL dosimetry (PRADHAN et al., 2008; YUKIHARA et al., 2015). Concerning barium sulphate ($BaSO_4$), there have been some attempts on measuring its OSL response (CHOUGAONKAR; BHATT, 2004; POLYMERIS et al., 2006; YOSHIMURA; YUKIHARA, 2006; FERREIRA et al., 2014; TWARDAK et al., 2014; KEARFOTT et al., 2015; NANTO et al., 2015).

The use of OSL dosimetry may be preferred to the traditional TLD because an OSL dosimeter may be read multiple times after a single exposure to radiation without a significant loss of the original radiation induced signal. When an OSL dosimeter is stimulated with light, only a small portion of the trapped electrons are released. This is unlike a TLD in which, when the dosimeter material is heated up, the thermal stimulation causes almost all radiation induced excited states to be de-excited by releasing the trapped electrons. This essentially resets the dosimeter reading to zero i.e., to a background reading (JURSINIC, 2007).

Other advantages of OSL over conventional TL techniques are:

a) In OSL, the readout method is all optical, requiring no heating of the samples.
b) Thermal quenching is a reduction in the efficiency of luminescence. In TL, thermal quenching occurs. As the heating rate is increased, the TL peak shifts to higher temperatures and luminescence efficiency is reduced. However, by using optical stimulation, the readout of the luminescence can be performed at lower temperatures, so there is no thermal quenching, and thus a significant increase in sensitivity is achieved. In this way, OSL avoids thermal quenching.
c) Deep traps may not be useful in TL but some of these may be used in OSL.
d) Traps for TL and OSL may be different and residual TL may also be carried out after OSL.
e) Possibility of real time remote dose monitoring among others.

2.3.1 OSL Phenomenon

The basic principle of operation of an OSL dosimeter is that a material absorbs some energy when it is irradiated and stores this energy in the form of trapped electronic states. When the material is subsequently exposed to a stimulating light,

the OSL material will emit light (i.e., luminescence response) which is proportional to the amount of energy the material has absorbed (BØTTER-JENSEN et al., 2003).

In the case of OSL dosimeters, when the material is stimulated with light, these trapped charges are released, generating visible light because of the decay of these trapped states. More the number of trapped states, the more intensity of the emitted light received. This light intensity is proportional to the dose of ionizing radiation absorbed by the OSL dosimeter.

In regard to the trap states mentioned above, an electron will become trapped in one of three general types of traps. These traps are distinguished by the energy difference between them and the valence band. They are shallow, intermediate, and deep traps. Shallow traps do not require a large amount of energy to be released. Typically, these traps release electrons when the OSL material is at room temperature. This causes an almost immediate decay in signal after the OSL has been recorded. Deep traps, unlike shallow traps, require a large amount of energy to free the trapped electrons. Electrons in deep traps are stable and require that the OSL material be heated to 900°C before these electrons are released (LANDAUER, INC., 2012). Due to the large amount of energy required to release these deep traps, these electrons will not be set free through light stimulation. The third type of traps is the intermediate traps. These traps are stable at a room temperature, but these electrons can be released with light stimulation, unlike the electrons in deep traps. To release the electrons from these intermediate traps, a wide spectrum of light can be used. This spectrum of light ranges from 400-700 nm, though the most efficient trap release will occur with light that has a peak wavelength of about 475 nm. Since these electrons will remain trapped until stimulated and the resulting signal is proportional to exposure, the material is ideal for use in dose determination. A schematic of the OSL phenomenon can be seen in Figure 4.

Figure 4 – Schematic diagram of OSL phenomenon

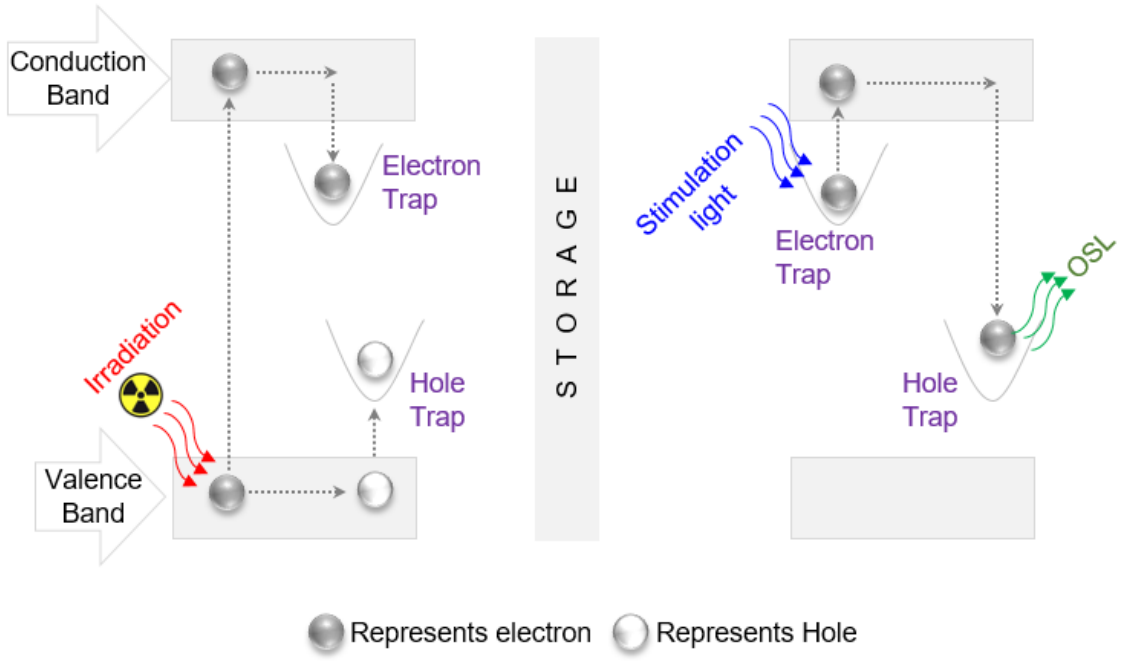

2.4 MODES OF OSL

Optical stimulation can be done in three ways according to the purpose of investigations.

a) Stimulation light intensity can be kept constant (Continuous-Wave OSL).

b) Stimulation source can be pulsed and the OSL can be measured between the pulses (Pulsed OSL).

c) Stimulation light intensity can be ramped linearly (Linearly Modulated OSL).

2.4.1 Continuous-Wave OSL

In this mode, the irradiated sample is stimulated with a constant light source and simultaneously the light emitted by the sample is measured. In this case, the light used for sample stimulation has a different wavelength than the emission light and filters are used to discriminate between these two lights, thus avoiding interference of the stimulation light on the detector response.

Figure 5 shows the schematic OSL reader and Figure 6 shows the OSL decay curve with the time. It is possible to observe the exponential decrease of the OSL signal as the traps are emptied, forming the decay curve, shown in Figure 6.

In Continuous-Wave OSL (CW-OSL) the discrimination of the stimulation light and the emitted light is required. This is achieved by using the combination of suitable optical stimulation and detection filters. So, as it appears, the OSL traps which have certain energies can be investigated and the emission can be observed in a specific wavelength range in this stimulation mode. The shape of the OSL signal obtained from this method was given in Figure 6. There are two main OSL stimulation types with respect to wavelength of the stimulation light: Infrared stimulated luminescence (IRSL) and Blue light stimulated luminescence (BSL).

In many cases, the decay curve has an exactly exponential or it may be the sum of several exponentials. There are cases where the decay curve is not exponential and shows an initial growth before decay. This wide variety of decay curve shapes suggests a multitude of possible OSL recombination paths and processes (MCKEEVER, 2001).

In the CW-OSL even the most sophisticated combinations and filters cannot absorb or reject the stimulation light completely, and a background signal can be observed resulting in difficulties for measurements at low doses. One way to solve this problem is to separate the stimulation stage from the luminescence measurement stage in time. This technique is called pulsed OSL mode.

Figure 5 – Scheme of OSL readout system

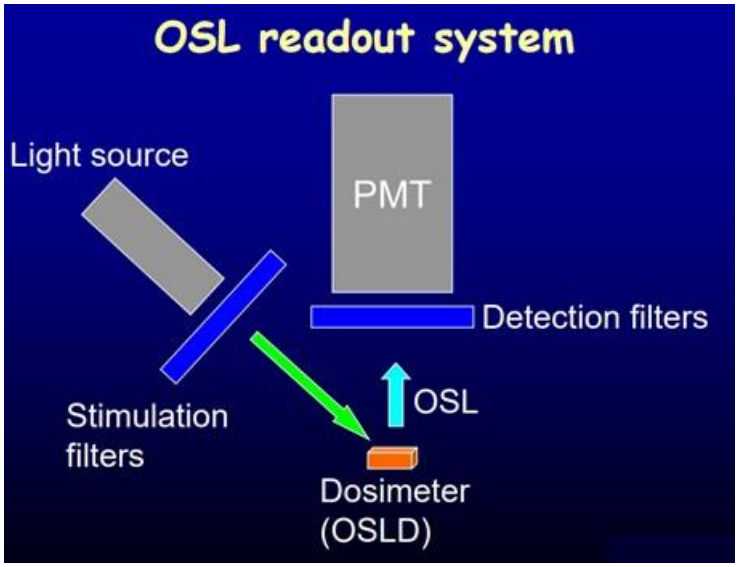

Figure 6 – Typical curve of the luminescence decay in the continuous OSL process

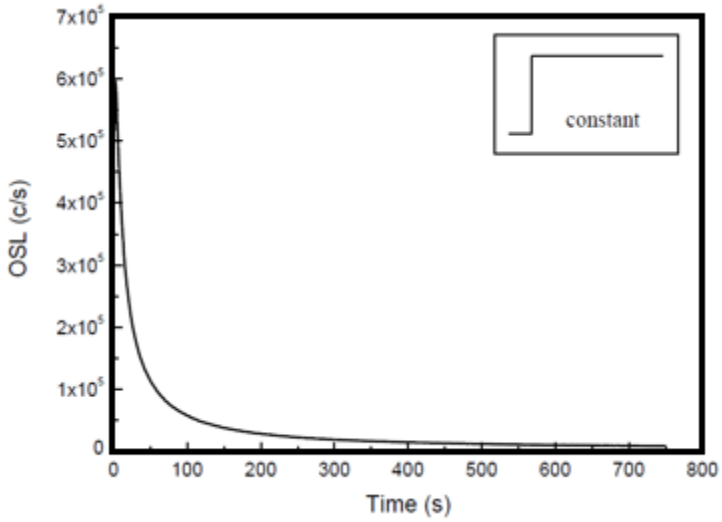

Source: Bøtter-Jensen, 2000.

2.4.2 Pulsed OSL- POSL

The pulsed OSL mode consists in stimulating the previously irradiated samples with light pulses and detecting the luminescence after the light pulse is turned off. The pulse width is selected so that it is smaller than the average luminescence center life of the sample material (AKSELROD; MCKEEVER, 1999). The detector used for luminescence measurement is triggered to record only the luminescence between the pulses.

Figure 7 shows the operating diagram of the OSL system in pulsed mode. It can be seen from Figure 7(a) that a series of laser pulses used for sample stimulation is 300ns wide. In the 15μs interval, the detector remains locked and during the 235μs period the detector is opened and the luminescence emitted by the sample is recorded.

Figure 7 – Schematic diagram of the OSL system in pulsed mode

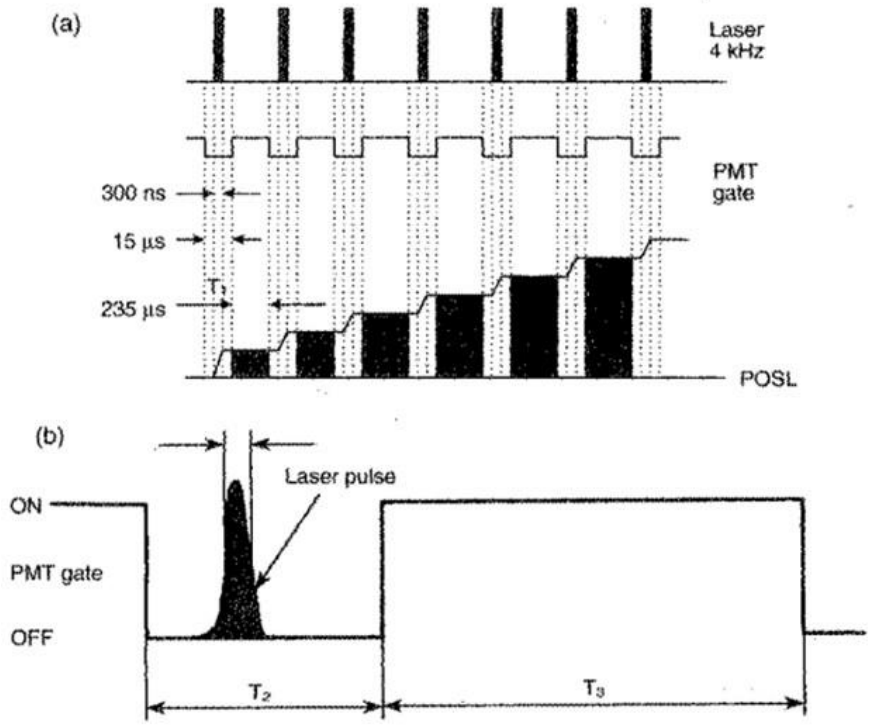

After: Akselrod; Mckeever, 1999.

This technique shows excellent results for Al_2O_3:C samples (MCKEEVER, 2001). Figure 8 shows the OSL response of samples of Al_2O_3:C irradiated with a dose of 40 mGy from $^{90}Sr/^{90}Y$ β-source and stimulated by laser beam of during 0.1 s. The dotted line indicates the end of the stimulation pulse.

2.4.3 Linear Modulation OSL (LM-OSL)

The Linear Modulation OSL (LM-OSL) method is based on the linear increase of the stimulation light intensity from zero to a maximum value during the reading of the sample. Unlike the decay curves obtained with CW-OSL, the LM gives luminescence curves containing peaks. The parameters of the luminescence curve i.e., peak height (L_{max}) and peak position (T_{max}) are related to the physical parameters of the traps involved.

Figure 8 – OSL signal of Al_2O_3:C stimulated with a laser pulse with 0.1s.

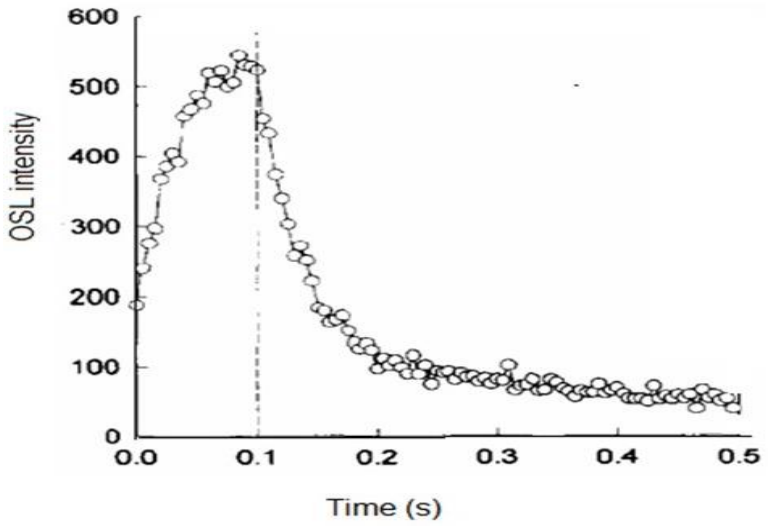

Figure 9 shows a typical LM-OSL curve. In case where more than one trap is involved in OSL production, the LM-OSL luminescence curve shows an overlap of luminescence peaks with different detrapping coefficients, separating the individual OSL components from different traps as a function of time.

Figure 9 – A typical LM-OSL signal

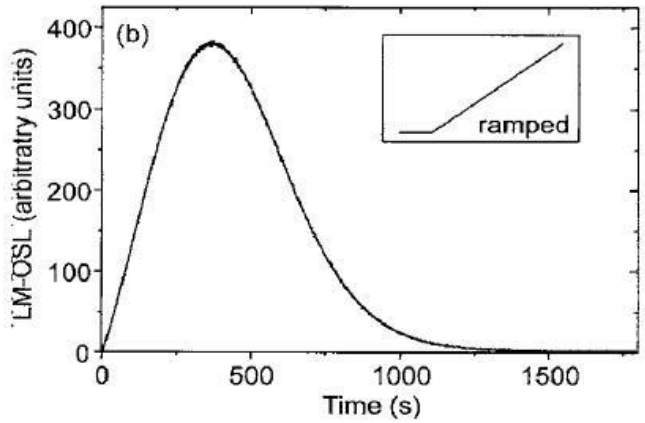

After: Bøtter-Jensen *et al*., 2003.

2.5 LUMINESCENT PROPERTIES OF BARIUM SULFATE ($BaSO_4$) DOPED WITH RARE EARTH IONS

Barium (Z=56) is a heavy metal which reacts with water exothermically and releases hydrogen gas, so the soluble ion is a toxic material, however barium sulfate i.e., $BaSO_4$, possesses low solubility in water and consequently less toxic for the patients. $BaSO_4$ has molecular mass 233.38 g/mol and density 4.49 g/cm^3. It is a

white crystalline odorless inorganic compound with orthorhombic crystal structure (JENSEN, 2002). The orthorhombic structure of barium sulfate is shown in the Figure 10.

Figure 10 – Orthorhombic crystal structure of $BaSO_4$ molecule. Green sphere represents barium (Ba) atoms; Yellow tetragon as sulfur (S) atoms and Red spheres represent oxygen (O) atoms

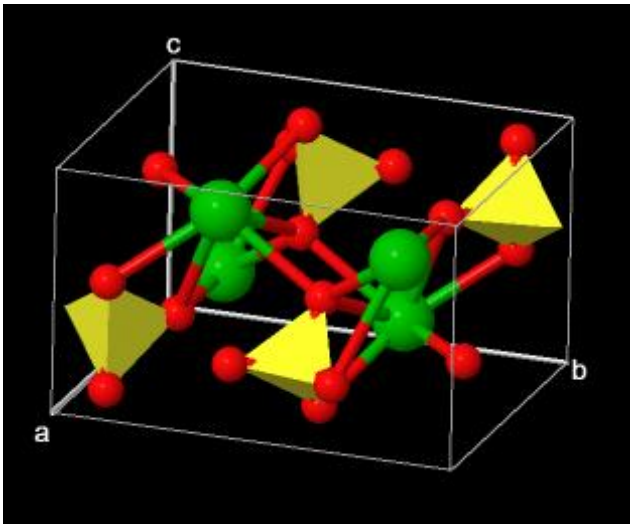

After: Jensen, 2002.

The crystallographic parameters of orthorhombic structure of $BaSO_4$ are $a = 7.154$ Å, $b = 8.879$ Å, $c = 5.454$ Å, $\alpha = \beta = \gamma = 90°$. It has melting point of 1580°C (JENSEN, 2002).

$BaSO_4$ is frequently used as a radiocontrast agent in X-ray imaging of the digestive system (BONTRAGER; LAMPIGNANO, 2013).

Considerable studies have been carried out on barite doped with either transition-metal or rare-earth ions. These include, measurement of spatial distribution of radiation dose around $BaSO_4$:Eu (RAMASWAMY et al., 2010) and environmental dosimetry using samples from shielding blocks of barite from CERN (KIYAK et al., 2010; KITIS et al., 2010). Other applications are the use of $BaSO_4/Y_2O_3:Eu^{3+}$ core-shell micro-spheres for lighting and plasma display (ZHANG et al., 2009) and the use of $BaSO_4$:Eu nanoparticles (SALAH et al., 2009), $BaSO_4:Cu^{2+}$ (MANAM; DAS, 2009) and $BaSO_4:Mn^{2+}$ (MANAM; DAS, 2010) for radiation dosimetry.

Manam and Das (2010) examined the trapping dynamics in Mn doped synthetic $BaSO_4$ samples and reported glow peaks at 420K and 498K with trap depths of 0.597±0.006 eV and 0.6370±005 eV, respectively.

ANNALAKSHMI et al. (2012) studied the TL characteristics of $BaSO_4:Eu^{2+}$ phosphor prepared by a solid-state reaction in different reducing atmospheres. The glow curves obtained by the samples prepared by the solid state diffusion methods and sintered in reducing atmosphere have shown TL sensitivity better than $CaSO_4$:Dy with a single peak at 513 K, as shown in Figure 11. The co-precipitation samples, which are fired in an argon atmosphere, have shown lower TL sensitivity as well as the TL peaks occurred at a lower temperature. Reducing atmosphere is required to incorporate more Eu in the divalent state in $BaSO_4$ during sintering. $BaSO_4:Eu^{2+}$ phosphor prepared in ammonia atmosphere has shown maximum TL sensitivity. The TL glow curve has a dominant single peak at 513 K unlike $CaSO_4$:Dy where the significant presence of the low and higher temperature peaks are seen.

Devi and Singh, 2012, studied the response of the $BaSO_4$ activated with different concentrations of Eu and Dy made by chemical co-precipitation method. They also evaluated the response of $BaSO_4$ co-doped by Eu and Dy ($BaSO_4$:Eu,Dy). Figure 12 shows comparison of TL glow curves of $Ba_{96}SO_4:Eu_{02}:Dy_{02}$, $Ba_{99}SO_4:Eu_{01}$ and $Ba_{98}SO_4:Dy_{02}$ recorded with a linear heating rate of 2.17 K/s. TL glow curve of $BaSO_4$:Dy shows two peaks at 383K and 458K. On the other hand, TL glow curves of $BaSO_4$:Eu:Dy and $BaSO_4$:Eu show an intense peak at 451 and 455K, respectively. It is evident from Figure 12 that TL peak intensity of $BaSO_4$:Eu,Dy at 452K is 15 times that of peak intensity of $BaSO_4$:Dy. Similarly peak intensity of TL glow peak of $BaSO_4$:Eu,Dy at 452K is 5.2 times that of $BaSO_4$:Eu at 455K.

SARAEE et al., (2013) studied the TL response of nanocrystalline of pure $BaSO_4$ and $BaSO_4$:Dy,Tb of grain size 45–55nm, prepared by the co-precipitation method. Figure 13 shows the TL glow curves of pure $BaSO_4$ and $BaSO_4$:Dy,Tb pellets exposed to 1Gy of gamma rays from a ^{60}Co source. TL glow curve of TLD-100 is shown as standard phosphor for comparison.

Figure 11 – Comparison of TL glow curves of (a) Standard $CaSO_4$:Dy powder with gamma irradiated (2.41 Gy) $BaSO_4$:Eu prepared at different conditions: solid-state diffusion in atmosphere; b) NH_3; c) CO; d) argon; and coprecipitation by e) H_2SO_4; f) $(NH_4)_2SO_4$ irradiated at 2.41Gy of gamma radiation

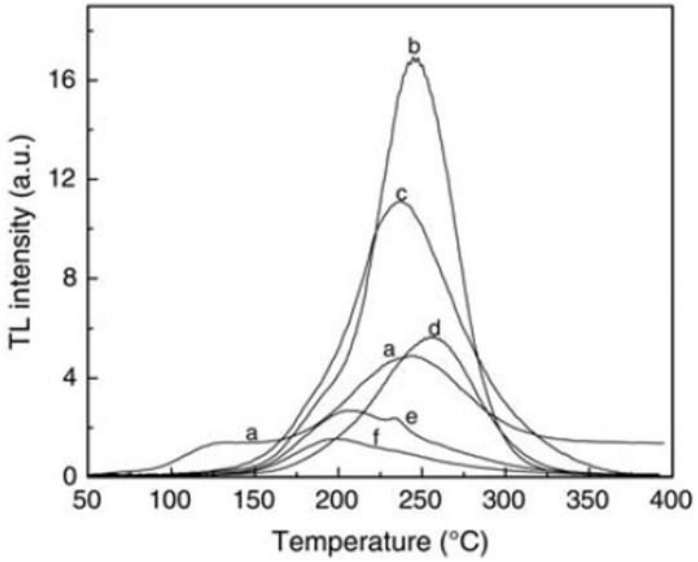

After: Annalakshami *et* al., 2012.

Figure 12 – Comparison of TL glow curves of (a) $Ba_{96}SO_4$:Eu_{02},Dy_{02} (b) $Ba_{99}SO_4$: Eu_{01} (c) $Ba_{96}SO_4$:Dy_{02} annealed at 873K and irradiated with 300Gy of □-rays

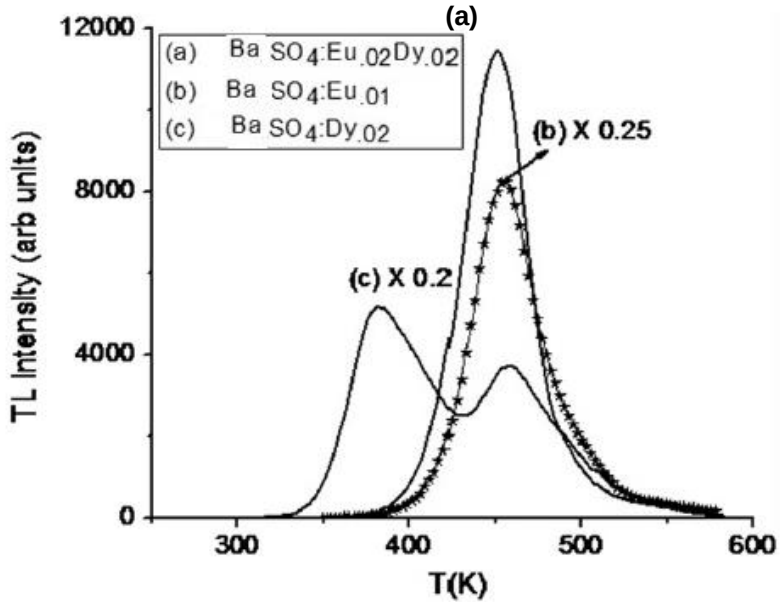

After: Devi; Singh, 2012.

Figure 13 – The glow curve of $BaSO_4$, $BaSO_4$:Dy,Tb and TLD-100 respectively irradiated with gamma ray of ^{60}Co at 1Gy dose

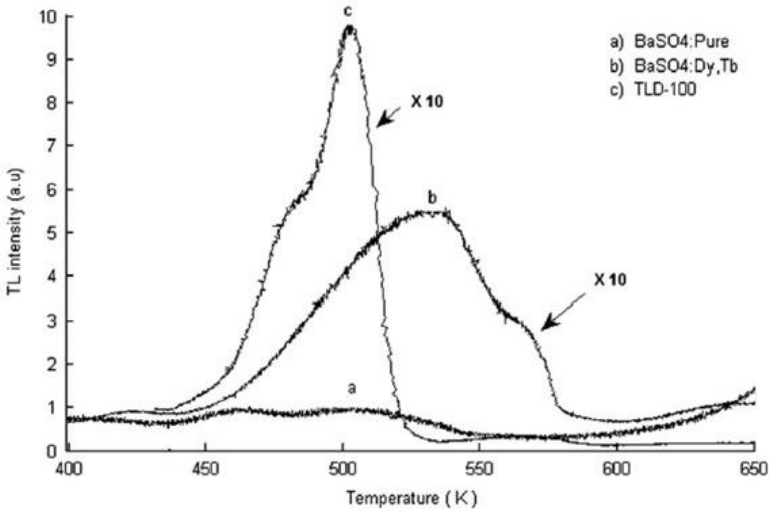

After: Saraee et al., 2013.

The response of the nanocrystalline powder versus dose was evaluated by irradiation with gamma radiation of ^{60}Co, and the results are shown in Figure 14. The results show that $BaSO_4$ and $BaSO_4$:Dy,Tb present a linear response from 0.1Gy to 1kGy and from 0.1Gy to 7KGy, respectively. Above 1kGy and 7kGy the TL response of $BaSO_4$ and $BaSO_4$:Dy,Tb, respectively, present a saturation.

Figure 14 – Dose response of $BaSO_4$ and $BaSO_4$:Dy:Tb nanocrystals irradiated with $_{60}Co$

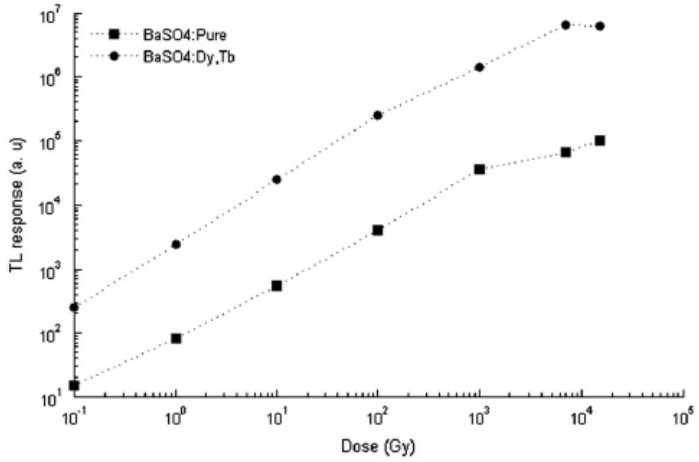

After: Saraee et al, 2013.

Figure 15 shows the TL response of commercial $BaSO_4:Eu^{2+}$ pellets produced by the company Nemoto from Japan, and evaluated by Bhatt et al., (2014). The TL curves of $CaSO_4$:Dy and a commercial α-Al_2O_3:C (TLD-500) irradiated to the same dose are plotted for comparison with the $BaSO_4:Eu^{2+}$ response. It is observed that

the response of $BaSO_4:Eu^{2+}$ is 6 times higher the response of $CaSO_4$:Dy and 4 times the response of a commercial α-Al_2O_3:C (TLD-500).

Figure 15 – Comparison of TL intensity of $CaSO_4$:Dy, □-Al_2O_3:C and $BaSO_4:Eu^{2+}$ phosphors for 100 mGy beta dose with heating rate 4 K/s

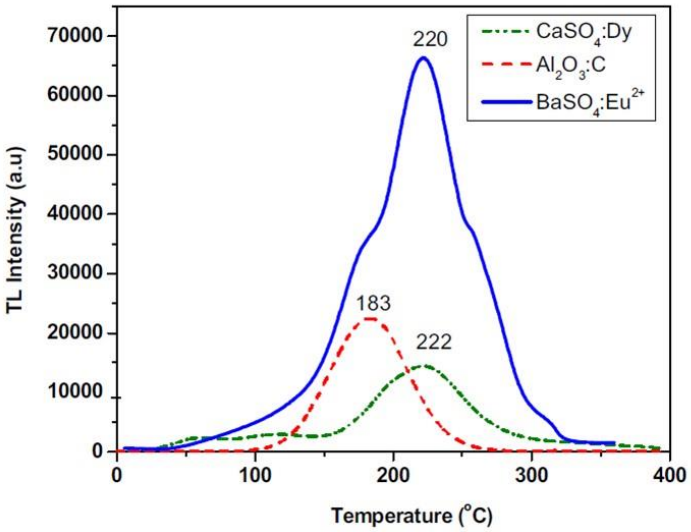

After: Bhatt et al., 2014.

Figure 16 shows the typical CW-OSL response of $BaSO4:Eu^{2+}$ for 200 mGy beta dose. It is found to possess three OSL components having photoionization cross-sections of 1.4×10^{-17}, 1.2×10^{-18} and 5.2×10^{-19} cm^{-2} respectively. Its OSL sensitivity for beta/gamma exposure is found to be 75% of commercial α-Al_2O_3:C, as shown in Figure 16.

Bhatt et al (2014) also evaluated the calibration curve of the commercial $BaSO_4:Eu^{+2}$ with beta irradiation and they found a linear response up to 10Gy, as shown in Figure 17.

Figure 16 – Comparison of OSL signal for Al_2O_3:C and $BaSO_4$:Eu^{2+} phosphors

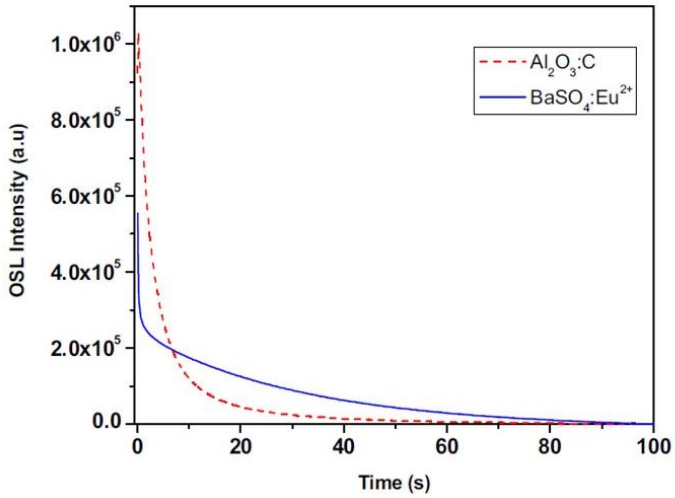

After: Bhatt et al., 2014.

Figure 17 – Dose vs OSL intensity for $BaSO_4$:Eu^{2+} phosphor

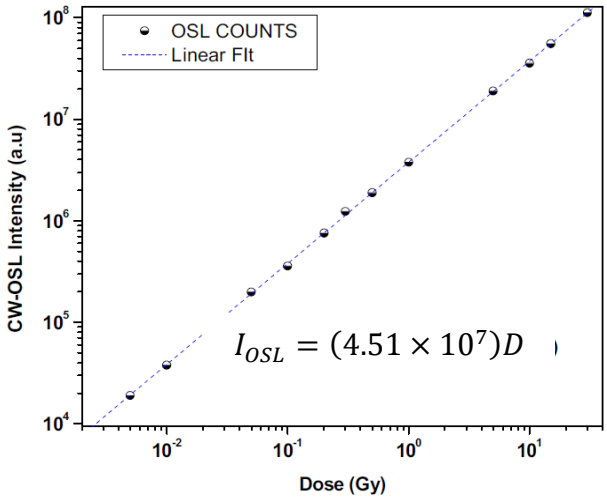

After: Bhatt et al., 2014.

3 MATERIALS AND METHODS

3.1 PRODUCTION OF THE SAMPLES

Samples of $BaSO_4$ phosphors doped with rare earth ions were produced via solid state combustion technique. Initially we prepared the samples by mixing barium nitrate ($Ba(NO_3)_2$) as oxidant, urea (CH_4N_2O) as fuel and a dopant material in the form of nitrate. This synthesis technique does not present ignition so it should not be confused with that of the solution combustion technique.

The methodology used in this study to get the barium sulfate phosphors doped with the selected rare earth ions (i.e., Eu, Tm, Dy, Ce and Pr) is the same. We explain here the methodology for europium doped barium sulfate phosphor ($BaSO_4$:Eu) which is as follows. In order to avoid confusions in understanding the steps of the methodology used, the scheme of the sample preparation of $BaSO_4$:Eu is shown in Figure 18.

Firstly, stoichiometric amounts of barium nitrate ($Ba(NO_3)_2$ and 0.02mol% of europium nitrate ($Eu(NO_3)_3 \cdot 5H_2O$) were added in 20mL distilled water in porcelain beaker 1. Secondly, stoichiometric amounts of ammonium sulfate $(NH_4)_2SO_4$ and urea (CH_4N_2O) were added in 7mL of distilled water in porcelain beaker 2. The ingredients were of pro-analysis purity. Both the porcelain beakers were put on a magnetic stirrer at a temperature of 200°C for 15 minutes to get well homogeneous solutions. Then solution of porcelain beaker 1 is transferred to porcelain beaker 2. This porcelain beaker 2 containing whole solution is then placed on a magnetic stirrer at a temperature of 300°C for 30 minutes with constant stirring. The chemical reaction is shown in equation (3).

$$6Ba(NO_3)_2 + 6(NH_4)_2SO_4 + 22CH_4N_2O + 6Eu(NO_3)_3 \cdot 5H_2O \xrightarrow{\text{yields}} 6BaSO_4{:}\,Eu + 22CO_2 + 43N_2 + 98H_2O \quad (3)$$

The homogeneous solution thus found was placed in an oven at 700ºC for 4h and after cooling, the resulting powder was removed and ground in an agate mortar and transferred to rectangular crucible combustion barge. After that, the sample powder was heated at different synthesis temperatures to found the higher luminescence response. Table 1 shows the synthesis temperature used for this purpose.

After these thermal treatments the powder sieved to obtain grains with size between 75 μm and 150μm. This range of grain size was selected based on the previous studies of our research group (VASCONCELOS et al., 2016)

For each thermal treatment given in Table 1, six pellets of $BaSO_4$:Eu were prepared with teflon as a binder, using a cold pressing machine with pressure of 1 ton for 2 minutes. The diameter of 6 mm and thickness of 1 mm were the dimensions of the prepared pellets. The scheme of the sample preparation of $BaSO_4$:Eu is shown in Figure 18 while the image of the pellets of $BaSO_4$:Eu is shown in Figure 19.

Table 1 – Synthesis temperature used to obtain $BaSO_4$:Eu (0.02 mol%) samples (SSCT)

Trial	Heat Treatments to SSCT sample	Short Explanation
1	500°C for 8h	Constant heating for 8h
2	700°C for 8 h	Constant heating for 8h
3	500°C for 4h + 700°C for 30 min	Samples after 500°C/4h taken out to cool, grabbed homogenously and again heated at 700°C/30 min
4	500°C for 4h + 900°C for 30 min	Samples of 500°C/4h taken out to cool, grabbed homogenously and again heated at 900°C/30 min
5	500°C for 4h + 1100°C for 30 min	Samples of 500°C/4h taken out to cool, grabbed homogenously and again heated at 1100°C/30 min

To erase any possible signal due to the background radiation, the pellets were annealed at 400°C for 1.0 h, using a programmable oven and then cooled at room temperature. The pellets were then irradiated, under electronic equilibrium, with absorbed dose of 5 mGy from ^{137}Cs γ–source and the thermoluminescent (TL) glow curve was recorded up to 350°C, using Harshaw 3500 reader at a linear heating rate of 2°C/s. The results of the glow curves of $BaSO_4$:Eu (0.02 mol%) thermally treated at different synthesis temperatures given in Table 1 are shown in Figure 20.

Figure 18 – Scheme of the sample preparation of $BaSO_4$:Eu

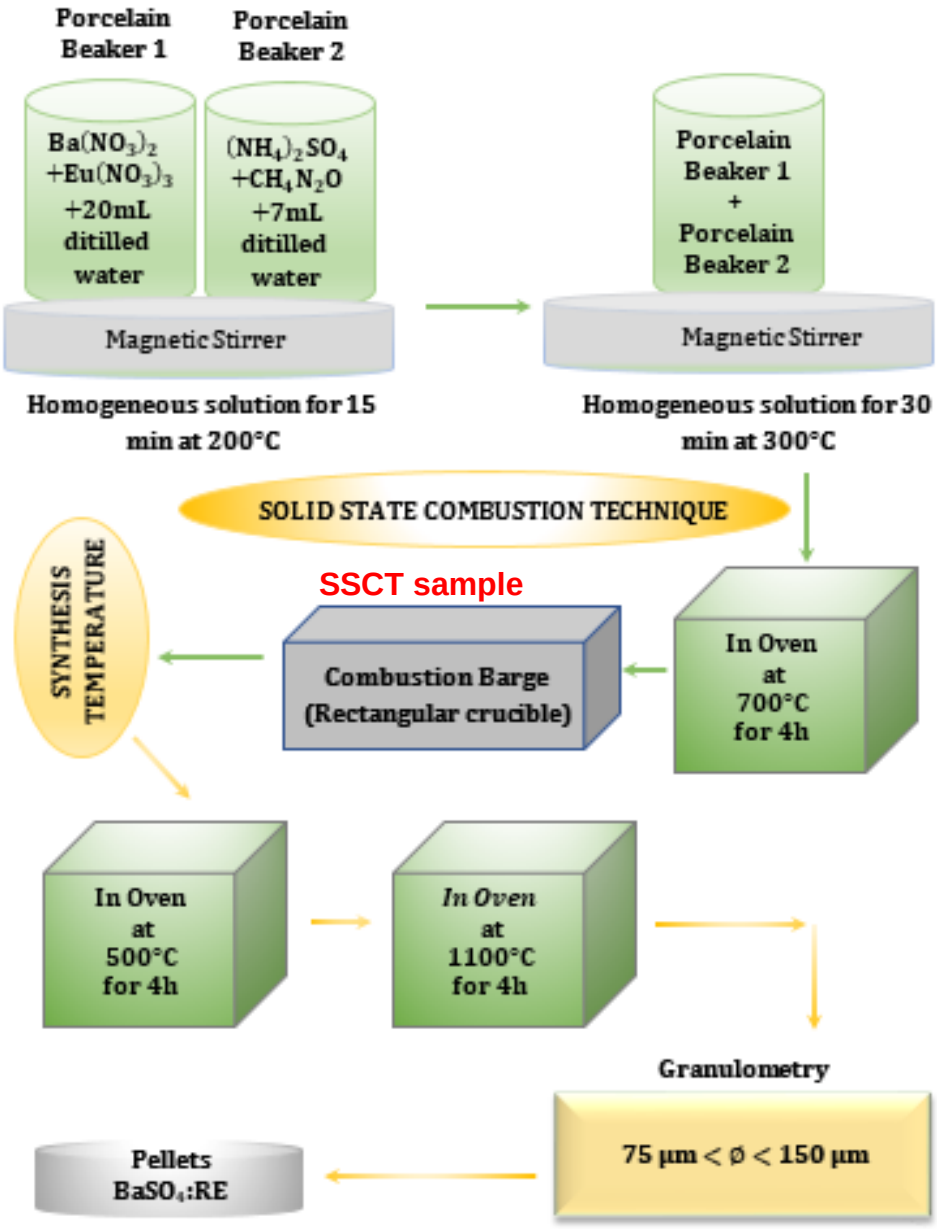

Figure 19 – Image and dimensions of the pellets of $BaSO_4$:Eu of this study

Figure 20 – Effect of synthesis temperature on TL glow curve of $BaSO_4$:Eu (0.02mol%) irradiated at 5 mGy from Cs^{137} γ-source

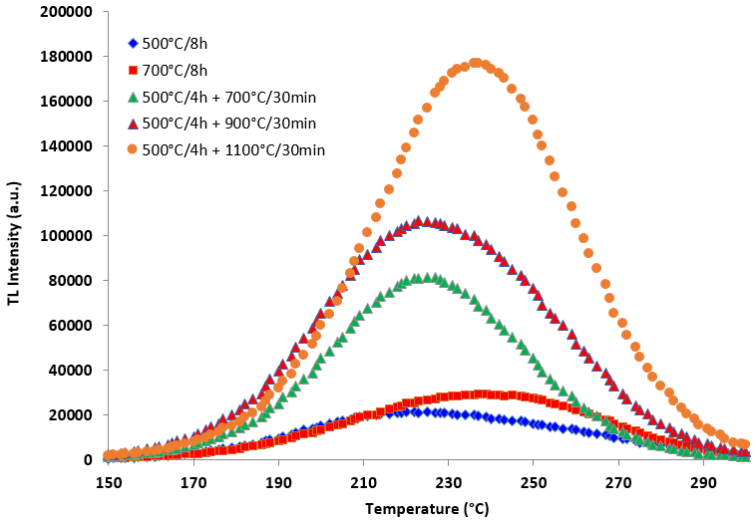

This increase in TL intensity with respect to increase in treatment temperature might be attributed to a favorable redistribution of the traps and a change in the efficiency of the trapping or the luminescence centers during the thermal treatment (NAGPAL; VARADHARAJAN, 1982). It can arise because of the changes in charge mobility or removal of certain competitive non-radiative transitions.

3.2 CHARACTERIZATION OF THE SAMPLES

3.2.1 X-Ray Diffraction (XRD)

The structure of the sample was checked by X-ray diffraction (XRD) using Bruker D2 PHASER equipment, operating at a voltage of 30 kV and a current of 10 mA (P = 300W), Cu-Kα radiation with $\lambda = 1.54060$ Å and using Bruker-AXS-Lynxeye detector. The scanning range (2θ) was from 10 to 80°, with the goniometer pitch of 0.02019° and constant sample rotation of 10 rpm. The opening of the primary slit was 0.4 mm, the bulkhead used was 1 mm and the counting time per step of 1 second. The samples were indexed using the Inorganic Crystal Structure Database (ICSD) n. COD9000159BaO4S Barite (COLVILLE; STAUDHAMMER, 1967). The measurements were performed in Mineral Technology Laboratory (LTM) of the Department of Mining Engineering (DEMINAS), UFPE.

3.2.2 Scanning Electron Microscopy (SEM)

To analyze the microstructural morphology of the pellets of $BaSO_4$:Eu (0.02 mol%), the Scanning Electron Microscopy (SEM) was performed using the Vesc 3 SEM Tescan Scanning from the Materials Science Research Institute of the Federal

University of Vale do São Francisco - UNIVASF - Campus Juazeiro-BA. To increase the conductivity of the surface of the samples, a thin layer of gold was used to cover the surfaces.

3.2.3 Differential Thermal Analysis and Thermal Gravimetric Analysis

The Differential Thermal analysis (DTA) and Thermal Gravimetric Analysis (TGA) gives information about changes in material properties as function of temperature. While TGA only measures changes caused by mass loss, DTA also register changes in material where no mass loss occurs, e.g., crystal structure changes, melting, glass transition etc. The measurements were made in the Mineral Technology Laboratory (LTM-UFPE), using a DTG-60H-Schimadzu analyzer, provided with DTA and TGA measurements simultaneously. The settings of the analyzer were such that; temperature range of 25°C to 800°C with heating rate $10°C/min$, Nitrogen flux was $70ml/min$ with reference as Alumina BP.

3.3 THERMOLUMINESCENT CHARACTERIZATION

In order to obtain a group of pellets with similar sensitivity, 13 pellets were prepared according the procedure described above and were irradiated simultaneously in air, at same time, with the absorbed dose of 20 mGy of ^{137}Cs. Their mass was measured and the average value was 46.7 mg ± 3%. Throughout this study, all the pellets of this group were considered to have the same mass.

The TL measurements were made using Harshaw 3500 reader at a linear heating rate of 2°C/s, in the range of 50 to 350°C. The area under the main TL peak was calculated and used to evaluate the radiation response of the pellet. The response of the un-irradiated pellet was subtracted from response of each pellet to obtain the net value. Figure 21 shows the results obtained. Each point corresponds to the average of 3 measurements with the indication of the standard deviation. After each measurement, the pellets were annealed at 400°C for 1.0h, using a programmable oven and then followed 100°C for 2h. The solid line represents the overall average of the measurements; the outermost dashed lines correspond to the range ($\bar{x} \pm 2s$) while the innermost represents the range ($\bar{x} \pm 1s$). The coefficient of variation (CV), also known as relative standard deviation was calculated by the ratio of the standard deviation to the mean. The pellets P 03, 06 and 07 showed a response outside the $\bar{x} \pm 2s$ range and were therefore excluded from the batch, and

the pellets 8 and 12 presented the coefficient of variation (CV) above 5% and were also removed from the group. As 5 pellets have been excluded so the TL response characterization was performed using the 8 pellets from the selected batch of 13 that have similar TL sensitivities, with a coefficient of variation CV < 5%.

3.3.1 Glow curve of $BaSO_4$:Eu

In order to acquire the glow curve of the $BaSO_4$:Eu (0.02 mol%), sample pellets were irradiated in air, under electronic equilibrium, at an absorbed dose of 100 mGy from ^{137}Cs γ-source. The TL measurements were made using Harshaw 3500 reader at a linear heating rate of 2°C/s, in the range of 50 to 350°C. After each measurement, the pellets were annealed at 400°C for 1.0h, using a programmable oven and then followed 100°C at 2h.

Figure 21 – TL reproducibility response of pellets of $BaSO_4$:Eu (0.02 mol%) irradiated at 200 mGy from ^{137}Cs γ-source

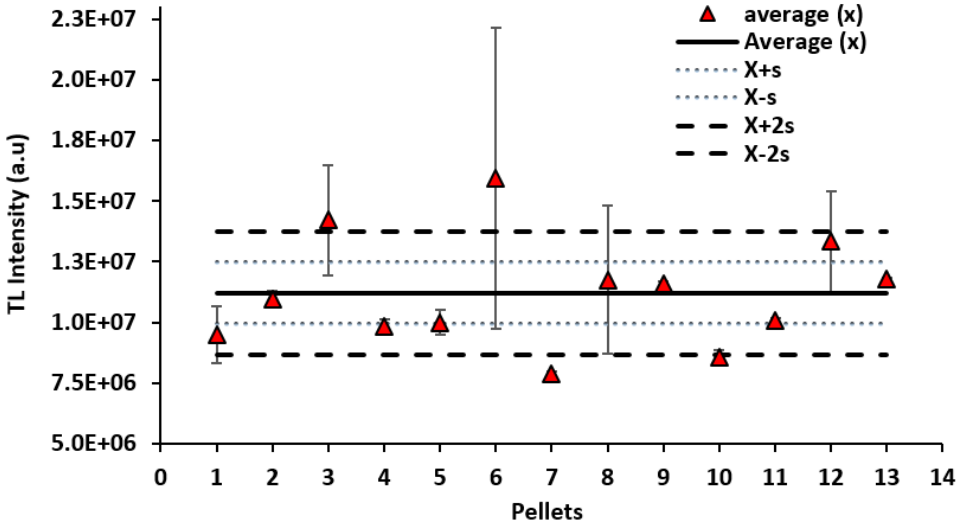

3.3.2 Effect of Eu Concentration on TL Glow curve

Samples of $BaSO_4$:Eu, with different dopant concentrations were prepared according the methodology described above and synthesized at the temperature of 500°C/4h+1100°C/30min. Dopant concentration was varied from 0.02 to 2mol%.

3.3.3 Dose Response for TL

The dose response of the $BaSO_4$:Eu (0.02 mol%) was studied by irradiating the sample pellets of $BaSO_4$:Eu to different doses using ^{137}Cs γ-source. The TL measurements were carried out using an automated Lexsyg Smart reader equipped with a bialkaline type photomultiplier tube from Hamamatsu H7360-02 and a wide

band blue filter. The glow curves were acquired at temperatures ranging from 50 to 350°C with heating rate of 2°C/s. For annealing, the samples were treated at a two-steps annealing cycle at 400ºC for 1 h, followed by 100°C for 2 h, before each irradiation. The area of the main peak was calculated by the integration of the TL intensity in the region of 130°C to 230°C, and plotted as a function of the absorbed radiation dose.

The dose response of the pellets was also evaluated for X-ray beam with different energies. The irradiation of the pellets was performed at the Metrology Laboratory of Ionizing Radiation of DEN/UFPE using the quality X-ray narrow series X-ray beams according ISO DIS: 4037-1, 1994. The sequence of Annealing-Irradiation-Reading was repeated three times for each dose and photon-energy. Table 2 presents the characteristics of the X-Ray beams used in this study.

Table 2 - Characteristics of the X-Ray beams used in this study

Beam quality	**Tube Potential** (kV)	**Mean Energy** (keV)	**Additional filter** (mm)	**1st HVL** (mm)
LMRI-N40	40	33	0.21Cu + 4.0Al	0.058 Cu
LMRI-N60	60	48	0.60Cu + 4.0Al	0.240 Cu
LMRI-N80	80	65	2.00Cu + 4.0Al	0.600 Cu

3.3.4 Emission Spectra and TL Glow curve for different dopant ions

To evaluate the effect of the type of dopant, sample pellets of $BaSO_4$ with the selected dopants (i.e., Eu, Ce, Dy, Tm, and Pr) were prepared according to the methodology described in section 3.1, for the concentrations of 0.02 mol%, 0.05 mol% and 2 mol%.

The samples with 2mol% were used to evaluate the emission spectra of these samples. The TL spectra were acquired using samples irradiated at 1 kGy from Co^{60} γ-source. Readout was performed using a Hammamatsu mini spectrometer equipped with a cooled CCD detector and a diffraction grating, sensitive to the visible to near IR (320 and 1000 nm) range. The spectrometer was coupled to a hot planchet with a linear heating rate from 50 to 400°C. The maximum spectral resolution (FWHM) for this spectrometer is 8 nm.

The wavelength of light emitted is determined by the depth of the recombination center, over a given temperature range. In this way, we can expect each TL emission peak to be associated with a spectral band of a set of recombination centers.

3.4 OSL CHARACTERIZATION

The OSL response was measured using an automated Lexsyg Smart OSL reader equipped with an internal $^{90}Sr/^{90}Y$ β-source with a dose rate of 100 mGy/min and a Hamamatsu H7360-02 bialkaline photomultiplier tube.

Blue light stimulation luminescence (BSL) measurements were acquired under constant illumination intensity mode (CW) with blue LEDs with peak emission at 458 nm and power set to 50 mW/cm^2. The “TL-380” filter pack used comprised the BP365-50, LF101581 and KG3 filters.

For the Infra-Red stimulation luminescence (IRSL), LEDs with peak emission at 850 nm and power set to 250 mW/cm^2 were used.

Initially the response of a group of 20 pellets was evaluated to obtain a group of pellets with similar sensitivity. Figure 22 shows the results of BSL response of the pellets irradiated at 20 mGy from $^{90}Sr/^{90}Y$ β-source. The blue stimulation light was at 458 nm with 50 mW/cm^2 during 100s. The acquisition time per channel was 0.1s. The response of the non-irradiated pellet was subtracted from response of each irradiated pellet to obtain a net value. The area of the OSL curve was calculated and each point corresponds to the average of 3 measurements with the indication of the standard deviation. After each measurement, the pellets were annealed at 400°C for 1.0 h, using a programmable oven and then followed 100°C at 2h. In Figure 22, the solid golden line represents the overall average of the measurements ($\bar{x}$); the dotted lines correspond to the response in range ($\bar{x} \pm 1s$) while the outermost solid black lines represent the range ($\bar{x} \pm 2s$). The coefficient of variation (CV), also known as relative standard deviation was calculated by the ratio of the standard deviation to the mean. All pellets selected for evaluation, presented response between the interval of $\bar{x} \pm 2s$ and they were used to characterize the OSL response of the $BaSO_4$:Eu (0.02 mol%).

Figure 22 – Reproducibility of the BSL response of the pellets irradiated at 200 mGy from $^{90}Sr/^{90}Y$ β-source

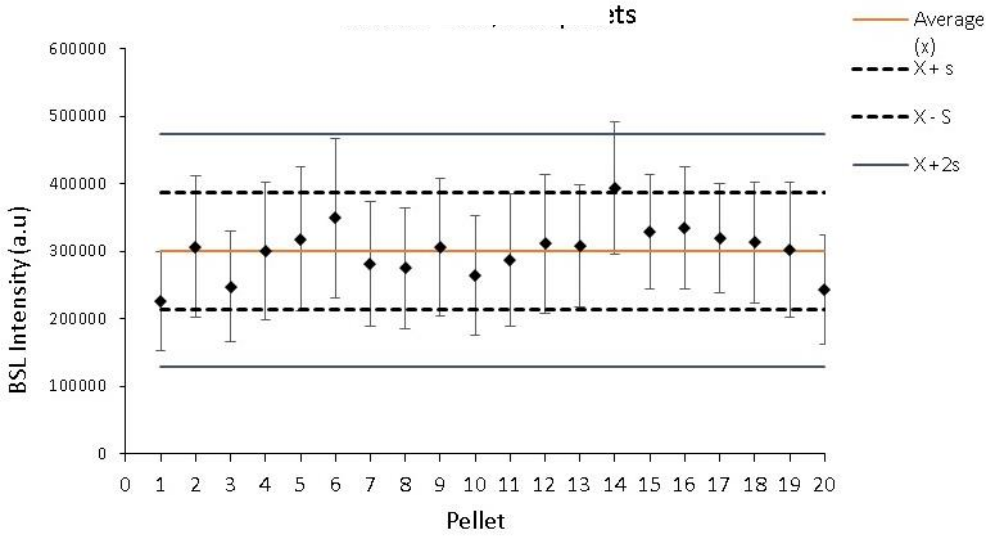

3.4.1 OSL emission and residual TL

For blue light stimulation luminescence (BSL) measurements were acquired under constant illumination intensity mode (CW) of blue LEDs with peak emission at 458 nm and power set to 50 mW.cm^2. The “TL-380” filter pack used comprised the BP365-50, LF101581 and KG3 filters. Residual thermoluminescent (TL) glow curves were recorded after BSL. A heating rate of 5°Cs^{-1}, with Wide-Band-Blue filter pack, was used for all TL measurements.

For the Infra-Red stimulation luminescence (IRSL), LEDs with peak emission at 850 nm and power set to 250 mW/cm^2 was used. The “Wide-Band-Blue” filter pack composed of BG39, BG25 and KG3 filters were used. Residual thermoluminescent (TL) glow curves for IRSL were recorded after IRSL.

The OSL decay curves were analyzed using the methods proposed by BULUR (2000) for first order kinetics. In this method the luminescence output in a CW-OSL measurement can be manipulated, so that the results are mathematically similar to the LM-OSL situation. For the first order kinetics, BULUR gave the luminescence decay function as:

$$\mathrm{L(t)} = \mathrm{n_o b}\exp(-bt) \qquad (4)$$

where, “n_0” is the initial concentration of trapped electrons, “b” is a constant describing the decay of the luminescence curve and is proportional to the detrapping

probability. Moreover, $b = I_o \alpha$ with "α" being the photoionization cross-section and "I_o" as the stimulation light intensity.

In order to convert the CW-OSL curve to an LM-OSL curve one may introduce a new independent variable u, which is defined as $\mathrm{u} = \sqrt{2tP}$ where, "P" is the measurement period, and t is the stimulation time. Notice that u has the dimension of time. Substituting u in Equation (4), we get;

$$\mathrm{I(u)} = \mathrm{n_o} \frac{\mathrm{b}}{P} u \exp(-\frac{b}{2P} u^2) \tag{5}$$

This is similar to the emitted LM-OSL intensity relation as:

$$\mathrm{L(t)} = -\frac{\mathrm{dn}}{dt} = \mathrm{L_o} \frac{\mathrm{t}}{\theta} \exp(-\frac{\alpha \mathrm{I_o}}{2\theta} t^2) \tag{6}$$

Where "$\mathrm{L(t)}$" is the emitted LM-OSL intensity, "$\mathrm{L_o}$" is the initial intensity, "θ" is the total time of measurement; "α" is the proportionality constant and "$\mathrm{I_o}$" is the initial intensity of stimulation light. In the first-order case the maximum intensity is proportional to the initial concentration of trapped carriers, the maximum intensity "u_m" can be used for evaluating the absorbed dose in cases where one is convinced that this concentration is proportional to the dose. Obviously, this may not be the case in non-first-order cases.

KREUTZER et al (2012) developed an **R** package 'Luminescence' using this mathematical formalism and this package includes a set of functions for analysis of luminescence properties. Using the **R** package "Luminescence" version (0.1.7) we obtained the pseudo LM-OSL of the samples. We have avoided to give detail about **R** package "Luminescence" version (0.1.7) to maintain the continuity of our own project, however, interested readers may have a look on the detailed work of (KREUTZER et al., 2012).

3.4.2 Dose Response for OSL

The OSL dose response of the $BaSO_4$:Eu (0.02 mol%) was studied by irradiating the phosphor to different doses using a ^{137}Cs γ-source. The OSL measurements were carried out using an automated Lexsyg Smart reader and the conditions described above for BSL and IRSL measurements. The OSL curves were acquired for a period of 20s. For annealing, the samples were treated at a two-steps annealing cycle of 400ºC at 1 h, followed 100°C at 2 h, before each irradiation. The

area of the OSL curve during the period of acquisition was calculated and plotted as a function of the absorbed radiation dose.

3.4.3 Effect of the Eu concentration on OSL response and residual TL

Samples of $BaSO_4$:Eu with different concentrations of Eu ions were prepared according to the methodology described in section 3.1 and synthesized at the temperature of 500°C/4h+1100°C/30min. Concentration of Eu ions was varied from 0.02 to 2.0 mol%. The BSL and IRSL signals were measured as well as the residual TL response.

3.4.4 Effect of Different Dopants on OSL response

To evaluate the effect of the type of dopant, sample pellets of $BaSO_4$ with the selected dopants (i.e., Eu, Dy, Tm, Ce and Pr) were prepared according to the methodology described in section 3.1, for the concentrations of 0.02 mol% and 0.05 mol%. The BSL and IRSL signals were measured as well as the residual TL response.

4 RESULTS AND DISCUSSION

4.1 CHARACTERIZATION OF THE SAMPLES

4.1.1 X-Ray Diffraction (XRD)

The XRD pattern of the $BaSO_4$:Eu (0.02 mol%), thermally treated at 500°C/4h+1100°C/30min, samples prepared is shown in Figure 23. The red lines inside this Figure belongs to Inorganic Crystal Structure Database (ICSD) n. COD 9000159 BaO4S Barite (COLVILLE; STAUDHAMMER, 1967).

Figure 23 – XRD pattern of our synthesized $BaSO_4$:Eu (0.02 mol%) sample thermally treated at 500°C/4h+1100°C/30min as compared with the standard ICSD Standard n. code 9000159

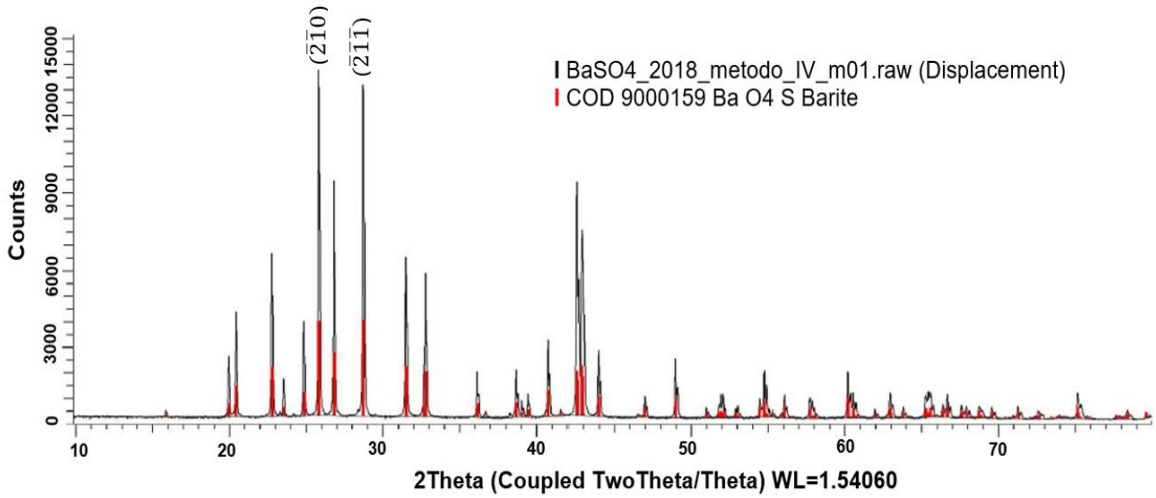

Source: Colville; Staudhammer, 1967.

The sharp and single peaks of XRD pattern suggest the formation of single-phase compound. The wide angle XRD pattern for the sample exhibits five intense peaks in the range 20°-45°, which are the main characteristic peaks of $BaSO_4$ having orthorhombic structure.

The average crystallite size for the crystalline sample was approximately estimated by taking into account the most prominent peak and using the Scherrer equation (SCHERRER, 1918) as given in equation (7).

$$D = \frac{0.9\lambda}{\beta \cos\theta} \qquad (7)$$

where, “D” is the average crystallite size; “θ” is the Bragg angle; “λ” is the incident wavelength and “β” is the diffracted full width at half maximum (FWHM) in radians

caused by the crystallites. Geometric parameters of the diffraction peaks of the planes $(\bar{2}\bar{1}0)$ and $(\bar{2}\bar{1}\bar{1})$ are given in Table 3.

Table 3 – Geometric parameters of the diffraction peaks corresponding to the planes $(\bar{2}\,\bar{1}\,0)$ and $(\bar{2}\,\bar{1}\,\bar{1})$

Parameters	Peak $(\bar{2}\,\bar{1}\,0)$	Peak $(\bar{2}\,\bar{1}\,\bar{1})$
Angle (2θ)	25.83°	28.72°
β (FWHM)	0.124	0.133
Crystallite Size	774.2 Å	744.7 Å

In case of europium doped barium sulphate ($BaSO_4$:Eu), we have for highest intense peak: $\theta = 25.83°$, $\lambda = 1.54060Å$ and $\beta = 0.124$, so this gave average crystallite size "D" equal to 77.4 nm.

Table 4 presents the values of the crystallite size of $BaSO_4$ synthetized by different author(s) using different synthesis techniques and dopants. The results show that the material produced in this study is similar to that of produced by other authors. It is evident from the results that the crystallite size of the $BaSO_4$:Eu produced in this study are in agreement with that of produced by other authors.

Table 4 – Crystallite size for rare earth doped $BaSO_4$ by some investigators

Year	Author(s)	Sample	Synthesis Technique	Thermal treatments	Crystallite Size
2010	Ramaswamy et al.,	$BaSO_4$	Micro emulsion technique	100°C/6h	50-70 nm
2012	Devi and Singh	$BaSO_4$:Eu,Dy	Chemical co-precipitation	100°C/1h+600°C/1h	67-73.3 nm
2017	Pandey et al	$BaSO_4$:Eu (0.2 mol%)	Chemical co-precipitation	90°C/2h+850°C/1h	40 nm
2018	Sharma et al	$BaSO_4$:Eu (0.2mol%)	Chemical co-precipitation	90°C/2h+850°C/1h	40 nm
2020	This study	$BaSO_4$:Eu (0.02 mol%)	Solid State Combustion Technique	500°C/4h+1100°C/0.5h	74.4 nm

4.1.2 Scanning Electron Microscopy (SEM)

Figure 24 shows the image of the surface of $BaSO_4$:Eu pellet obtained by SEM with different magnifications.

It is possible to observe by the Figure 24(d) that it is a polycrystalline structure formed by equiaxial grains. Particles of $BaSO_4$:Eu seen in SEM micrographs are ultrafine and having agglomeration. The size of the grains, corresponding to the agglomeration of the crystals, is ranging from 0.83-0.97μm and hence grain size is less than 1 micron. SALAH et al., (2009) has calculated the grain size of 30-50 nm for $BaSO_4$:Eu prepared by chemical co-precipitation technique.

Figure 24 – SEM micrographs of $BaSO_4$:Eu with Magnification (a) 25× (b) 2000× (c) 5000× and (d) 10000×

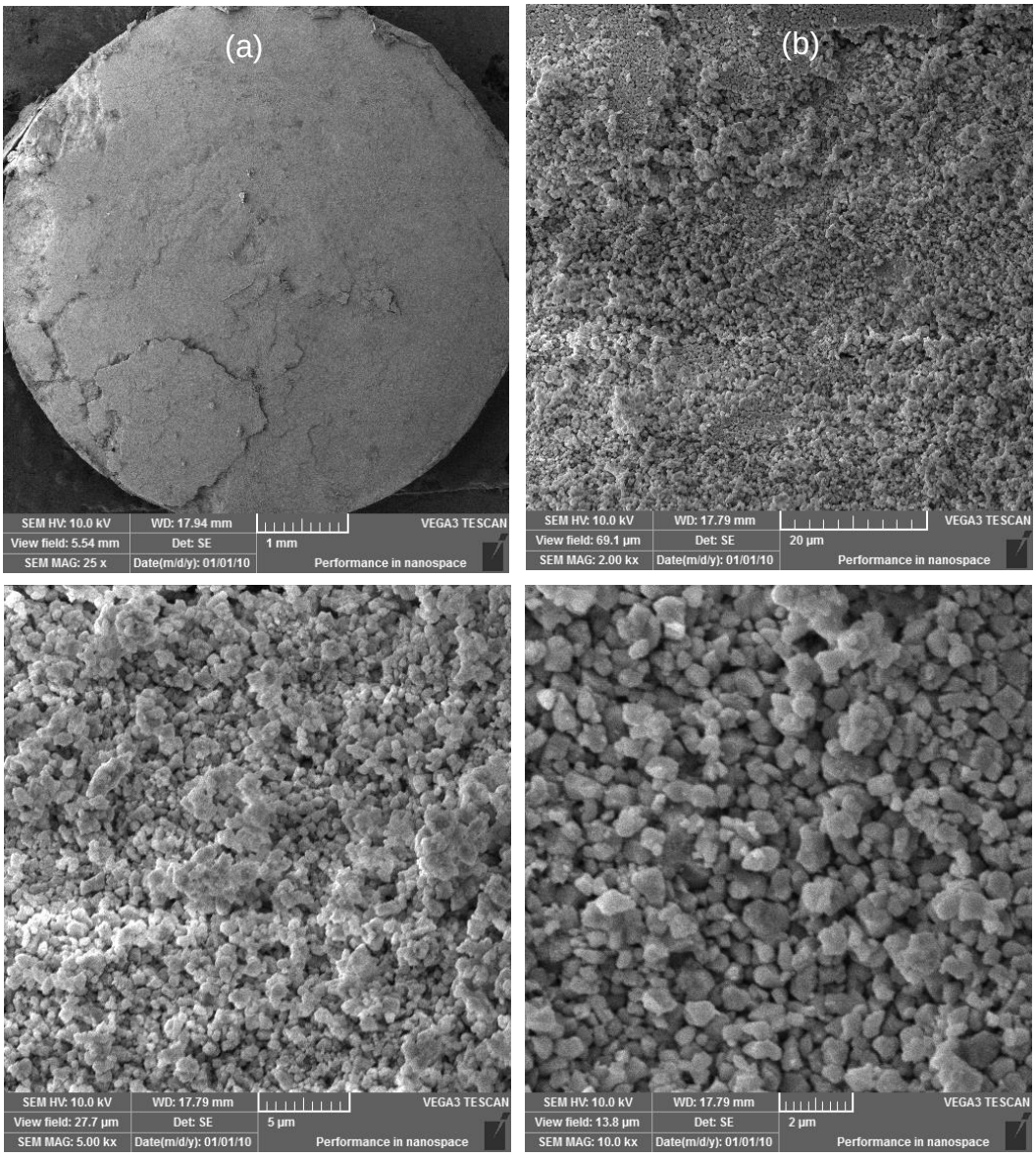

4.1.3 Differential Thermal analysis (DTA) and Thermal Gravimetric Analysis (TGA)

Figure 25 and Figure 26 show the Differential Thermal Analysis (DTA) and Thermal Gravimetric Analysis (TGA) of the samples prepared with the Synthesis temperature of 500°C/4h and 500°C/4h+1100°C/30min, respectively. The results show that for the sample treated at 500°C for 4h, there is a weight loss of 5.8% at temperature around 100°C, that is due to the evaporation of the water and a second weight loss of 5.3% at temperature around 680°C.

The TGA results obtained with the treatment at 500°C/4h+1100°C/30min does not show variation in the sample weight, which indicates an excellent crystallinity of the synthesized sample.

4.2 THERMOLUMINESCENT CHARACTERIZATION

4.2.1 TL Glow Curve of $BaSO_4$:Eu

Figure 27 shows the glow curve of the $BaSO_4$:Eu (0.02mol%), pellets were irradiated, in air under an electronic equilibrium, for an absorbed dose of 100mGy from ^{137}Cs γ-source. It can be seen from the graph that $BaSO_4$:Eu shows a simple glow curve structure with a main TL peak at approximately 186°C, a shoulder peak at 205°C and a high temperature peak at 270°C. This result is similar of the glow curves found in the literature.

ANNALAKSHMI et al, (2012) has mentioned the 240°C TL glow peak of $BaSO_4$:Eu prepared by solid state diffusion method sintered in reducing atmosphere as shown in Figure 11. Although they have not deconvoluted the TL glow curve but a sharp look can see the significant presence of the low and higher temperature peaks.

SALAH et al (2009) has mentioned the 224°C TL glow peak of $BaSO_4$:Eu nanophosphor prepared by the chemical co-precipitation method as shown in Figure 28.

PATLE et al., (2015) has mentioned the intense TL peak at 190°C with shoulder at 282°C for the TL/OSL dual phosphor $BaSO_4$:Eu (0.1 mol%) using thiourea ($SC(NH_2)_2$). They dried the precipitate at 60°C for 2h and then annealed at 1000°C. TL response of $BaSO_4$:Eu before BSL and after BSL is shown in Figure 29.

Figure 25 – TGA and DTA graphs of $BaSO_4$:Eu samples thermally treated at 500°C for 4h

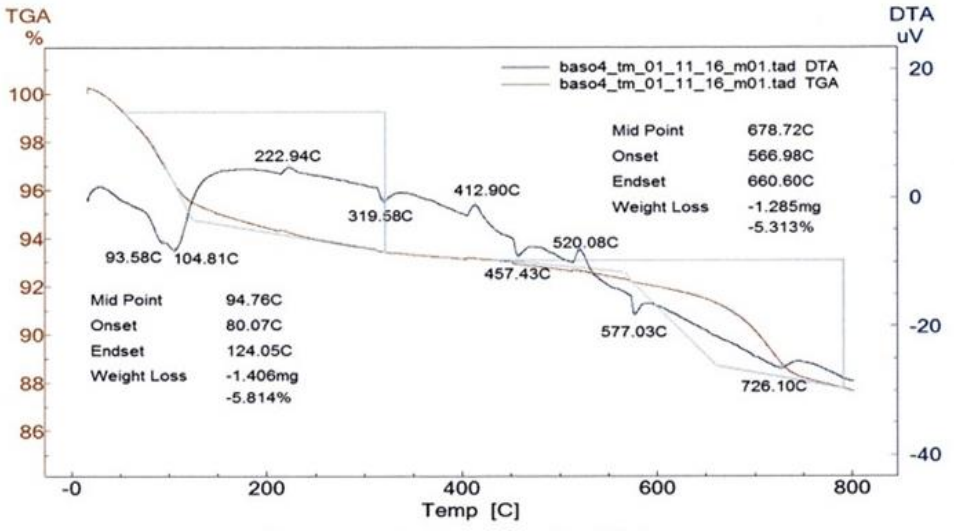

Figure 26 – TGA and DTA graphs of $BaSO_4$:Eu samples thermally treated at 500°C/4h+1100°C/30min

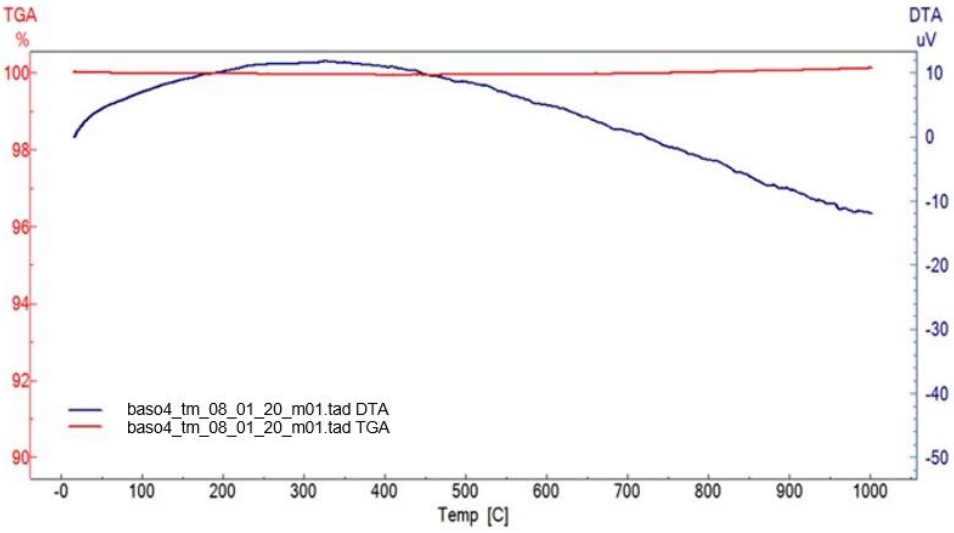

BHATT et al., (1997) found the TL Glow curves for $CaSO_4$:Dy and $BaSO_4$:Eu Teflon disks, as well as for $BaSO_4$:Eu and $BaSO_4$:Eu,P TL phosphor samples at a test gamma dose of 0.01Gy. The TL sensitivity of $BaSO_4$:Eu was 5.8 and 11 times that of $CaSO_4$:Dy teflon disks. $BaSO_4$:Eu pellets prepared by co-precipitation technique and annealed at 850°C for 3h presented three TL peaks at 170, 215 and 270°C.

Table 5 presents some literature results of TL peaks obtained in the glow curves of samples of $BaSO_4$:Eu prepared by different methods. It is possible to observe that depending of the preparation method is possible to obtain more than one peak, but in all of the methods the most intense TL peak is in the region around 200°C.

Figure 27 – TL Glow curve of sample pellets of $BaSO_4$:Eu (0.02 mol%) thermally treated at 500°C/4h+1100°C/30min irradiated at 100 mGy from ^{137}Cs γ–source

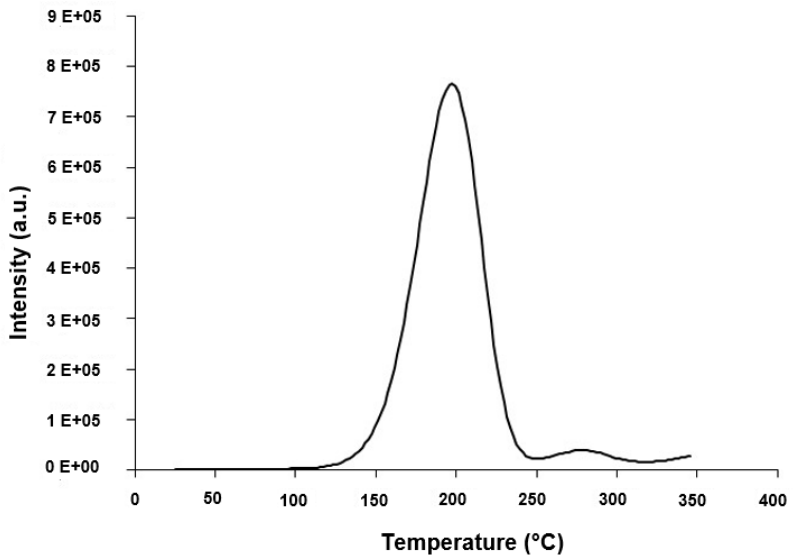

Figure 28 – Typical TL glow curves of $BaSO_4$:Eu micro- and nanocrystalline samples exposed to 10 Gy from ^{60}Co γ-source. TL glow curve of $CaSO_4$:Dy phosphor is also shown for comparison

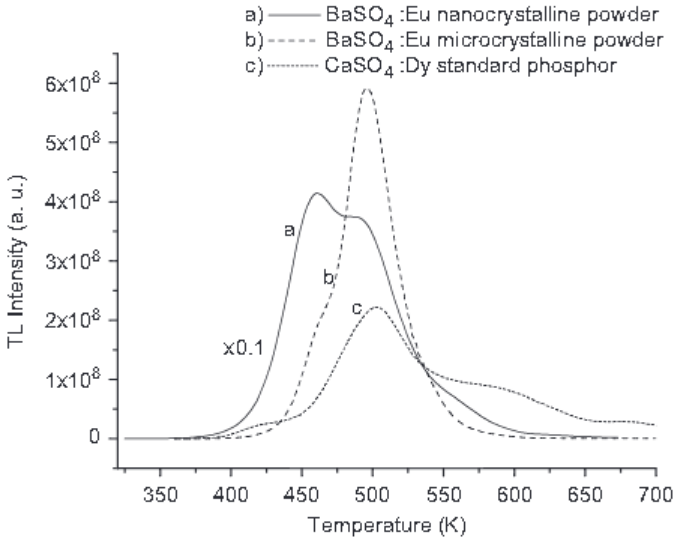

After: Salah *et al*., 2009.

Figure 29 – TL response of sample $BaSO_4$:Eu a) TL before OSL b) TL after OSL

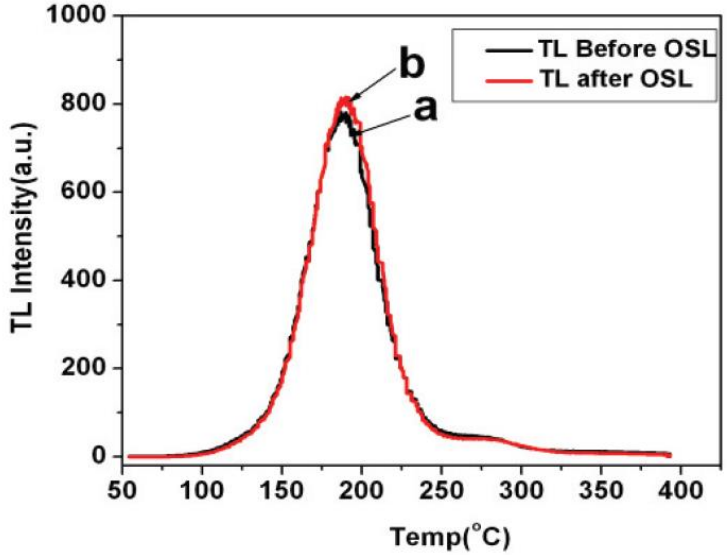

(After: PATLE et al., 2015)

Figure 30 – Typical Glow curves for $BaSO_4$:Eu Teflon disks, $CaSO_4$:Dy Teflon disks, $BaSO_4$:Eu,P (0.2, 0.5 mol%) phosphor, $BaSO_4$:Eu (0.5 mol%) phosphor. Test gamma dose was 0.01 Gy. Sensitivities of the various materials can be compared by multiplying the indicated numbers

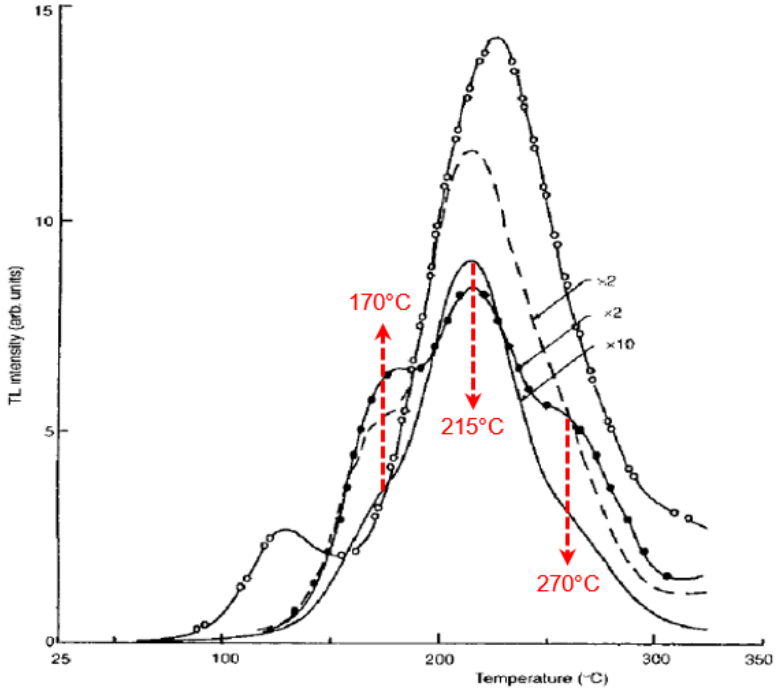

After: Bhatt *et al.*, 1997.

Table 5 – TL Glow Peak of $BaSO_4$:Eu by different researchers with different methodologies

Year	Authors	Phosphors	Preparation Method	Peak temperature (°C)				
				Intense peak	2nd peak	3rd peak	4th peak	5th Peak
1997	Rao et al	$BaSO_4$:Eu	Recrystallization & Coprecipitation Technique	170	215	280	-	-
1997	Bhatt et al.,	$BaSO_4$:Eu	Co-precipitation Technique	170	215	270	-	-
1999	Madhusoodanan	$BaSO_4$:Eu	Co-precipitation Technique	180	230	280	-	-
2007	Gonzalez et al	$BaSO_4$:Eu	Crystallization technique	167	131	205	235	-
2009	Salah et al.,	$BaSO_4$:Eu	Chemical Co-precipitation method	224	-	-	-	-
2012	Annanlakshmi et al	$BaSO_4$:Eu	Solid state diffusion method	240	-	-	-	-
2012	Devi & Singh	$BaSO_4$:Eu	Chemical Co-precipitation method	182	-	-	-	-
2013	Singh et al	$BaSO_4$:Eu	Chemical co-precipitation	180	208	-	-	-
2014*	Bhatt et al	$BaSO_4$:Eu	Received Nemoto and Co, Japan	220	130	190	280	330
2015	Patle et al	$BaSO_4$:Eu	Precipitation Technique (with Thiourea)	190	282	-	-	-
2015*	Aboelezz et al	$BaSrSO_4$:Eu (nano)	Chemical co-precipitation	183	212	268	-	-
		$BaSrSO_4$:Eu (micro)		211	-	-	-	
2016*	Hassan et al	$BaSrSO_4$:Eu	Chemical co-precipitation	181.2	209.7	253.1	290.2	-
2016	Rani et al	BaSO4:Eu (M-I)	Chemical co-precipitation	250	180	-	-	-
2017	Pandey et al	$BaSO_4$:Eu (Co^{60})	Chemical co-precipitation	187	278	-	-	-
		$BaSO_4$:Eu (Cs^{137})		187	278	-	-	
2018*	Sharma et al	$BaSO_4$:Eu	Solid State Diffusion Method	185	217	279	-	-
2020*	This study	$BaSO_4$:Eu	Solid State Combustion Technique (With urea)	186	205	270	-	-

*TL Glow curve was deconvoluted.

There are various methods for evaluation of the kinetic parameters of TL glow curves. Some methods such as the initial rise (IR), variable heating rates (VHR) and peak shape methods are suitable for single or thermally cleaned glow peaks. Computerized Glow Curve Deconvolution (CGCD) method is suitable for analyzing complex TL glow curves. The most attractive feature of the deconvolution technique is the simultaneous determination of kinetic parameters i.e., activation energy (E), frequency factor (s) and order of kinetics (b).

To better identify the TL peaks, the experimental curves were deconvoluted using the GlowFit program (PUCHASKA; BILSKI, 2006). This program was developed based on the functions and equations presented by KITIS et al. (1998) and KITIS (2001) and also based on the Randall and Wilkins model for first-order kinetics (CHEN; MCKEEVER, 1997; PAGONIS et al. 2002).

The deconvolution of the TL curve was performed on TL curves obtained from samples irradiated at 60 mGy from ^{137}Cs γ-source. TL readings were performed on the Lexsyg Smart TL/OSL Reader, with a heating rate of 2°C/s and between 25 and 300°C.

The Figure of merit (FOM) used to assess the degree of deconvolution quality was initially proposed by BAILIAN and EDDY (1977) to analyze gamma-ray spectrum peaks, but has since been commonly used to compare deconvolution analysis on TL curves (BOS et al., 1994). The Figure of merit as a percentage is defined as:

$$FOM = \sum_{j_{inicial}}^{j_{final}} \frac{|y_j - y(x_j)|}{A} \times 100\% \qquad (8)$$

where: $j_{inicial}$ is the first channel of TL peak corresponding to the region being deconvoluted; j_{final} is the last channel of this region; y_j is the corresponding intensity of channel j; $y(x_j)$ is the theoretical value of channel j estimated by the deconvolution, and A is the integral of the deconvoluted TL peak.

The coefficient C_b was also used to evaluate the deconvolution parameters. According to KITIS (2001) this coefficient varies between 0.38 and 0.40, for first order peaks, and can be used as criteria in order to accept or reject the results of the deconvolution analysis. It is calculated by the equation:

$$C_b = \exp\left(\frac{2kT_m}{E} - 1\right) \qquad (9)$$

where, k is the Boltzmann constant ($8.617 \times 10^{-5}\ eV/K$); T_m is the temperature in K attributed to maximum TL intensity, and E is the activation energy (eV).

The intensity of the TL peak as well as the peak temperature (T_m) and activation energy (E) were determined and their values found are presented in the Table 6. Figure 31 shows an experimental TL curve and the deconvolution peaks. The main TL peak was deconvoluted in two peaks, at 186°C and 205°C and the third peak is at 270°C. The FOM value obtained was 8.38%, indicating a good adjust.

OKAMOTO et al., (1986) found three TL peaks for $BaSO_4$:Eu and according to them the lower temperature peak is affected by fading effects and higher temperature peak is near the background region, so they believed to achieve middle temperature TL peak for the dosimetric applications.

Figure 31 – TL Glow curve of $BaSO_4$:Eu and deconvolution peaks

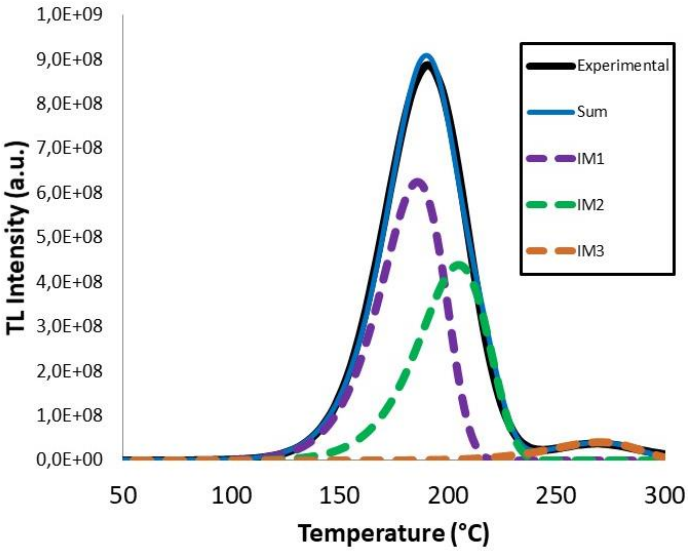

Table 6 – Deconvolution parameters of TL glow curve of $BaSO_4$:Eu (0.02 mol%)

Peak	T_m (°C)	I_m (a.u.)	E (eV)
1	186	6.24×10^9	1.19
2	205	4.38×10^9	1.22
3	270	3.97×10^8	1.22

4.2.2 Effect of Eu Concentration on TL response

Figure 32 shows the variation of the TL glow curve obtained with samples prepared with different concentration (mol %) of the dopant Eu ions and irradiated at 5 mGy from ^{137}Cs γ–source. The results show that the sensitivity of the samples increases with the reduction in the concentration (mol %) of the Eu ions. It is inferred from the Figure that nanocrystalline $BaSO_4$:Eu has a simple glow curve structure with

a TL peak at 186°C. Also, the TL peak position is independent of the concentration of dopant (Eu) ions and shows no shift with change in dopant concentration (0.02−2.0 mol%). Our results are consistent with SHARMA et al., (2018). TL peak intensity firstly increased with decreasing Eu concentration and reaches a maximum at a 1 mol%, after which it decreased with further decrease in the concentration of the dopant until 0.5mol%. With further decrease in dopant concentration from 0.5 mol% to 0.02 mol% TL intensity kept on increasing again. It can be concluded that there is an increase in the number of defects/traps at Eu concentration of 0.02 mol%, which in turn implies an increase in the number of charge carriers being trapped upon irradiation. This phenomenon explains the initial rise in the peak intensity of the glow curves. Furthermore, on being thermally stimulated, these traps released the charge carriers which in turn recombined at the recombination center and gave rise to diverse glow peaks with increased height. The decline in the peak intensity after concentration (1 mol%) is attributed to concentration quenching (CHEN; PAGONIS, 2011).

Figure 33 shows the variation of the sensitivity of $BaSO_4$:Eu with the dopant concentration (mol%). The TL sensitivity is defined as the ratio between the TL reading per unit dose and pellet mass i.e., $(TL\ Intensity)/(mg.Gy)$ (FURETTA, 2003). The results show that the highest sensitivity has been achieved for a concentration of 0.02 mol% of Eu ions, therefore we optimized this concentration for further study.

Figure 32 – Variation of TL peak as a function of concentration (mol%) of Eu ions as dopant in $BaSO_4$ pellets irradiated at 5 mGy of Cs^{137} γ-source

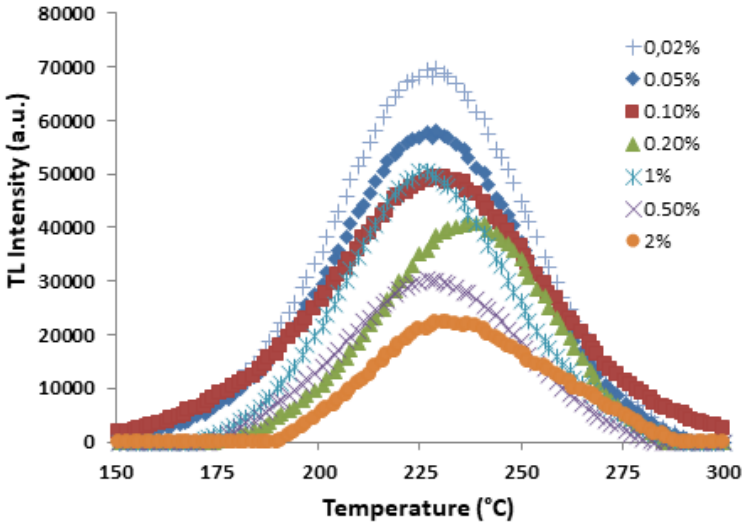

Figure 33 – Sensitivity (TL/Gy.mg) of $BaSO_4$:Eu as a function of dopant concentration (in mol%) irradiated with ^{137}Cs γ-source

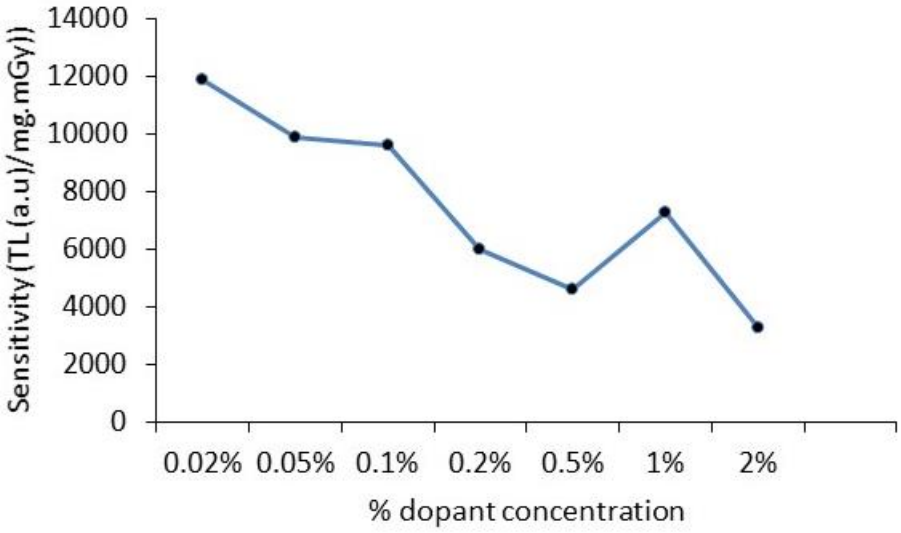

4.2.3 TL Dose Response of $BaSO_4$:Eu

Figure 34 represents the glow curve of the pellets of $BaSO_4$:Eu (0.02 mol%) irradiated with different radiation doses from ^{137}Cs γ-source. The area of the main peak was calculated by the integration of the TL intensity in the region of 130°C to 230°C. The results obtained are shown in Figure 34 as function of the absorbed dose (mGy) of gamma radiation of ^{137}Cs.

The angular coefficient (*a*) and the regression coefficient (R^2) of the linear fittings are also shown in Figure 35. It is observed that the results show a linear response of the phosphor with the absorbed dose in the investigated range. This

linear response shows that the phosphor can act as a good dosimeter for radiation dosimetry applications.

Figure 34 – TL Dose response of $BaSO_4$:Eu (0.02 mol%) irradiated at different radiation doses from ^{137}Cs γ-source

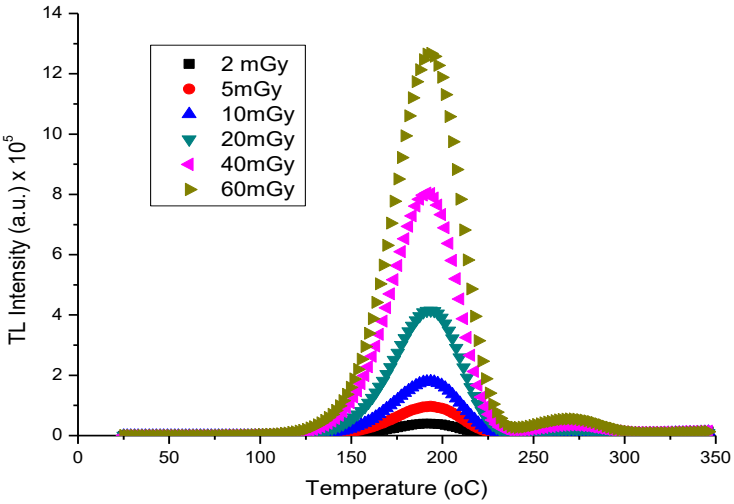

Figure 35 – Calibration curve of $BaSO_4$:Eu (0.02 mol%) irradiated at different doses from Cs^{137} γ-source

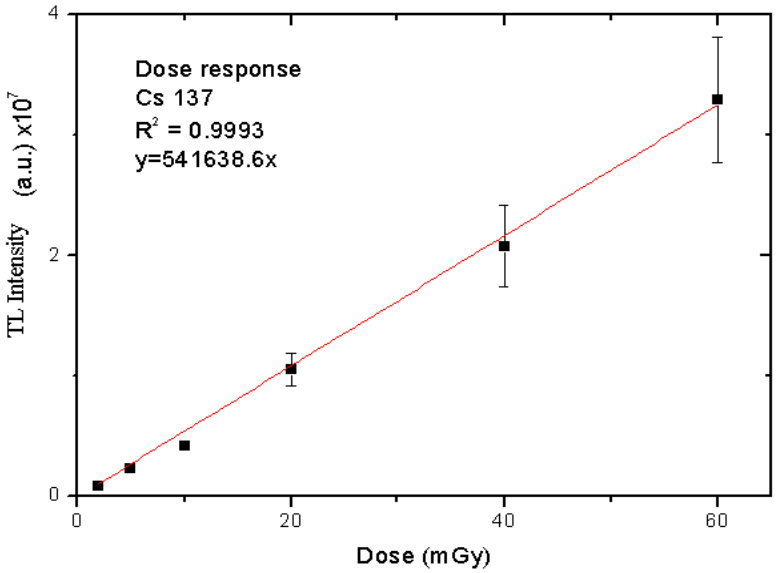

The lower detection limit (LDL) is the *lowest* dose that can be distinguished from the background value with a stated confidence level of 99%. The lower limit of detection of a TLD is currently defined as the reading of the dosimeter for a background radiation plus three times the standard deviation (FURETTA, 2003). The TL reading of the background of three pellets is 7758±647 (a.u.). Considering the dose response curve shown in Figure 35, the LDL value was equal to 17.9 μGy.

Literature reveals that an LDL of 28 μGy for TLD-100 (NASCIMENTO 2010); 20 μGy of $CaSO_4$:Dy (FERNANDEZ 2016); 25 μGy for synthetic Barite (Mn doped) for

498K TL glow peak (MANAM; DAS 2010); 135 μGy in $BaSrSO_4$:Eu (0.2 mol%) for 485K TL glow peak (ABOELEZZ at al., 2015) and 50 μGy in $BaSO_4$:Eu (0.2 mol%) for 485K TL glow peak (NAGPAL; VARADHARAJAN 1982) have been reported. Hence, we can safely say that our calculated LDL is lower than other investigators. However our result is consistent with the LiF:Mg,Cu,P that was 12μGy (FERNANDES 2016).

TL response of $BaSO_4$:Eu (0.02mol%) shown in Figure 34 is at low doses (in mGy). In order to observe high dose TL response, the sample pellets were irradiated at high doses in range 0.5-8Gy from Co^{60} γ-source. Since the sensitivity of the $BaSO_4$:Eu was very high so at high doses the TL intensity lied out of the range of Photomultiplier tube that's why a filter was used to reduce the TL intensity of Eu to 75% and only 25% response has been plotted in Figure 36 (a). Meanwhile, for quantitative analysis, calibration curves for $BaSO_4$:Eu is shown in Figure 36(b).

The qualitative TL response of $BaSO_4$:Eu shown in Figure 36 (a) describes that the TL response of Eu ions slowly increases at 0.5Gy to 2Gy but for the doses higher than 2Gy the TL response increases too high. Figure 36(b) explains that there is a linear behavior of TL response against gamma dose from 0.5Gy to 2Gy but there is another linear behavior of TL response seen from 2Gy to 5Gy. After 5Gy the response is too intense to be detected even with filter.

Figure 36 – TL Dose response (with filter) of $BaSO_4$:Eu (0.02mol%), thermally treated at 500°C/4h+1100°C/30min, irradiated at different doses of Co^{60} γ-source

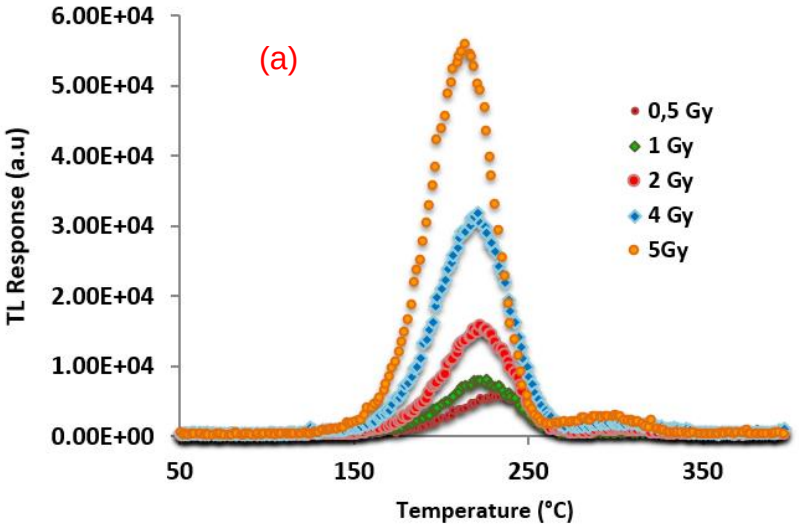

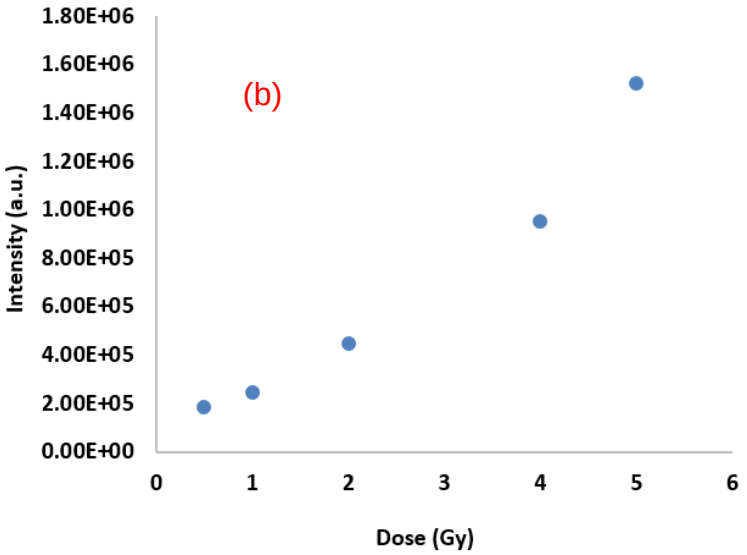

Figure 37 shows the calibration curves obtained with the X-ray beams with the ISO:4037 qualities of N-80, N-60 and N-40. The angular coefficient (*b*) and the regression coefficient (R^2) of the linear fittings are also shown.

Figure 37 – Calibration curve of $BaSo_4$:Eu (0.02mol%) with X-Ray beams of Quality a) N80 b) N60 c) N40

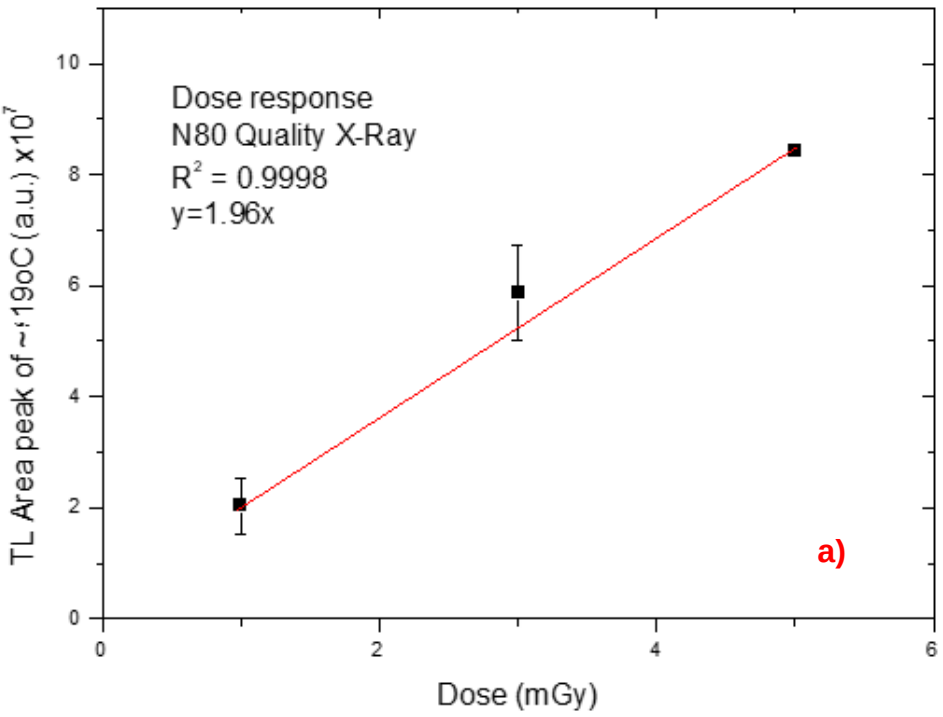

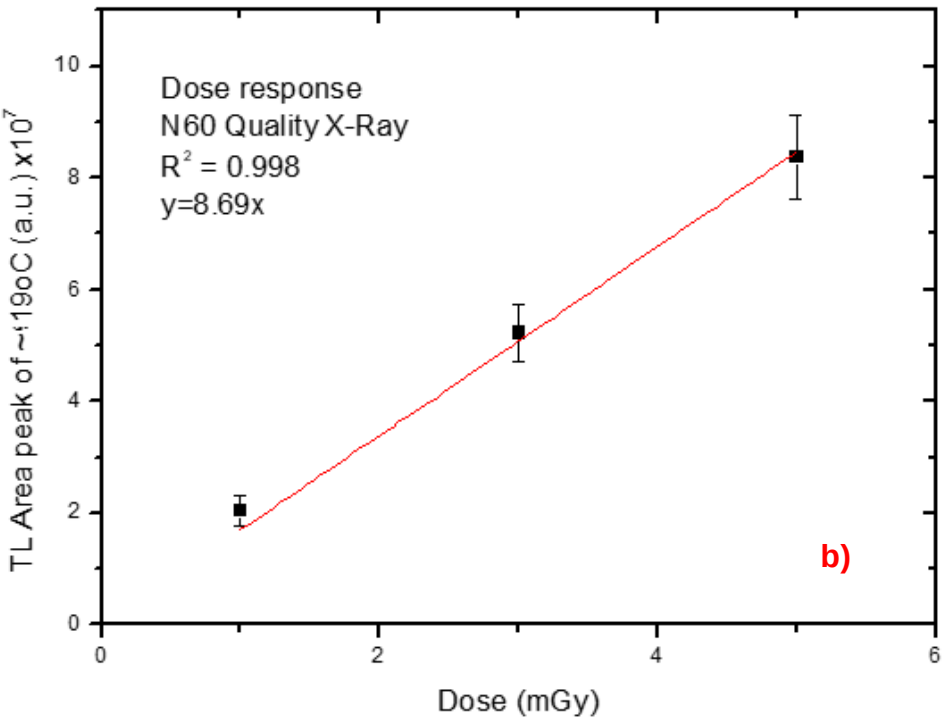

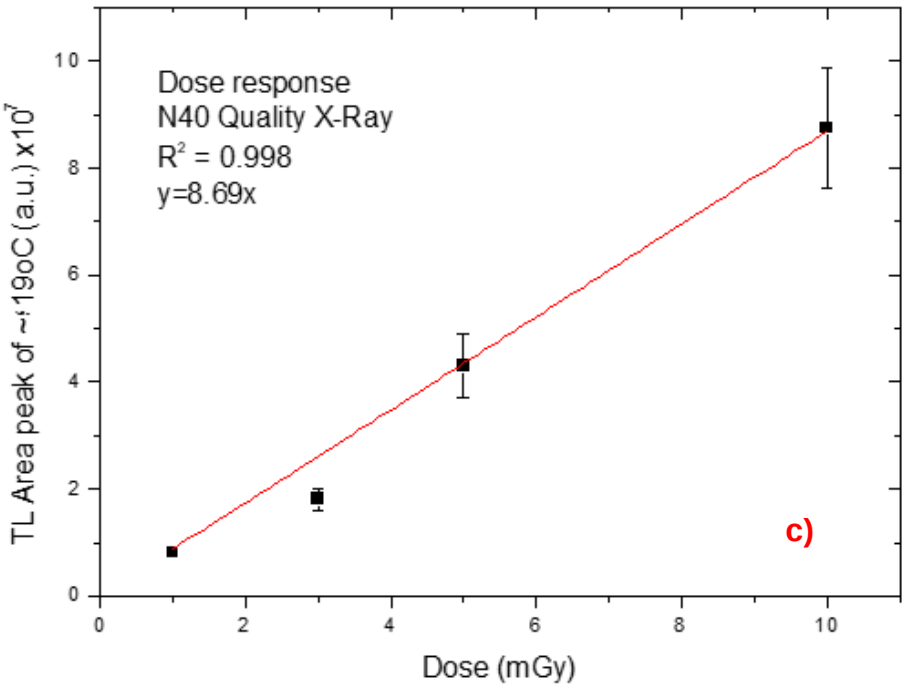

Figure 38 shows the energy dependence of $BaSO_4$:Eu given with respect of the ^{137}Cs.

The higher the value of Z_{eff} and the lower the energy of incident photons, the larger is the TL response to a given dose due to the dominant component of the photoelectric effect in the mass energy absorption coefficient (MCKEEVER, 1985). The values of Z_{eff} of $BaSO_4$ and $CaSO_4$ are 48.17 and 12.46 respectively (HAROLD; CUNNINGHAM;1983).

Figure 38 – Photon energy dependence of relative TL response of $BaSO_4$:Eu (0.02mol%) teflon pellets compared to Cs^{137} γ–source (Present Study)

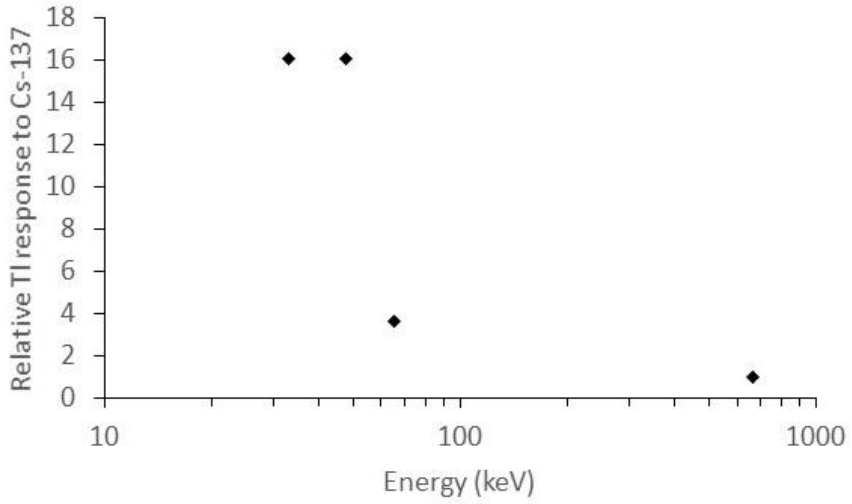

Figure 39 – Photon energy dependence response of $BaSO_4$:Eu Teflon disks, $BaSO_4$:Eu (0.5 mol%), $BaSO_4$:Eu,P (0.2, 0.5 mol%), $CaSO_4$:Dy Teflon disks

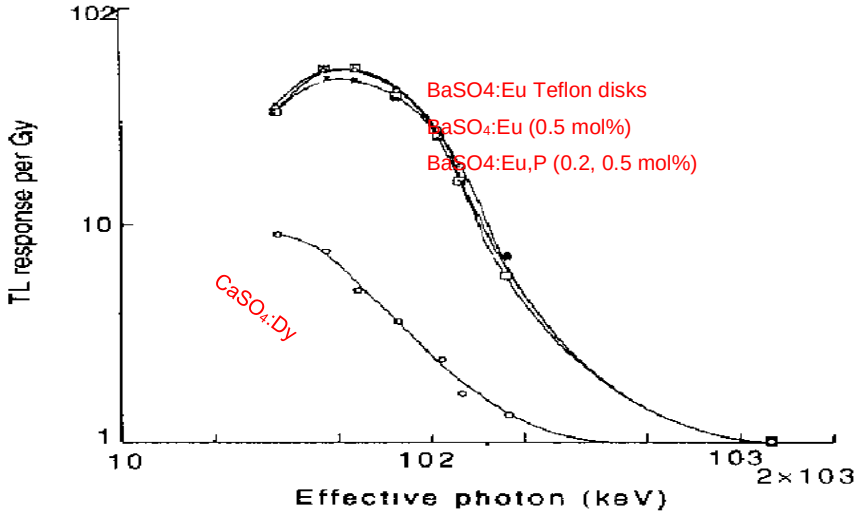

After: Bhatt *et al*., 1997.

Our result in Figure 38 is consistent with that of BHATT et al., (1997) as shown in Figure 39. BHATT et al., (1997) shows the photon energy response of $BaSO_4$:Eu and $CaSO_4$:Dy Teflon disks in the range 32-1250 keV.

Figure 40 – Energy response of $BaSO_4$:Eu, TLD-900 ($CaSO_4$:Dy) and TLD-100 (LiF:Mg,Ti)

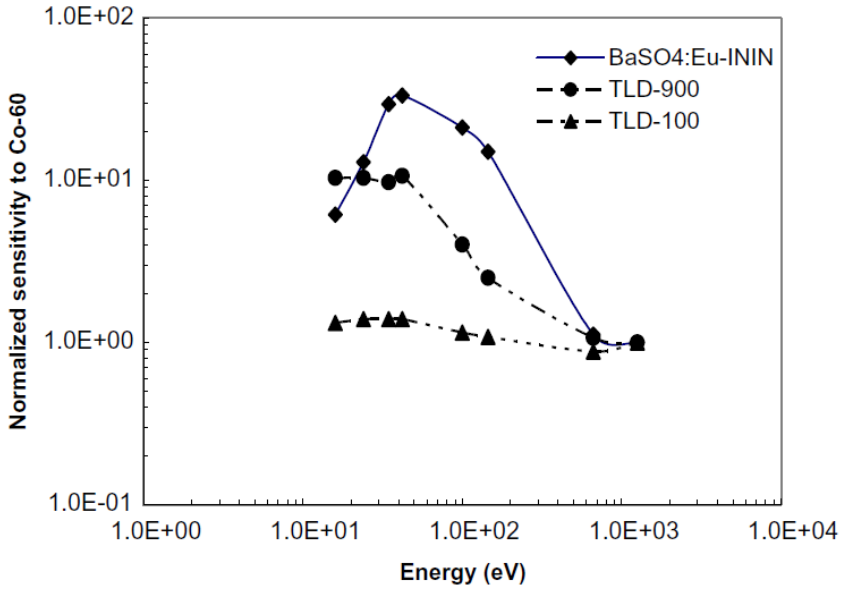

After: González *et al*., 2007.

The photon energy dependence factor of $BaSO_4$:Eu at 52 keV as compared to that of Co^{60} gamma ray energy was about 52; the corresponding factor for $CaSO_4$:Dy Teflon disks at 32 keV was about 9. Figure 39 explains that the photon energy dependence for all the barium sulphate phosphors i.e., $BaSO_4$:Eu Teflon disks, $BaSO_4$:Eu (0.5 mol%) and $BaSO_4$:Eu,P (0.2, 0.5 mol%) is same as compared to $CaSO_4$:Dy Teflon disks (BHATT et al., 1997). High TL sensitivity of $BaSO_4$:Eu could be exploited for environmental monitoring applications by using suitable combinations of filters in order to make its response energy independent in the range 0.3-3MeV. Similar pattern of energy dependence has been described for $BaSO_4$:Eu compared with TLD-900 and TLD-100 as shown in Figure 40 (GONZÁLEZ et al., 2007).

4.2.4 Emission Spectra and TL Glow curve of Different Dopant Ions

4.2.4.1 Emission Spectra

Figure 41 and Figure 42 present, 2D and 3D respectively, the TL emission spectra of samples of $BaSO_4$:Eu (2 mol%) irradiated with gamma radiation of ^{60}Co with absorbed dose of 1kGy. The results show an emission in the region of 337-417 nm with the peak at 375 nm. This emission is attributed to the electronic transition $^6P_{7/12} \rightarrow {}^6S_{7/2}$ which is in excellent agreement with Atone (et al. 1993). Yamashita el al (1985) suggested that in the Eu^{2+} ions the emission bands and their excitation

bands are ascribed to the electronic $4f^6$ ▪$5d \leftrightarrow 4f^7$ transitions. This divalent state of Eu possesses emission around 375nm. PATLE et al., (2015) have also described that the photoluminescence emission spectra of $BaSO_4$:Eu (0.1mol%) samples, prepared by precipitation method using thiourea annealing at 1100°C, has been observed around 376nm corresponding from the lowest band of $4f^65d^1$ configuration to $^8S_{7/2}$ state of $4f^7$ configuration of Eu^{2+} ion.

Figure 41 – TL emission spectra of $BaSO_4$:Eu (2mol%) irradiated with gamma radiation of ^{60}Co with absorbed dose of 1kGy

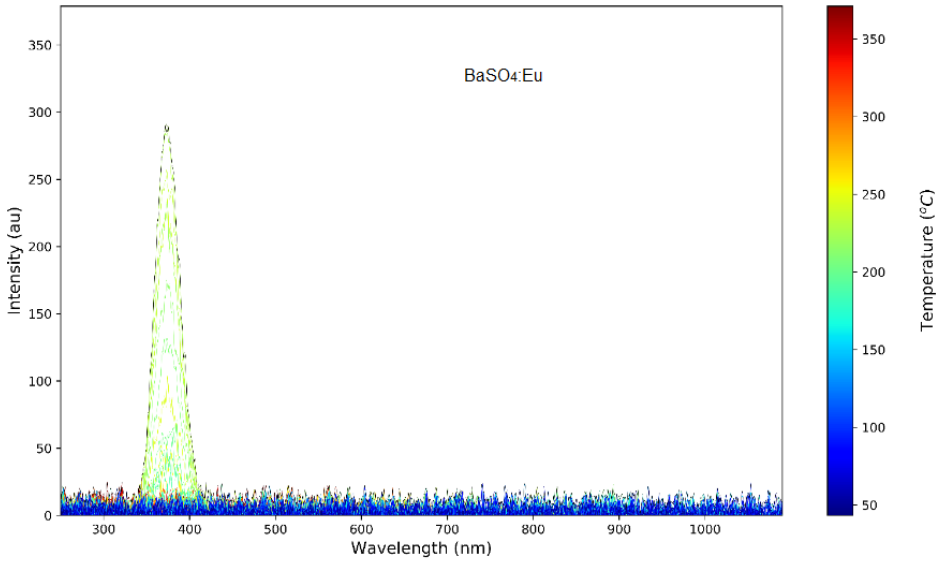

Figure 42 – A three dimensional view of TL emission spectra of $BaSO_4$:Eu (2mol%) irradiated with gamma radiation of ^{60}Co with absorbed dose of 1kGy

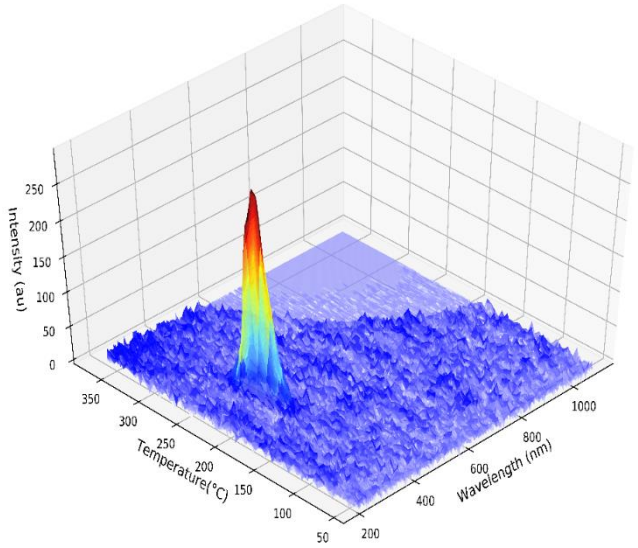

Figure 43 shows the TL emission spectra of samples of $BaSO_4$:Ce (2mol%) irradiated with gamma radiation of ^{60}Co with absorbed dose of 1kGy. The results

show that for the samples doped with Ce (2mol%) there is no emission in the visible luminescent region.

Figure 43 – TL emission spectra of $BaSO_4$:Ce (2mol%) irradiated with gamma radiation of ^{60}Co with absorbed dose of 1kGy

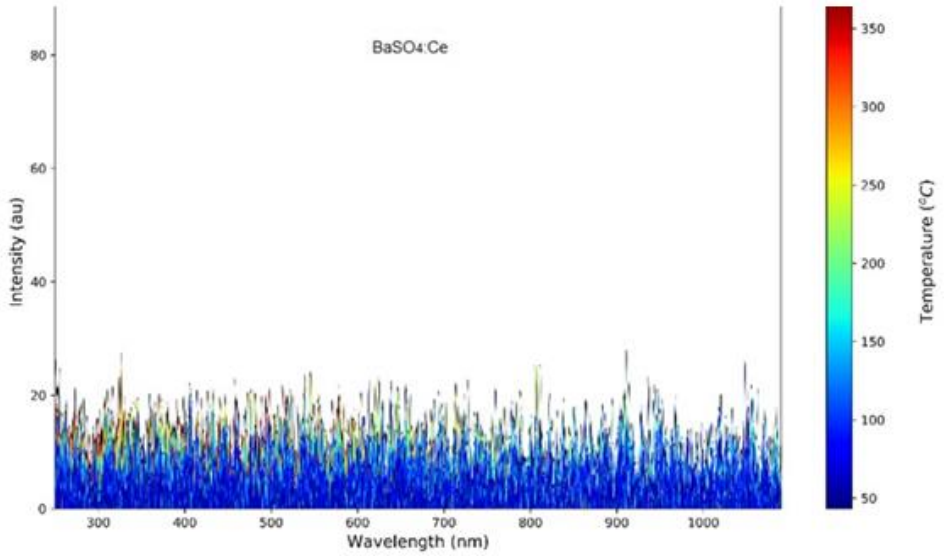

Figure 44 shows the TL emission spectra of samples of $BaSO_4$:Dy (2mol%) irradiated with gamma radiation of ^{60}Co with absorbed dose of 1kGy. The results show low peaks in the region of 460-480 nm. Yamashita et al., 1968, found emission lines of $CaSO_4$:Dy at 478 and 571nm, which can be associated with $^4F_{9/2} \rightarrow {}^6H_{15/2}$ and $^4F_{9/2} \rightarrow {}^6H_{13/2}$ optical transitions in the Dy^{3+} ion due to electron rearrangement in the incomplete 4f shell. The 571nm peak was not observed in our results.

Figure 45 shows the TL emission spectra of samples of $BaSO_4$:Tm (2mol%) irradiated with gamma radiation of ^{60}Co with absorbed dose of 1kGy. Thulium ion has shown luminescent emission peaks at 356 nm ($^1D_2 \rightarrow {}^3H_6$), 455 nm ($^3P_0 \rightarrow {}^3H_4$), 482 nm ($^1G_4 \rightarrow {}^3H_6$), 650 nm ($^1G_4 \rightarrow {}^3H_4$) and 799 nm ($^3F_4 \rightarrow {}^3H_6$) respectively. The spectral lines are very narrow because these electronic transitions are highly shielded from electric field generated by the lattice. These peaks are in accordance with the electronic transitions within the observed energy levels of divalent thulium rare-earth ion (Tm^{2+}) provided by Dieke and Crosswhite (1963). The same TL emission peaks have already been confirmed for CaF_2:Tm by Vilaithong, et al., (2002) and Vasconcelos et al., (2016).

Figure 44 – TL emission spectra of BaSO4:Dy (2mol%) irradiated with gamma radiation of ^{60}Co with absorbed dose of 1kGy.

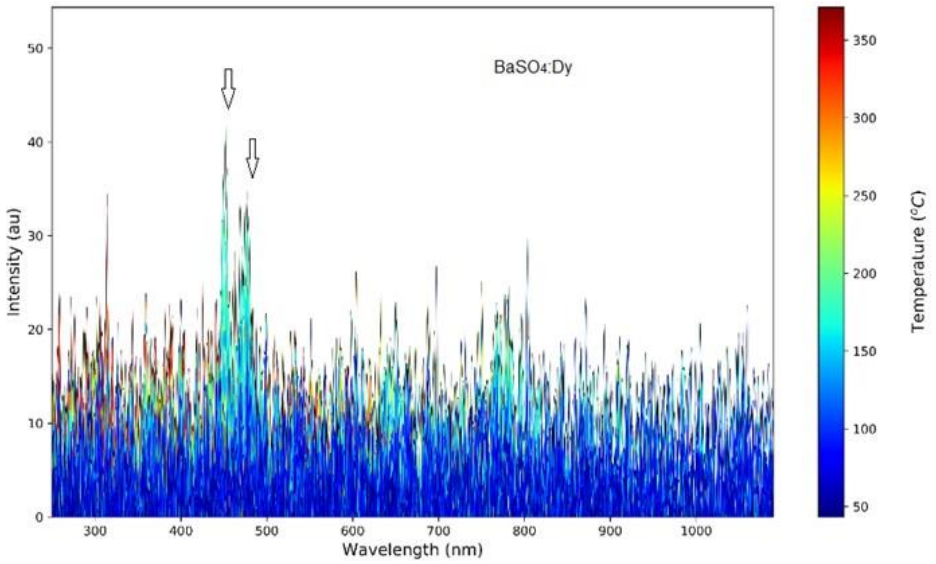

Figure 45 – TL emission spectra of $BaSO_4$:Tm (2mol%) irradiated with gamma radiation of ^{60}Co with absorbed dose of 1kGy

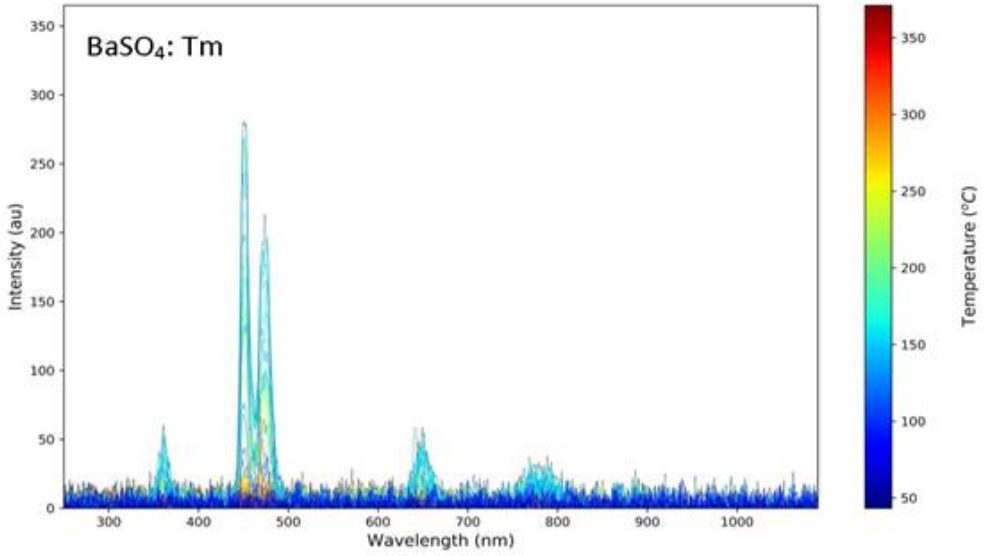

Figure 46 shows the TL emission spectra of samples of $BaSO_4$:Pr (2mol%) irradiated with gamma radiation of ^{60}Co with absorbed dose of 1kGy. The results show a luminescent emission in the region of 600 nm, outside the range of the sensitivity of the photomultiplier tube used to measure TL and OSL curves.

Figure 46 – TL emission spectra of $BaSO_4$:Pr (2mol%) irradiated with gamma radiation of ^{60}Co with absorbed dose of 1kGy

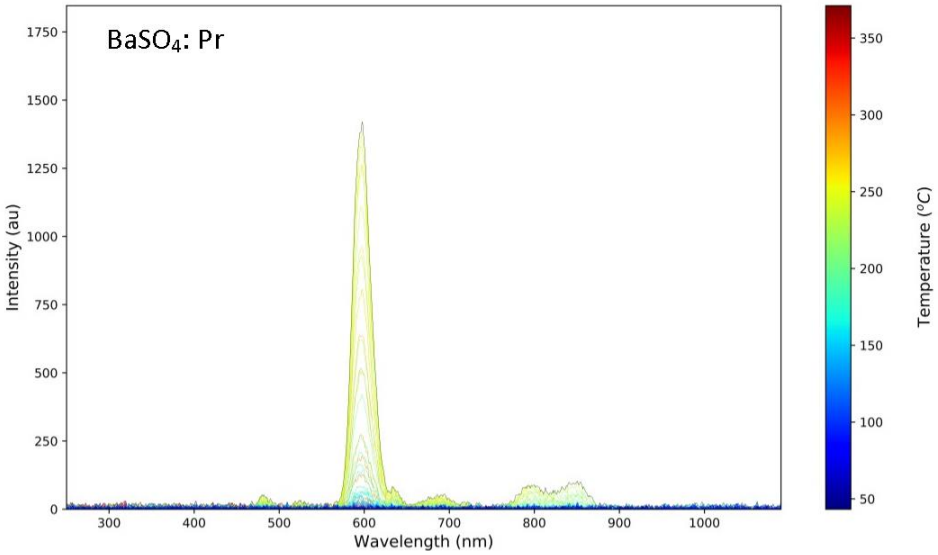

4.2.4.2 TL Glow curves with different dopants

Figure 47 shows the TL glow curves of the $BaSO_4$ pellets prepared with all the selected dopant ions (i.e., Ce, Pr, Tm, Dy and Eu) with the concentration of 0.02mol% and thermally treated at 500°C/4h+1100°C/30min. The samples were irradiated at 100mGy of ^{137}Cs gamma source. The TL intensity of $BaSO_4$:Eu was divided by 20 to fit in the same plot along with the other dopant ions. The results show that the highest response is obtained with $BaSO_4$:Eu (0.02mol%). The samples of $BaSO_4$:Ce (0.02mol%) did not show a TL peak which is expected because it was not observed an emission spectrum. The pellets prepared with Dy, Tm and Pr present two TL peaks, being one in the region of 100°C and the other in the region of 200°C. $BaSO_4$:Pr presents low sensitivity because its emission spectra lied outside the range of the photomultiplier tube.

4.2.5 TL dose response of $BaSO_4$:Dy and $BaSO_4$:Tm

In Figure 47, among all the selected rare earth dopant ions, Dy and Tm ions have also given a reasonable luminescent response under the same synthesis conditions, therefore, so we studied their TL response for high doses.

Figure 47 – TL glow curve of $BaSO_4$:RE (RE: Ce, Pr, Tm, Dy, Eu) sample pellets with 0.02mol% concentration, thermally treated at 500°C/4h+1100°C/30min and irradiated at 100 mGy of ^{137}Cs γ-source

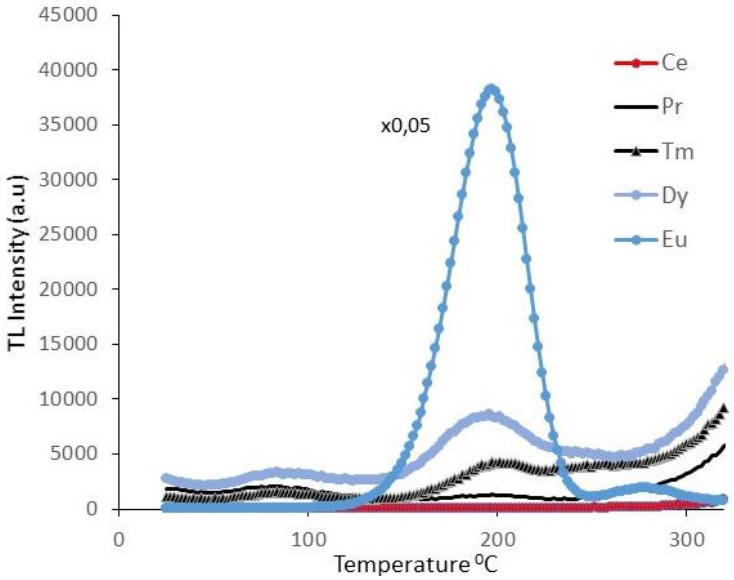

In order to observe the effect of high doses on the TL response of the sample pellets of $BaSO_4$:Dy and $BaSO_4$:Tm with concentration 0.02mol%, thermally treated at 500°C/4h+1100°C/30 min; have been irradiated at high doses 0.5-8Gy from gamma source of Co^{60}. The TL response for Dy and Tm were not too intense compared with Eu so we have not used any filter for them and the results of TL response (without filter) for $BaSO_4$:Dy and $BaSO_4$:Tm are shown in Figure 48(a) and Figure 50(a) respectively. Meanwhile, for quantitative analysis, calibration curves for $BaSO_4$:Dy and $BaSO_4$:Tm are shown in Figure 48(b) and Figure 50(b), respectively.

The qualitative TL response of $BaSO_4$:Dy shown in Figure 48(a) without using any filter. The glow curve of $BaSO_4$:Dy represents the peak shape and peak position of the TL response of $BaSO_4$:Dy. Figure 48(b) explains that TL response of $BaSO_4$:Dy keeps on increasing against irradiation gamma doses with a gradual pattern until 5Gy but there is saturation after 5Gy. With the use of filter, the TL response of $BaSO_4$:Dy could have been measured at high doses of Co^{60}.

Figure 48 – TL Dose response (without filter) of $BaSO_4$:Dy (0.02mol%), thermally treated at 500C°/4h+1100°C/30min, irradiated with different doses of Co^{60} gamma source

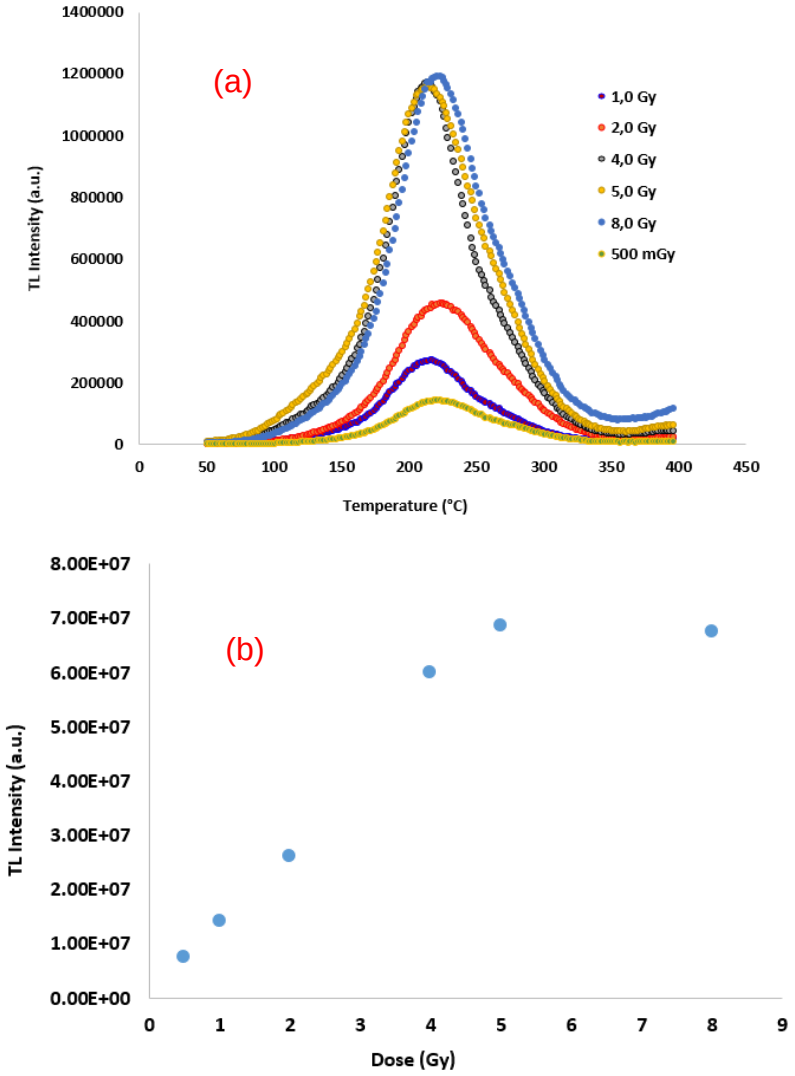

Figure 49 – a) Typical TL glow curve of $BaSO_4$:Dy at 300K irradiated with 1Gy of Co^{60} γ–source. b) Thermoluminescence response of $BaSO_4$:Dy as a function of Co^{60} γ–radiation dose (After: AZORIN; RUBIO 1994)

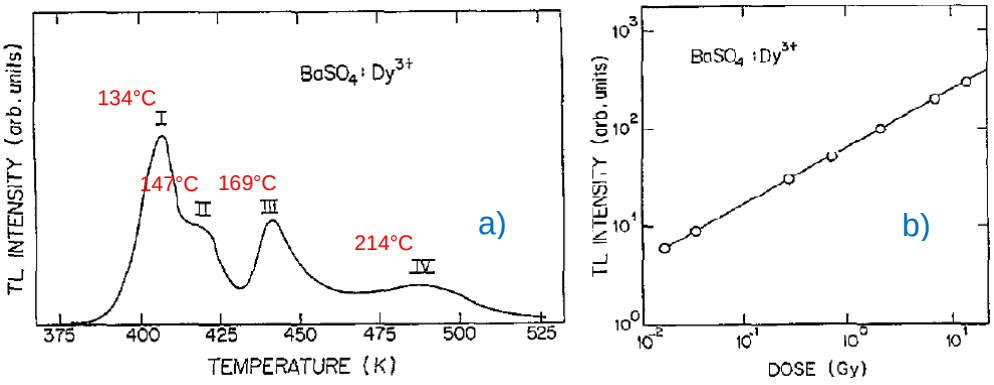

This result is consistent with TL results of $BaSO_4$:Dy^{3+} prepared by solution-evaporation growth technique as shown in Figure 49 (AZORIN; RUBIO 1994). They

claimed that a high gamma ray dose up to 10Gy did not reveal any significant change in the shape of the glow curve except a nominal increase in the overall intensity. The TL peaks for $BaSO_4$:Dy were 407, 420, 442 and 487K (i.e., 134, 147, 169 and 214°C respectively). The absorption due to radiation induced trapped hole centers (SO_4^-, SO_3^-, O^-) were found to be responsible for the multiple TL glow peaks for the $BaSO_4$:Dy phosphor. One may also see the TL glow peaks at 110°C and 185°C for $BaSO_4$:Dy produced by chemical co-precipitation method, annealed at 873K/1h and irradiated at 300Gy of gamma rays (DEVI; SINGH 2012).

The qualitative TL response of $BaSO_4$:Tm shown in Figure 50(a) without using any filter. The glow curve of $BaSO_4$:Tm represents the peak shape and peak position of the TL response of $BaSO_4$:Tm. Figure 50(b) explains that there is a linear behavior of TL response against gamma dose from 0.5Gy to 2Gy but there is another linear behavior of TL response seen from 5Gy to 8Gy. With the use of filter, the TL response of $BaSO_4$:Tm could have been measured at high doses of Co^{60}.

Figure 50 – TL Dose response (without filter) of $BaSO_4$:Tm (0.02mol%), thermally treated at 500°C/4h+1100°C/30min, irradiated with different doses of Co^{60} gamma source

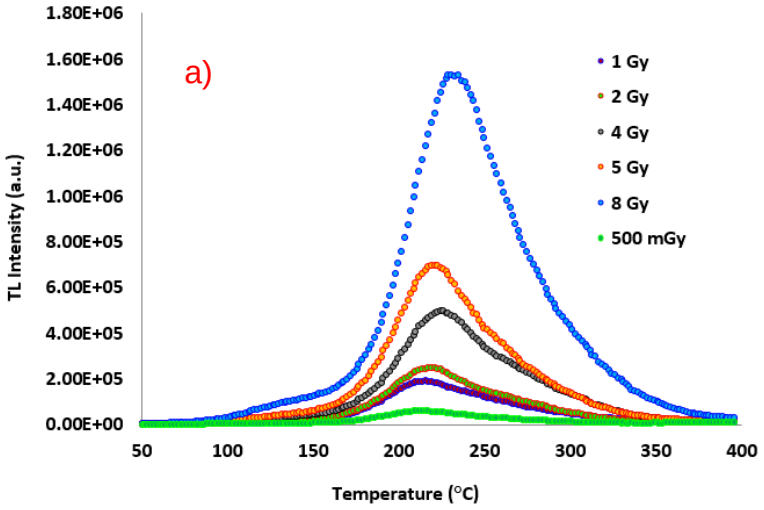

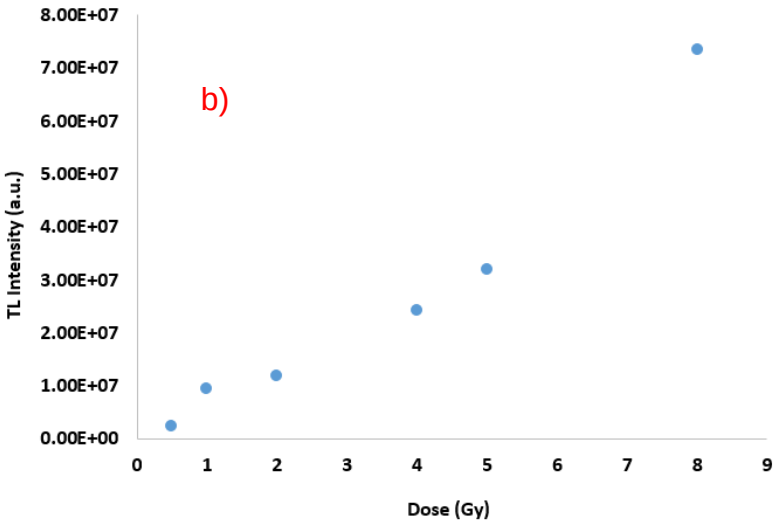

4.3 OSL CHARACTERIZATION

4.3.1 BSL emission of $BaSO_4$:Eu

Figure 51 shows the CW-OSL response of the pellets of $BaSO_4$ undoped and doped with Eu (0.02mol%), stimulated with blue light and irradiated at an absorbed dose of 100 mGy from $^{90}Sr/^{90}Y$ β-source. $BaSO_4$:Eu showed an OSL response for stimulation with blue light.

Using the R package luminescence (KREUTZER et al., 2012), the CW-OSL curve was deconvoluted in three components and the pseudo LM-OSL was obtained considering four components. Both curves are shown in Figure 52 and Figure 53 respectively. The fourth component corresponds to the contribution of the background. The values of decay constant of the luminescence “b” and the initial concentration of trapped electrons “n_0” are given in Table 7.

Figure 51 – BSL curve for $BaSO_4$ undoped and doped with Eu (0.02mol%) thermally treated at 500°C/4h+1100°C/30min, irradiated at 100 mGy of $^{90}Sr/^{90}Y$ β-source

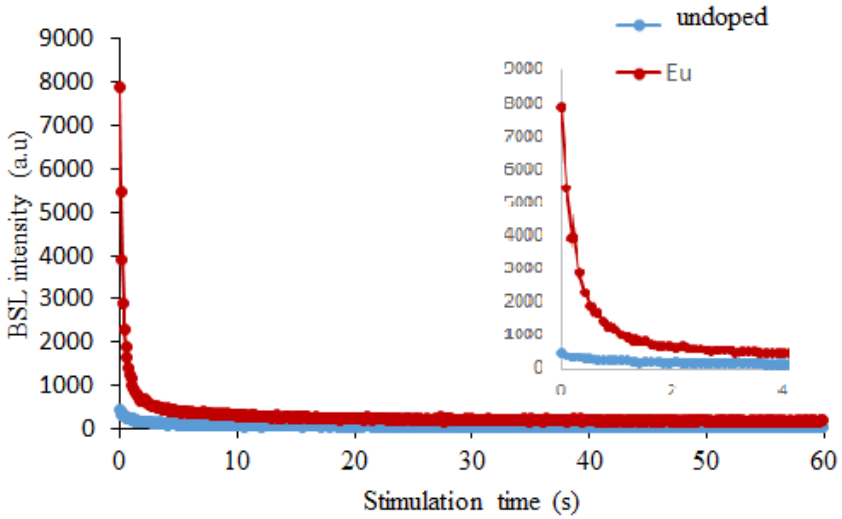

Figure 52 – BSL curve of $BaSO_4$:Eu (0.02 mol%) thermally treated at 500°C/4h+1100°C/30min and irradiated at 100mGy of $^{90}Sr/^{90}Y$ β-source, is deconvoluted into its three individual components as deduced by curve fitting

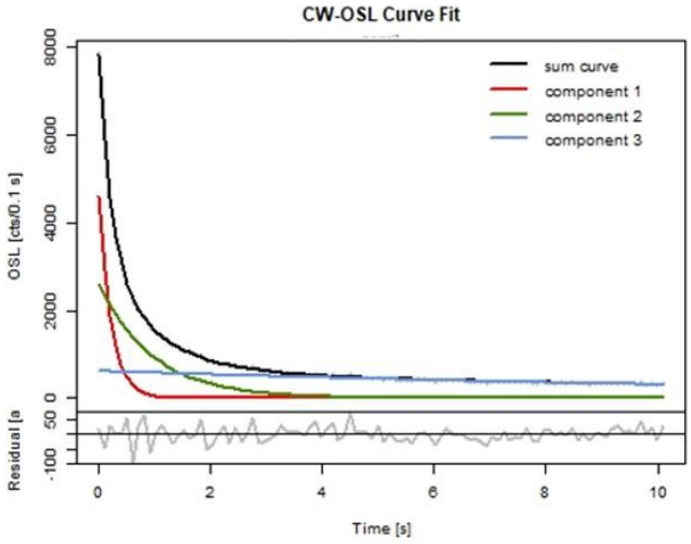

Figure 53 – Pseudo LM-OSL curves for Blue-OSL of $BaSO_4$:Eu (0.02 mol%) pellets irradiated with 100mGy of $^{90}Sr/^{90}Y$ β-source

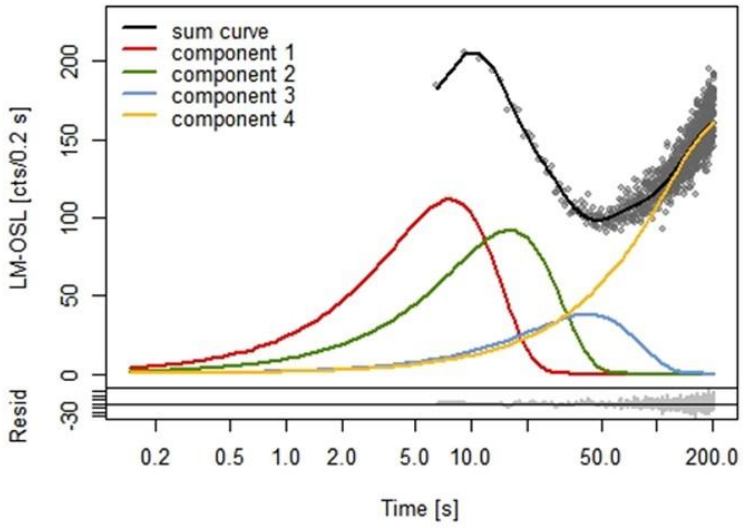

Table 7 – Pseudo-LM OSL corresponding values for b and n_0

Component	**b value**	**n_0 value**
Component 1	3.50×10^{0}	1.40×10^{3}
Component 2	7.96×10^{-1}	2.42×10^{3}
Component 3	1.14×10^{-1}	2.65×10^{3}
Component 4	3.97×10^{-3}	6.08×10^{4}

Source: Bulur, 2000.

These results are similar to that of obtained by Bhatt et al., (2014) for commercial pellets of $BaSO_4$:Eu as shown in Figure 54. These components were further confirmed and quantified by nonlinearly modulated optically stimulated luminescence measurements (BHATT et al., 2014).

PATLE et al., 2015 observed the CW-OSL for intense blue stimulated luminescence in $BaSO_4$:Eu sample. They found OSL curve of $BaSO_4$:Eu faster and 11% more sensitive than Al_2O_3:C under identical conditions as shown in Figure 55(i). For BSL of $BaSO_4$:Eu sample, a linear dose response was found in dose range of 10mGy to 1Gy from $^{90}Sr/^{90}Y$ beta source having dose rate of 20 mGy/min as shown in Figure 55(ii).

Figure 54 – LM-OSL curve of $BaSO_4:Eu^{2+}$ de-convolved into its three individual components, a background signal and a phosphorescence component. Open circles experimental points and solid lines the fit and each individual LM-OSL component

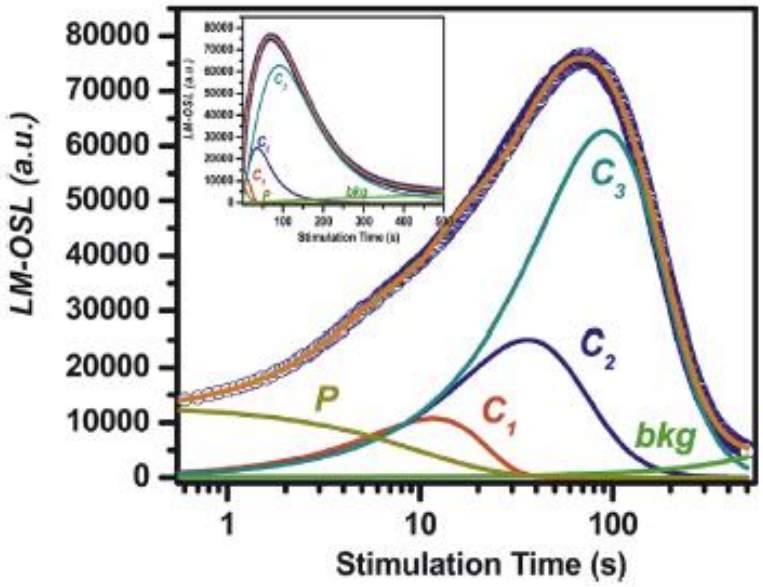

Source: Bhatt *et al*., 2014.

Figure 55 – (i) CW-OSL of a) $BaSO_4:Eu$ and b) $Al_2O_3:C$ for blue (470nm) light stimulation for a test dose of 100mGy from $^{90}Sr/^{90}Y$ β-source with dose rate 20mGy/min. Inset showing normalized OSL curve. (ii) Dose response of $BaSO_4:Eu$ samples for irradiation doses 10mGy-1Gy from $^{90}Sr/^{90}Y$ beta source

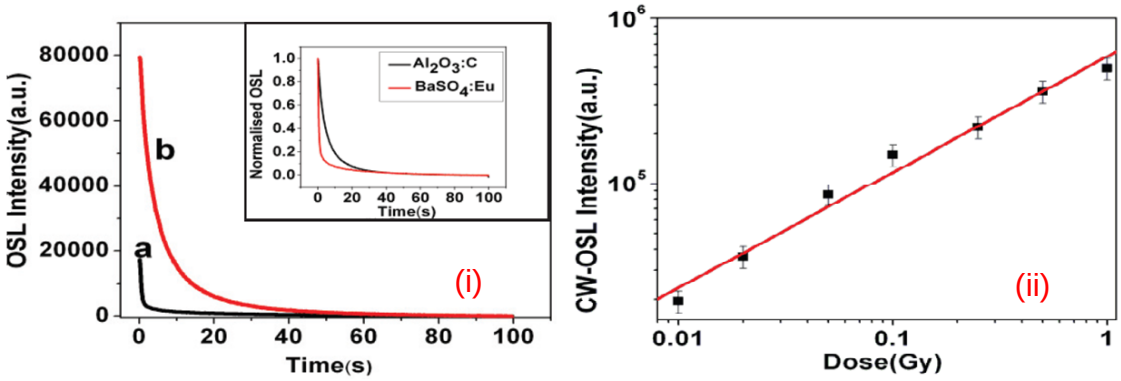

After: Patle *et al*., 2015.

4.3.2 IRSL emission of $BaSO_4:Eu$

Figure 56 shows the IRSL response of pellets of $BaSO_4$ undoped and doped with Eu (0.02 mol%), stimulated with IR light and irradiated at an absorbed dose of 100 mGy from $^{90}Sr/^{90}Y$ β-source. It can be observed that the IRSL response of doped $BaSO_4:Eu$ is similar to that of the IRSL response of undoped pellet, indicating if $BaSO_4:Eu$ is not stimulated by infrared (IR) light.

Figure 56 – IRSL curve for $BaSO_4$ undoped and doped with Eu (0.02 mol%), thermally treated at 500°C/4h+1100°C/30min and irradiated at 100 mGy of $^{90}Sr/^{90}Y$ β-source

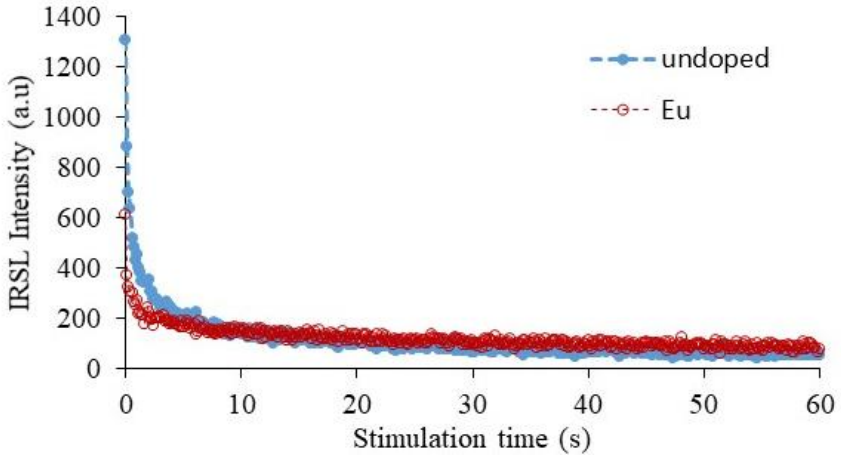

4.3.3 BSL Dose-Response of $BaSO_4$:Eu

In order to observe the effect of different doses on the BSL response, the sample pellets made of $BaSO_4$:Eu (0.02 mol%), thermally treated at 500°C/4h+1100°C/30 min, have been irradiated at doses 2-60 mGy from Cs^{137} γ–source as shown in Figure 57.

Figure 57 – BSL response of $BaSO_4$:Eu (0.02 mol%) thermally treated at 500°C/4h+1100°C/30 min, irradiated at low doses of Cs^{137} γ-source

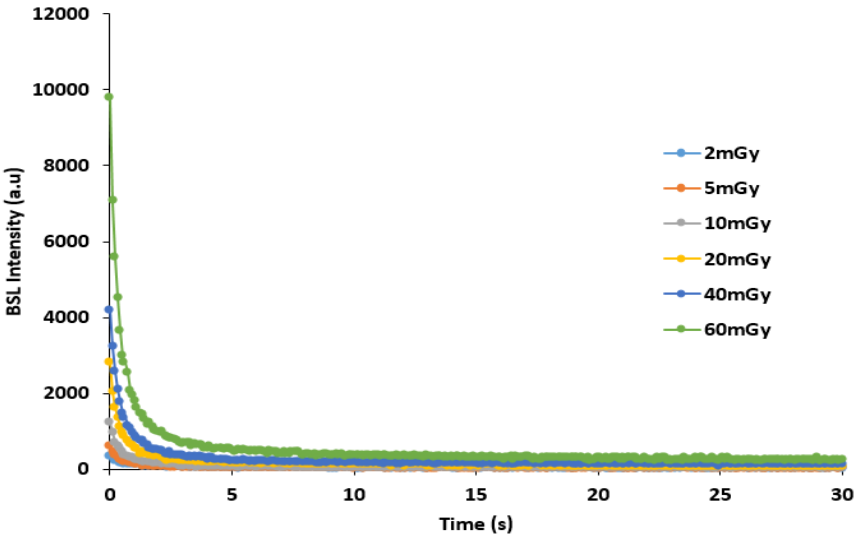

Figure 58 present the calibration curve for the BSL signals of the pellets of $BaSO_4$:Eu (0.02 mol%) irradiated with different gamma radiation doses of ^{137}Cs. The area of the BSL curve was calculated and subtracted from the BG in the region 0 to 60s. The results obtained are shown in Figure 58 as function of the absorbed dose of gamma radiation of ^{137}Cs.

The angular coefficient (*a*) and the regression coefficient (R^2) of the linear fit are shown in Figure. The results show a linear BSL response of the phosphor with the absorbed dose in the range investigated. This linear response shows that the phosphor can act as a good dosimeter for radiation dosimetry applications (BHATT et al., 2014; PATLE et al., 2015).

The low detection limit (LDL) was calculated taking into account the value of the BSL response of the pellet unirradiated plus three times the value of standard deviation which is 16.6 ± 4.6 (a.u.). Considering the BSL calibration curve shown in Figure 58, the LDL value was equal to 0.6 mGy. Notice that this LDL value, of $BaSO_4$:Eu for OSL study, is higher than we have earlier Figured out for TL response of the same phosphor.

Figure 58 – BSL Dose response for $BaSO_4$:Eu (0.02mol%) thermally treated at 500°C/4h + 1100°C/30min and irradiated at different radiation doses from ^{137}Cs γ-source

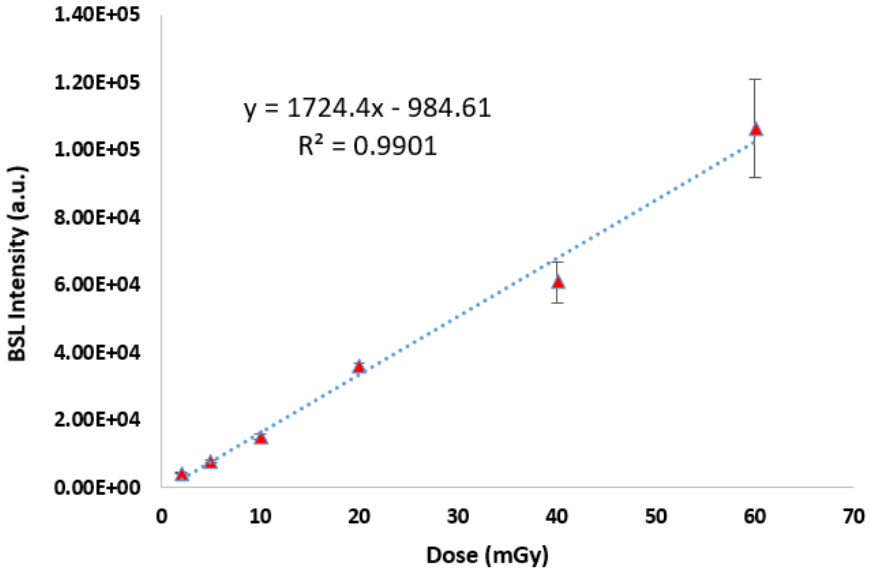

4.3.4 Residual TL after BSL for $BaSO_4$:Eu

In order to observe the effect of high doses on the TL residual after BSL response, the TL and as well as residual TL after BSL for $BaSO_4$:Eu (0.02 mol%) was measured at 100 mGy from ^{90}Sr/^{90}Y β-source and is shown in Figure 59. In $BaSO_4$:Eu (0.02 mol%), still shows a small or almost no significant difference between TL and residual TL after BSL, suggesting that traps responsible for OSL signal are different to those of responsible for the TL signal.

Figure 59 – TL glow curves for $BaSO_4$:Eu (0.02mol%) irradiated at 100 mGy of $^{90}Sr/^{90}Y$ β-source, after and before BSL measurement

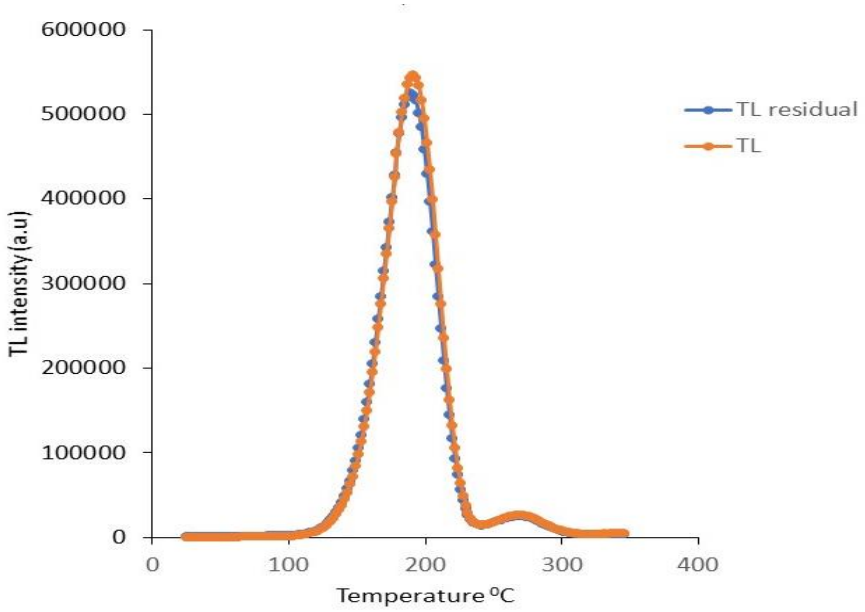

The saturation problem was handled by using a filter as we have done in section 4.2.3 and is presented in Figure 36. Now let us check the effect of high doses i.e., 0.5-4 Gy from Co^{60} γ-source.

The comparison results of TL and residual TL after BSL for the pellets of $BaSO_4$:Eu (0.02 mol%) irradiated at 0.5-4 Gy doses from Co^{60} γ-source, are shown in Figure 60, Figure 61 and Figure 62.

It is obvious that at low doses, TL and residual TL after BSL for the pellets of $BaSO_4$:Eu are not showing any significant difference (Figure 59). However, upon increasing the irradiation doses we have found the decreases in the residual TL intensity. The residual TL after BSL intensity at 500 mGy (Figure 60) was yet found to be resistant and then 100 mGy (Figure 59). But a further increase in the absorbed dose until 1 Gy = 1000 mGy (Figure 61) has changed this behavior and residual TL after BSL intensity started decreasing than the TL intensity of $BaSO_4$:Eu (0.02 mol%) under the same conditions. The more absorbed dose i.e., 4Gy, the residual TL after BSL intensity was reduced almost half of the TL intensity (Figure 62).

Figure 60 – TL glow curves for $BaSO_4$:Eu (0.02mol%) irradiated at 500 mGy of Co^{60} γ-source, after and before BSL measurement

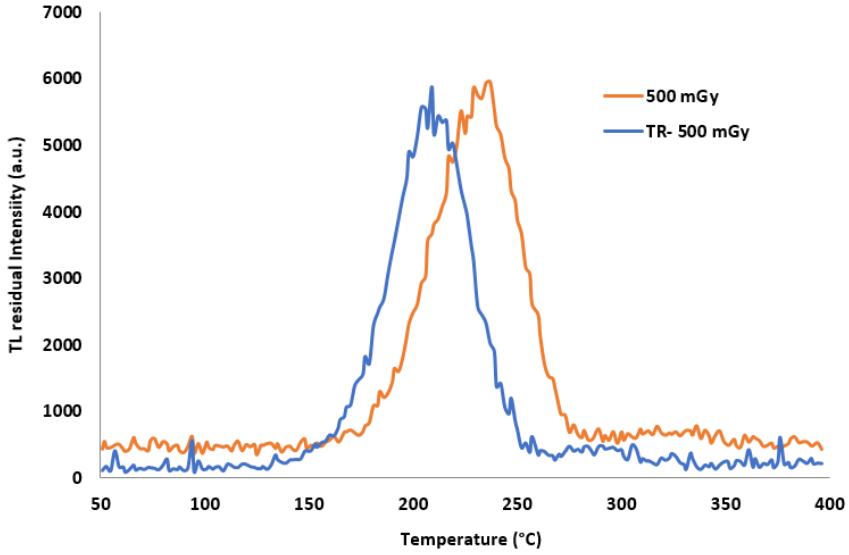

Figure 61 – TL glow curves for $BaSO_4$:Eu (0.02mol%) irradiated at 1 Gy of Co^{60} γ-source, after and before BSL measurement

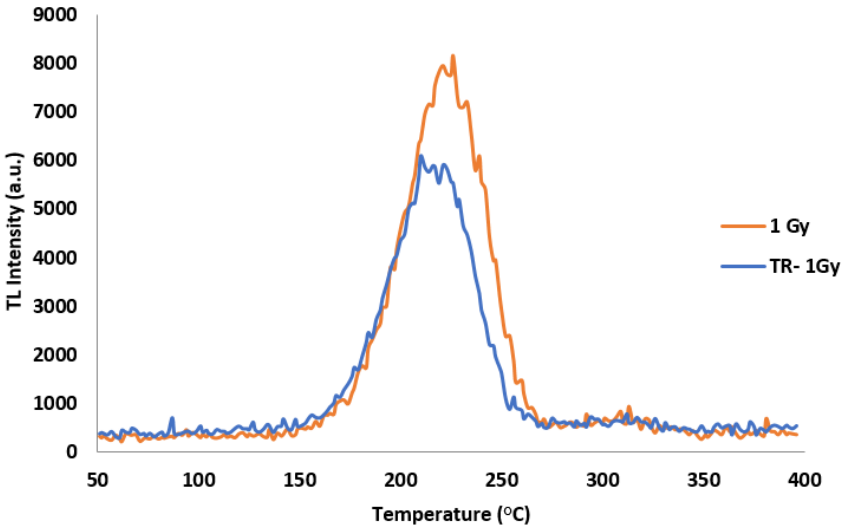

Figure 62 – TL glow curves for $BaSO_4$:Eu (0.02mol%) irradiated at 4 Gy of Co^{60} γ-source, after and before BSL measurement

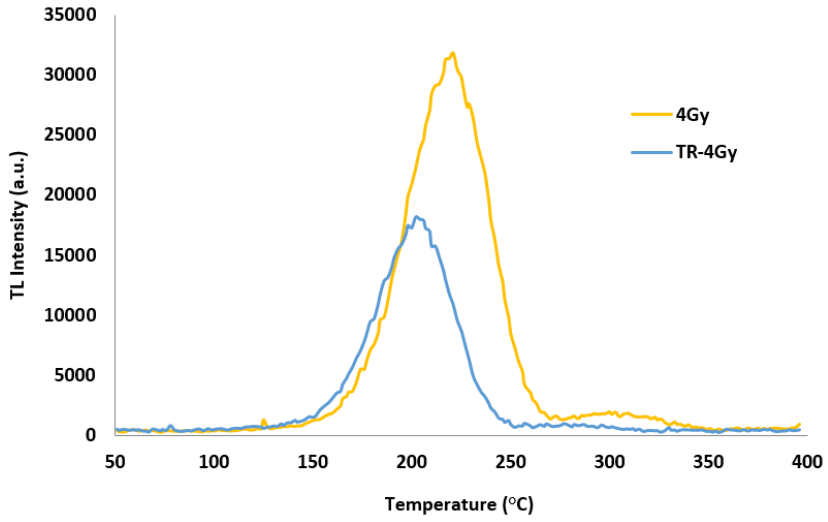

4.3.5 BSL and Residual TL after BSL of $BaSO_4$:Eu (0.02 mol%) versus stimulation time period

Area of the TL curve and OSL curve for the $BaSO_4$:Eu (0.02mol%) sample pellets have been achieved by conventional intensity integration method within the reasonable limits of temperature/time of TL/OSL response respectively, and is plotted jointly to see the variation in TL/OSL response of the selected phosphor material. It is clear from Figure 63 that the stimulation time period has influence on the BSL response of $BaSO_4$:Eu. However, the TL response of $BaSO_4$:Eu (0.02 mol%) seems to be independent from stimulation time period being almost constant and do not vary much in the present study as compared to OSL response under the same synthesis conditions. In first 5 seconds of stimulation time period, the TL response seems to increase but after that it looks like saturation. Contrarily, OSL response seems to have sharp vertical shoot out which is attributed to the fast component of BSL response in first 5 seconds. If we subtract the residual TL after BSL for 5 seconds readout from the total TL, the 186°C and 270°C peaks will be responsible for the fast component. This result is in agreement with BHATT et al., (2014).

Figure 63 – Inter-comparison of BSL and residual TL after BSL response of $BaSO_4$:Eu (0.02ml%) with the help of luminescent response as a function of stimulation time

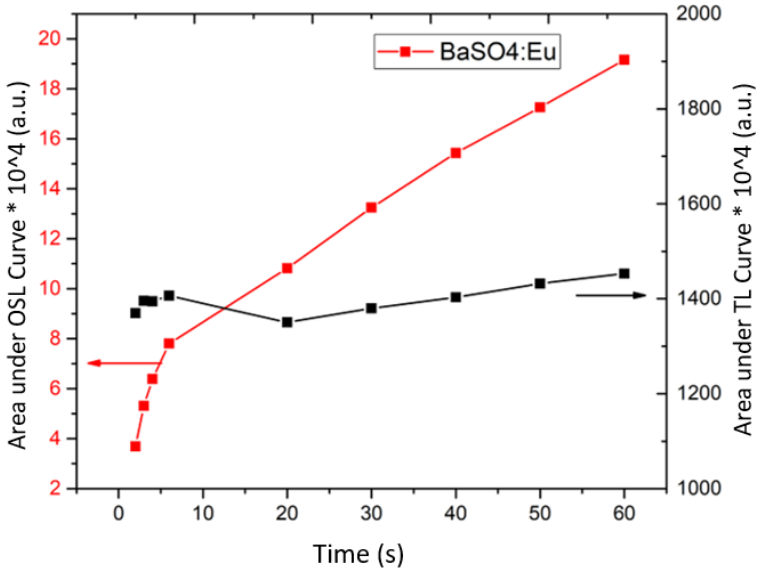

4.3.6 BSL emission of different dopants ions ($BaSO_4$:RE)

BSL response of pellets of $BaSO_4$ doped with different rare earth ions with the concentration of 0.02 mol%, thermally treated at 500°C/4h+1100°C/30min and irradiated with absorbed dose of 100 mGy of $^{90}Sr/^{90}Y$ β-source is shown in Figure 64. The results show that, unlike the TL response, there is no significant difference between the BSL response of pellets of $BaSO_4$ doped with 0.02mol% of selected rare earth ions (i.e., Eu, Dy, Tm, Ce, Pr). Table 8 shows the percentage variation of the BSL response of pellets in relation to the BSL response of Eu. Samples doped with Dy and Tm with 0.02 mol% present, respectively, a BSL response of 63.3% and 54.5% of BSL response compared with Eu. The results suggest that these three types of dopants can be used to obtain BSL dosimeters.

Table 8 – Variation of BSL intensity of selected dopant ions compared with that of Eu

Selected Dopant	BSL signal (a.u.)	Variation of BSL response of selected dopant ions as compared to that of Eu
Eu	1.22×10^5	100.00 %
Dy	7.69×10^4	63.20 %
Tm	6.63×10^4	54.50 %
Ce	1.95×10^4	16.00 %
Pr	9.26×10^4	7.60 %

The samples doped with Ce presents a small BSL signal for the absorbed dose of 100mGy. Future investigations are recommended to evaluate its BSL response for high doses. There is no BSL response for the pellets doped with Pr (0.02mol%) under identical conditions.

Figure 64 – BSL response of pellets of $BaSO_4$:RE (RE: Eu, Dy, Tm, Ce, Pr) with 0.02mol% irradiated at 100 mGy from $^{90}Sr/^{90}Y$ β-source

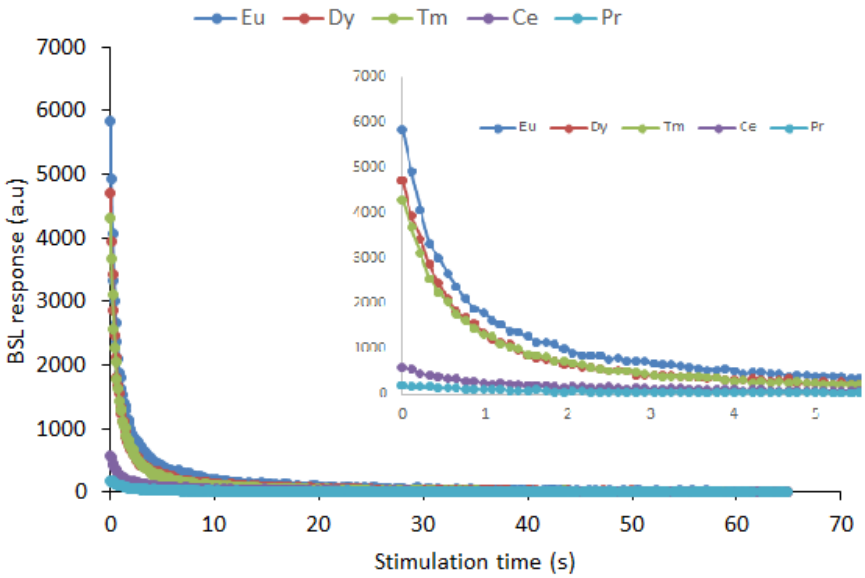

4.3.7 IRSL emission of different dopant ions ($BaSO_4$:RE)

Figure 65 shows the IRSL response of the pellets of $BaSO_4$ doped with different rare earth ions with the concentration of 0.02 mol% and irradiated with absorbed dose of 100 mGy of $^{90}Sr/^{90}Y$ β-source. The results show that all the pellets investigated, do not present any significant IRSL response.

Figure 65 – IRSL response of pellets of $BaSO_4$:RE (RE: Eu, Ce, Pr, Tm, Dy) with 0.02mol% irradiated at 100 mGy of $^{90}Sr/^{90}Y$ β-source

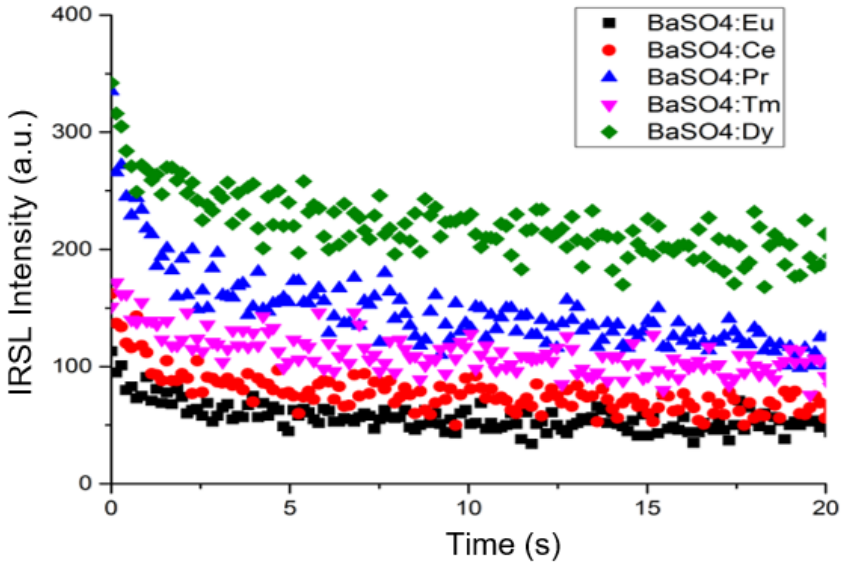

4.3.8 BSL dose response of $BaSO_4$:RE

Since three of the selected dopant ions i.e., Eu, Dy and Tm have shown good BSL response earlier, therefore we decided to see their response for some low doses of gamma radiations from ^{137}Cs.

Figure 66 shows the BSL dose response curves obtained with pellets of $BaSO_4$ doped with Eu, Dy and Tm (0.02mol% each) irradiated with radiation doses between 2-60 mGy from ^{137}Cs γ-source. The equation of the fitting curves and the R^2 values are also presented in the Figure. The results indicate a linear response of the three phosphors and therefore they can act as a good dosimeter for radiation dosimetry applications. For personal dosimetry and medical applications, it is necessary to evaluate their response at high doses.

Figure 66 – BSL dose response for $BaSO_4$ phosphor doped with Eu, Dy and Tm (0.02mol%) and irradiated with different doses from ^{137}Cs γ-source

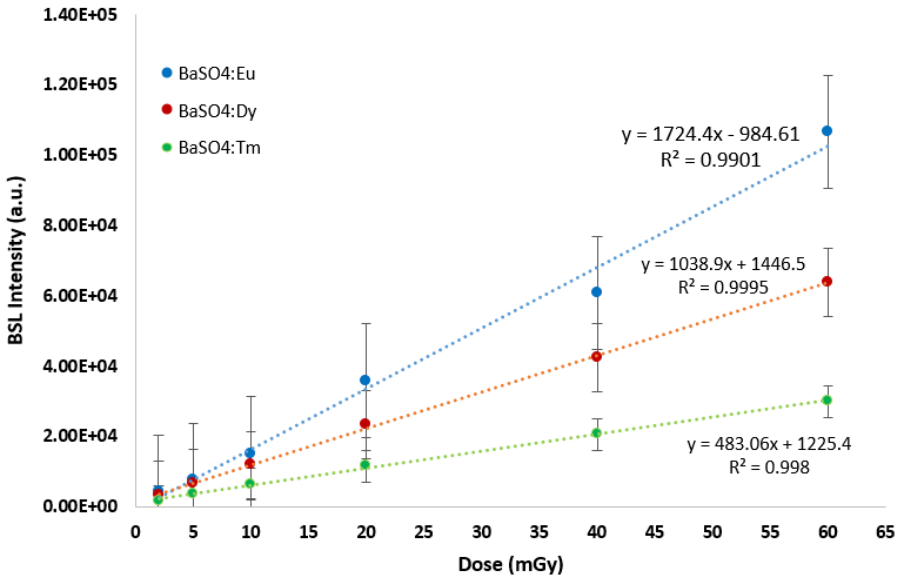

4.3.9 Residual TL after BSL of $BaSO_4$:Dy and $BaSO_4$:Tm

The residual TL after BSL response of the sample pellets of $BaSO_4$:Dy (0.02mol%) and $BaSO_4$:Tm (0.02mol%) irradiated at 100 mGy from $^{90}Sr/^{90}Y$ β-source are presented in Figure 67 and Figure 68 respectively. The TL glow curve measured after and before BSL excitation is presented.

Figure 67 - TL glow curves for $BaSO_4$:Dy (0.02mol%) irradiated at 100 mGy of $^{90}Sr/^{90}Y$ β-source, after and before BSL measurement

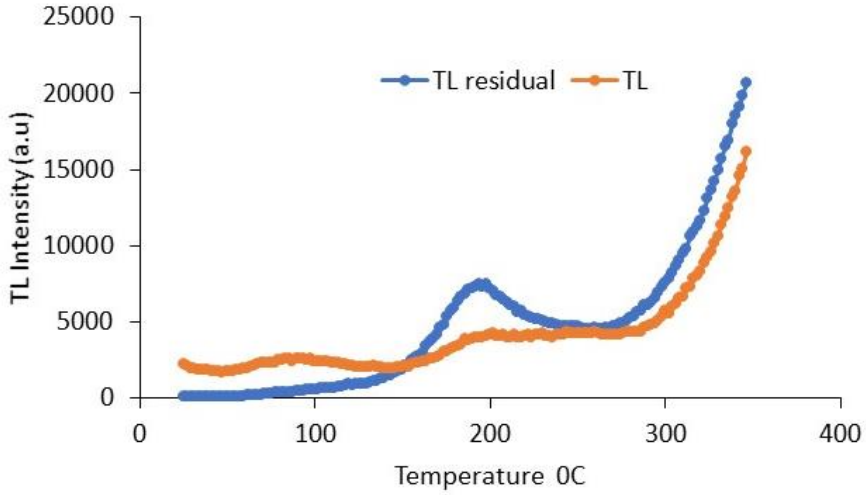

Figure 68 - TL glow curves for $BaSO_4$:Tm (0.02mol%) irradiated at 100 mGy of $^{90}Sr/^{90}Y$ β-source, after and before BSL measurement

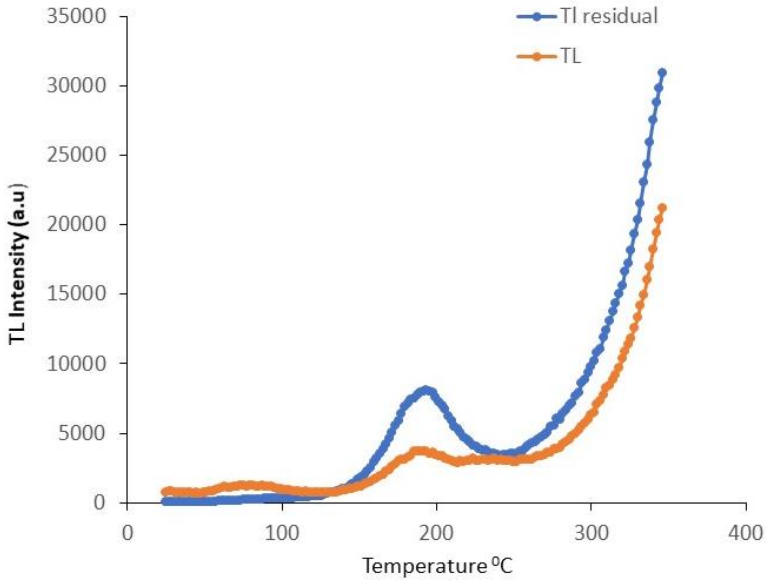

Figure 67 and Figure 68 show that the OSL signal of $BaSO_4$:Dy (0.02mol%) and $BaSO_4$:Tm (0.02mol%) are related to the traps of the TL peak around 100°C, and probably by the excitation with the blue light a phototransfer thermoluminescence (PTTL) phenomenon occurs, contributing to increase the intensity of the TL peak in the region of 200°C. There is no report in the literature so far about this behaviour and more study is needed to try to understand the BSL mechanism in these two types of phosphors.

4.3.10 Effect of the dopant concentration on BSL response

Among our selected dopant ions i.e., Eu, Dy, Tm, Ce and Pr; none of them responded in IRSL study, however, for BSL study Eu, Dy and Tm have been optimized for further study. Therefore, we planned to observe the effect of concentration of the selected three dopant ions on the BSL response. For this purpose, the pellets were irradiated at 100 mGy from $^{90}Sr/^{90}Y$ β-source and the BSL response was recorded in the Lexsyg Smart reader, keeping in mind the already optimized synthesis and characterization conditions described earlier.

The net BSL response for pellets of $BaSO_4$:Eu (0.02mol%) and $BaSO_4$:Eu (0.05mol%) are presented in the Figure 69. The net BSL response for pellets of $BaSO_4$:Dy (0.02mol%) and $BaSO_4$:Dy (0.05mol%) are presented in the Figure 70. The net BSL response for pellets of $BaSO_4$:Tm (0.02mol%) and $BaSO_4$:Tm (0.05mol%) are presented in the Figure 71. The net response corresponds to the BSL response subtracted by the BSL background response.

The results show that for the $BaSO_4$:Eu pellets, it is not observed a significant difference in the BSL response between the selected concentration of 0.02 and 0.05 mol%.

Figure 69 - Net BSL response for pellets of $BaSO_4$:Eu (0.02 and 0.05 mol%) irradiated at 100 mGy from $^{90}Sr/^{90}Y$ β-source

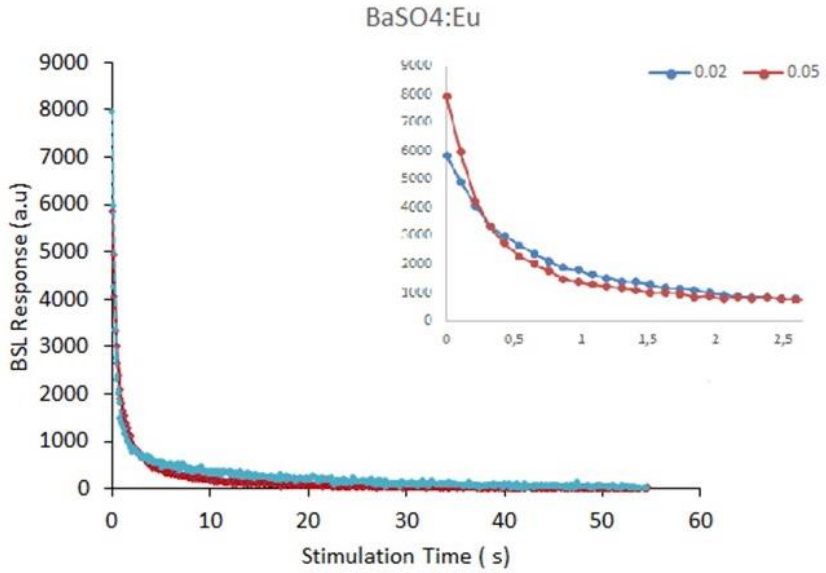

Figure 70 and Figure 71 show that BaSO4:Dy and BaSO4:Tm do not show the BSL response like BaSO4:Eu. Both Dy and Tm show that the BSL response for the pellets prepared with 0.02 mol% present higher BSL response than the pellets

prepared with 0.05 mol%. Hence, $BaSO_4$:Dy and $BaSO_4$:Tm can also be further studied at high doses under the similar synthesis conditions.

Figure 70 - Net BSL response for pellets of $BaSO_4$:Dy (0.02 and 0.05 mol%) irradiated at 100 mGy from $^{90}Sr/^{90}Y$ β-source

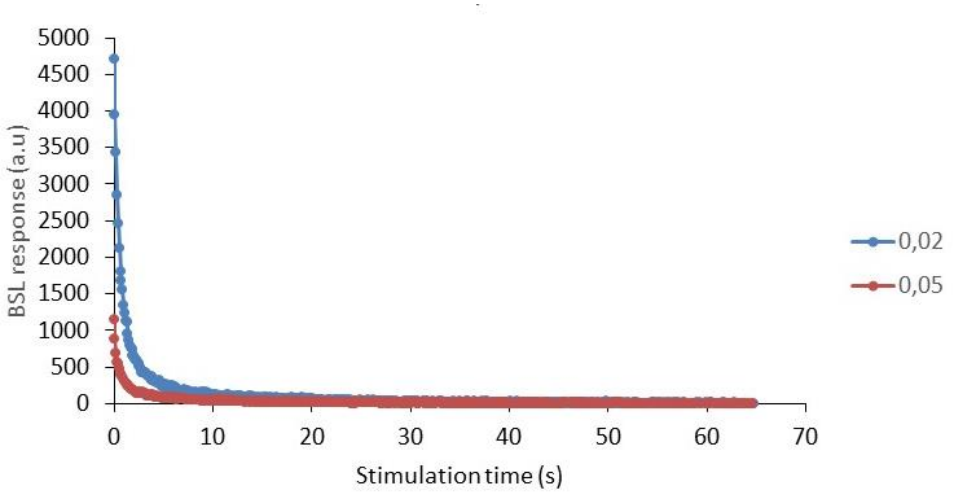

Figure 71 - Net BSL response for pellets of $BaSO_4$:Tm (0.02 and 0.05 mol%) irradiated at 100 mGy from $^{90}Sr/^{90}Y$ β-source

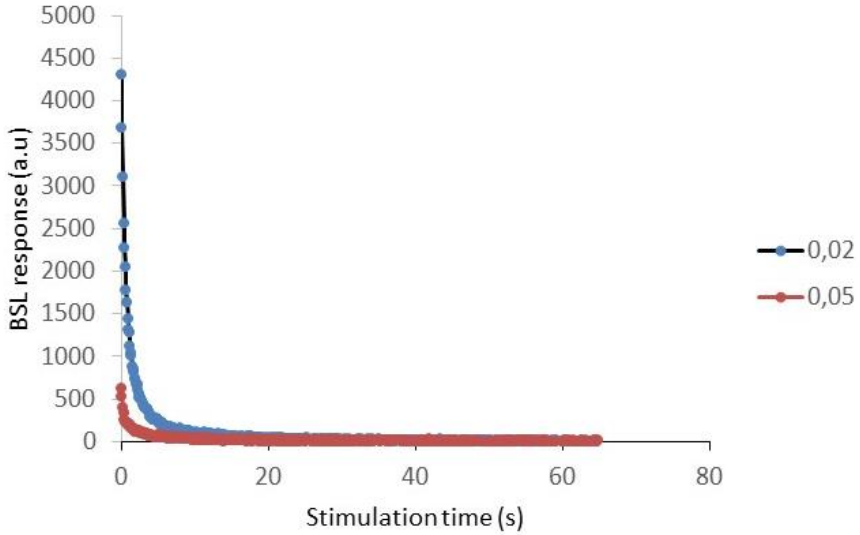

5 CONCLUSION

The results obtained allow us to conclude that the $BaSO_4$:RE synthesized by solid state combustion technique and thermally heated at 500°C for 4h followed by 1100°C for 30 min, present TL and OSL response for the dopants Tm, Eu and Dy. It was not observed any TL or OSL response for the $BaSO_4$ phosphor doped with Ce or Pr in this study.

The highest TL response was observed with the $BaSO_4$:Eu (0.02 mol%) phosphor, that is around 20 times higher than obtained with samples of $BaSO_4$:Dy and $BaSO_4$:Tm at the same concentration.

The difference between TL and residual TL after BSL response of $BaSO_4$:Eu phosphor remained insignificant at low doses but there was a significant difference seen between them at high doses. To explain this behavior more investigations is needed to identify the centers of luminescence. It is important to emphasis that this result is new and it is not found in the literature.

In case of the samples of $BaSO_4$:Dy and $BaSO_4$:Tm, the TL and residual TL after BSL showed that the first peak around 100°C decreased and the peak at high temperature increased. These results indicated a possible occurrence of phenomenon of phototransfer thermoluminescence.

For $BaSO_4$:RE (RE: Eu, Tm, Dy, Ce and Pr) we could not get any IRSL within the similar synthesis conditions.

Although $BaSO_4$:Eu is not a tissue equivalent material, its Low detection Limit for TL response of $BaSO_4$:Eu (0.02mol%), that is 17.9 μGy for gamma radiation of ^{137}Cs, and its linear dose response indicates that it can be used for dosimetry applications.

In the literature there is a few papers discussing the OSL response for $BaSO_4$:RE, so this research contributed with some information about the OSL response of $BaSO_4$ doped with Eu,Tm, Dy, Ce and Pr.

REFERENCES

ABOELEZZ, E.; SHARAF, M.A.; HASSAN, G.M.; EL-KHOUDARY, A. Nano-barium-strotium sulphate as a new thermoluminescent dosimeter. **Journal of Luminescence,** v. 166, p. 156-161, 2015.

AKSELROD, M.S.; KORTOV, V.S.; KRAVETSKY, D.J.; GOTLIB, V.I. Highly sensitive thermo-luminescent anion-defective alpha-Al_2O_3:C single crystal detectors. **Radiation Protection Dosimetry,** v. 32, n. 1, p. 15-20, 1990.

AKSELROD, M.S.; MCKEEVER, S.W.S. A radiation dosimetry method using pulsed optically stimulated luminescence. **Radiation Protection Dosimetry,** v. 81, p. 167-176, 1999.

ANNALAKSHMI, O.; JOSE, M.T.; MADHUSOODANAN, U. Synthesis and characterization of $BaSO_4$:Eu Thermoluminescence phosphor. **Radiation Protection Dosimetry,** v. 150, n. 2, p. 127-133, 2012.

ANTONOV-ROMANOVSKY, V.V.; KEIRUM-MARKUS, I.F.; POROSHINA, M.S.; TRAPEZNIKOVA, Z.A. **Dosimetry of Ionizing Radiation with the Aid of Infrared Sensitive Phosphors.** Conference of the Academy of Sciences of the U.S.S.R. on the Peaceful Uses of Atomic Energy, Moscow, USAEC Report AEC-tr-2435 (Pt. 1), 239–250, 1955.

ATONE, M.S; DHOBLE, S.J.; MOHARIL, S.V.; DHOPTE, S.M.; MUTHAL, P.M.; KONDAWAR, V.K. Luminescence in $BaSO_4$:Eu. **Radiation Effects and Defects in Solids,** v. 127, p. 225-230, 1993.

AZORIN, J.; GUTIÉRREZ, A.; GONZÁLEZ, A. **Tech. Rep. IA-89-07 ININ** (Mexico) (1989).

AZORIN, N.J.; RUBIO, J.O. Optical absorption and Thermoluminescence of Dy^{3+} doped BaSO4 γ-irradiated at room temperature. **Journal of Physics: Condensed Matter,** v. 6, p. 3831-3837, 1994.

BALIAN, H.G.; EDDY, N.W. Figure-of-merit (FOM), an improved criterion over the normalized chi-squared test for assessing goodness-of-fit of gamma-ray spectral peaks. **Nuclear Instruments and Methods,** v. 145, p. 389-395, 1977.

BHATT, B.C.; SANAYE, S.S.; SHINDE, S.S.; SRIVASTAVA, J.K. A comparative study of the dosimetric characteristics BaSO4:Eu and CaSO4:Dy Teflon TLD disks. **Radiation Protection Dosimetry**, v. 69, n. 2, 105-110,1997.

BHATT, B.C.; SONI, A.; POLYMERIS, G.S.; KOUL, D.K.; PATEL, D.K.; GUPTA, S.K.; MISHRA, D.R.; KULKARNI, M.S. Optically stimulated luminescence (OSL) and thermally assisted OSL in Eu^{2+}-doped $BaSO_4$ Phosphor. **Radiation Measurements,** v. 64, p. 35-43, 2014.

BONTRAGER, K.L.; LAMPIGNANO, J. Textbook of radiographic positioning and related Anatomy-E-Book. **Elsevier Health Sciences,** 2013.

BOS, A.J.J. Theory of Luminescence. **Radiation Measurements,** v. 41, supplement 1, S45-S56. 2006.

BOTTER-JENSEN, L.; MCKEEVER, S.W.; WINTLE, A.G. **Optically Stimulated Luminescence Dosimetry.** Elsevier, 2003.

BULUR, E.; BOTTER-JENSEN, L.; MURRAY, A.S. Optically stimulated luminescence from quartz measured using the linear modulation technique. **Radiation Measurements,** v. 32, p. 407–411, 2000.

BULUR, E.; GOEKSU, H.Y. OSL from BeO ceramics: new observations from an old material. **Radiation Measurements,** v. 29, p. 639-650, 1998.

CHEN, R.; PAGONIS, V. **Thermally and Optically Stimulated Luminescence: A Simulation Approach**. Edition 1, John Wiley & Sons, Ltd., 2011. ISBN: 978-0-470-74927-2

CHEN, R.; S.W.S. MCKEEVER. **Theory of Thermoluminescence and Related Phenomena,** World Scientific Publishing, Co., Singapore, 1997.

CHOUGAONKAR, M.P.; BHATT, B.C. Blue light stimulated luminescence in calcium fluoride, its characteristics and implications in radiation dosimetry. **Radiation Protection Dosimetry,** v. 112, n. 2, p. 311-321, 2004.

COLVILLE, A.A.; STAUDHAMMER, K. A Refinement of the Structure of Barite. **American Mineralogist,** v. 52, n. 11-12, p. 1877–1880. 1967.

DEVI, Y.R.; SINGH, S.D. Synthesis and TL glow curve analysis of $BaSO_4$:Eu,Dy phosphor. **Journal of Luminescence**, v. 132, p. 1575-1580, 2012.

DIEKE, G.H.; CROSSWHITE, H.M. The Spectra of the Doubly and Triply Ionized Rare Earths. **Applied Optics,** v. 2, n. 7, p. 675-686, 1963.

DIXON, R.L.; EKSTRAND, K.E. **Phys. Med. Biol.,** v. 19, p. 196, 1974.

DIXON,R. L.; WATTSF, C. **Phys. Med. Biol.**, v. 17, p. 81, 1972.

FERNÁNDEZ, S.D.S.; GARCÍA-SALCEDO, R.; MENDOZA, J.G.; SÁNCHEZ-GUZMÁN, D.; RODRÍGUEZ, G.R.; GAONA, E.; MONTALVO, T.R. Thermoluminescent characteristics of LiF:Mg,Cu,P and $CaSO_4$:Dy for low dose measurement. **Applied Radiation and Isotopes,** v. 111, p. 50-55, 2016.

FERREIRA, J.F.A.; YOSHIMURA, E.M; UMISEDO, M.K.; NASCIMENTO, R.P.D. Correlation of optically and thermally stimulated luminescence of natural fluorite pellets. **Radiation Measurements,** v. 71, p. 254-257, 2014.

FURETTA. C. **Handbook of Thermoluminescence**, World Scientific: New Jersey, London, Singapore, Hongkong, 2003.

GONZÁLEZ, P.R.; FURETTA, C.; CALVO, B.E.; GASO, M.I.; CRUZ-ZARAGOZA, E. Dosimetric characterization of a new preparation of $BaSO_4$ activated by Eu ions.

Nuclear Instruments and Methods in Physics Research B, v. 260, p. 685‑692, 2007.

GORBICS, S.G.; ATTIX, F.H. **Int. J. Appl. Radiat. Isotopes,** v. 19, p. 81, 1968.

GURVICH, A.M.; MIL' SHTEJN, R.S.; MYAKHKOVA, M.G.; GOLOVKOVA, S.I.; RUEDIGER, J.; KAVTOROVA, V.P. Photostimulable Luminescence Screens and Their Application in Clinical Dosimetry. **Radiation Protection Dosimetry.,** v. 34, n. 1-4, p. 265-267, 1990.

HAROLD, E.J.; CUNNINGHAM, J.R. **The Physics of Radiology**, Charles C Thomas Publisher, USA, 1983.

HUBBELL, J.H.; SELTZER, S.M. 1995. Available at: <http://www.nist.gov/pml/data/xraycoef> (Accessed on 05 February, 2018).

JENSEN, W.B. Holleman-Wiberg's Inorganic Chemistry (Book). **Journal of Chemical Education,** v. 79, n. 8, p. 944-946, 2002.

JURSINIC, P.A. Characterization of optically stimulated luminescent dosimeters, OSLDs, for clinical dosimetric measurements. **Medical Physics,** v. 34, n. 12, p. 4594-4604, 2007.

KEARFOTT, K.J.; GEOFFREY, W.W.; RAFIQUE, M. The optically stimulated luminescence (OSL) properties of LiF:Mg,TI, $Li_2B_4O_7$:Cu, $CaSO_4$:Tm, and CaF_2:Mn thermoluminescent (TL) materials. **Applied Radiation and Isotopes,** v. 99, p. 155-161, 2015.

KITIS, G. TL glow curve deconvolution functions for various kinetic orders and continuous trap distribution: Acceptance criteria for E and s values. **Journal of Radioanalytical and Nuclear Chemistry**, v. 247, n. 3, p. 697-703, 2001.

KITIS, G.; GOMEZ-ROS, J.M.; TUYN, J.W.N. Thermoluminescence glow-curve deconvolution functions for first, second and general orders of kinetics. **Journal of Physics D: Applied Physics,** v. 31, p. 2636-2641, 1998.

KITIS, G.; KIYAK, N.G.; POLYMERIS, G.S. Thermoluminescence and optically stimulated luminescence properties of natural barytes. **Applied Radiation and Isotopes,** v. 45, p. 543-545, 2010.

KIYAK, N.G.; POLYMERIS, G.S.; KITIS, G. TL/OSL properties of crystalline inclusions from heavy, barytes loaded, concrete. **Radiation Measurements**, v. 45, p. 543-545, 2010.

KNOLL, G.F. **Radiation Detection and Measurements.** Edition 4, John Wiley & Sons. 2010.

KREUTZER, S.; SCHMIDT, C.; FUCHS, M.C.; DIETZE, M.; FISCHER, M.; FUCHS, M. Introducing an R package for luminescence dating analysis. **Ancient TL,** v. 30, n. 1, p. 1-8, 2012.

KUNDUO, H.K.; MASSANDP, P.; MARATHE, K. VENKATARAMN, G. **Nuclear Instruments and Methods in Physics Research,** v. 175, p. 363, 1980.

MADHUSOODANAN, U.; JOSE, M.T.; LAKSHMANAN, A.R. Development of $BaSO_4$:Eu phosphor. **Radiation Measurements,** v. 30, p. 65-72, 1999.

MANAM, J.; DAS, S. Characterization and TSL dosimetric properties of Mn doped $BaSO_4$ phosphor prepared by recrystallisation method. **Journal of Alloys Compounds,** v. 489, n. 1, p. 84-90, 2010.

MCKEEVER, S.W.S. **Thermoluminescence of solids.** Cambridge University Press*;* 1985. http://dx.doi.org/10.1017/ CBO9780511564994

McKEEVER, S.W.S. **Thermoluminescence of solids.** Cambridge University Press, England, p. 376, 1988.

MCKEEVER, S.W.S.; CHEN, R. Luminescence Models. **Radiation Measurements,** v. 27, p. 625-661. 1997.

MEIJERINK, A.; BLASSE, G.; STRUYE, L. A new photostimulable phosphor – Eu^{2+} activated bariumbromosilicate ($Ba_5SiO_4Br_6$). **Materials Chemistry and Physics,** v. 21, n. 3, 261-270, 1989.

NAGPAL, J.S.; KATHURIA, K.; BAYATI, V.N. **J. appl. Radiation and Isotopes,** v. 32, p. 147, 1981.

NAGPAL, J.S.; VARADHARAJAN, G. Thermoluminescence of Rare Earth Doped $BaSO_4$ Phosphors and its Applications. **Int J Appl. Rad. Isot.,** v. 33. p 175-182, 1982.

NAKAJIMA, T.; MORAYAMA, Y.; MATSUZAWA, T.; KOYANO, A. **Nuclear Instruments and Methods in Physics Research,** v. 157, 155 (1978).

NANTO, H.; NAKAGAWA, R.; YANAGIDA, T.; FUJIMOTO, Y.; FUKUDA, K.; MIYAMOTO, Y.; HIRASAWA, K.; TAKEI, Y. Optically stimulated luminescence in Tm-doped calcium fluoride phosphor crystal for application to a novel passive type dosimeter. **Sensors and Materials,** v. 27, p. 277-282, 2015.

NASCIMENTO, S.R.V. **Thermoluminescent dosimetry of natural quartz from Solonópole (CE) for application in radio-diagnosis**. [Dissertation]. Recife: Universidade Federal de Pernambuco; 2010.

OKAMOTO, Y.; KAWAGUCHI, S.; KINO, S.; MIONO, S.; KITAJIMA, T.; MISAKI, A.; SAITO, T. Thermoluminescent sheets for the detection of high energy hadronic and electromagnetic showers. **Nuclear Instruments and Methods in Physics Research Section A: Accelerators, Spectrometers, Detectors and Associated Equipment,** v. 243, n. 1, p. 219-224, 1986.

PAGONIS, V.; MIAN, S.M.; KITIS, G. Fit of first order thermoluminescence glow peaks using the Weibull distribution function. **Radiation Protection Dosimetry**, v. 93, n. 1, p. 11-17, 2002.

PANDEY, A.; RAHEJA, K.; BAHL, S.; KUMAR, P.; LOCHAB, S.P.; SINGH, B. Nanocrystalline Europium doped barium sulphate as an energy independent thermoluminescent dosimeter. **AIP Conference Proceedings**, 1832, 050034-1-050034-3, 2017. doi: 10.1063/1.4980267

PATLE, A.; PATIL, R.R.; KULKARNI, M.S.; BHATT, B.C.; MOHARIL, S.V. Development of europium doped BaSO4 TL OSL dual phosphor for radiation dosimetry applications. **Advanced Materials and Radiation Physics**, AIP Conference Proceedings, v. 1675, n. 1, 020026-1-020026-5, 2015. Doi: https://doi.org/10.1063/1.4929184

POLYMERIS, G.S.; KITIS, G.; TSIRLIGANIS, N.C. Correlation between TL and OSL properties of CaF_2:N. **Nuclear Instruments and Methods in Physics Research Section B: Beam Interactions with Materials and Atoms**, v. 251, p. 133-142, 2006.

PRADHAN, A.S.; LEE, J.I.; KIM, J. Recent developments of optically stimulated luminescence materials and techniques for radiation dosimetry and clinical applications. **Journal of Medical Physics**, v. 33, n. 3, p. 85-99. 2008.

PUCHALSKA, M.; BILSKI, P. GlowFit - a new tool for thermoluminescence glow-curve deconvolution. **Radiation Measurements**, v. 41, p. 659-664, 2006.

RAMASWAMY, V.; VIMALATHITHAN R.M.; PONNUSAMY, V. Synthesis and characterization of $BaSO_4$ nano particles using micro emulsion technique. **Advances in Applied Science Research,** v. 1, n. 3, p. 197-204, 2010.

RAO, G.T.K.; SHINDHE, S.S.; BHATT, B.C.; SRIVASTAVA, J.K.; NAMBI, K.S.V. **J. Phys.: Condens. Matter**, v. 7, p. 6569, 1997.

SAHARE, P.D.; MOHARIL, S.V. A new high-sensitivity phosphor for thermoluminescence dosimetry. **Journal of Physics D: Applied Physics**, v. 23, n. 5, p. 567, 1990.

SALAH, N.; HABIB, S.S.; KHAN, Z.H.; AL-HAMEDI, S.; LOCHAB. S.P. Nanoparticles of $BaSO_4$:Eu for heavy-dose measurements. **Journal of Luminescence,** v. 129, p. 192-196, 2009.

SARAEE, K.R.E.; KHARAIEKI, A.A.; KHOSRAVI, M.; ABDI, M.R.; ZEINALI, H.Z. Thermoluminescence properties of nanocrystalline of $BaSO_4$:Dy,Tb, irradiated with gamma rays. **Journal of Luminescence**, v. 137, p. 230-236, 2013.

SCHERRER, P. Determination of the size and internal structure of colloidal particles by means of X-rays. **News from the Society of Sciences in Göttingen, Mathematical-Physical Class,** p. 98-100, 1918. Available at: <http://eudml.org/doc/59018>.

SEGGERN, H.V.; MEIJERINK, A.; VOIGT, T.; WINNACKER, A. Photostimulation mechanisms of x-ray-irradiated RbBr:Tl. **Journal of Applied Physics**, v. 66, n. 9, p. 4418-4424, 1989.

SEGGERN, H.V.; VOIGT, T.; KNÜPFER, W.; G. LANGE. Physical model of photostimulated luminescence of X-ray irradiated BaFBr:Eu^{2+}. **Journal of Applied Physics**, v. 64, n. 3, p. 1405-1412, 1988.

SHARMA, K.; BAHL, S.; SINGH, B.; KUMAR, P.; LOCHAB, S.P.; PANDEY, A. $BaSO_4$:Eu as an energy independent thermoluminescent radiation dosimeter for gamma ray and C^{6+} ion beam. **Radiation Physics and Chemistry**, v. 145, p. 64-73, 2018.

SHINDE, S.S.; BHATT, B.C.; SRIVASTAVA, J.K.; SANAYE, S.S. Development and characterization of a $BaSO_4$:Eu,P Phosphor as a high sensitivity TL dosimeter. **Radiation Protection Dosimetry,** v. 65, n. 1‑4, p. 305-308, 1996.

TWARDAK, A.; BILSKI, P.; MARCZEWSKA, B.; LEE, J.I.; KIM, J.L.; GIESZCZYK, W.; MROZIK, A.; SĄDEL, M.; WRÓBEL, D. Properties of lithium aluminate for application as an OSL dosimeter. **Radiation Physics and Chemistry,** v. 104, p. 76-79, 2014.

VASCONCELOS, D.A.A.D.; BARROS, V.S.M.; KHOURY, H.J.; ASFORA, V.K.; OLIVEIRA, R.A.P. Thermoluminescent properties of CaF_2:Tm produced by combustion synthesis. **Radiation Physics and Chemistry,** v. 121, p, 75-80, 2016.

VILAITHONG, T.; WANWILAIRAT, S.; RHODES, M.; HORFFMANN, W.; MESSARIUS, T. High resolution emission spectra of TL materials. **Radiation Protection Dosimetry,** v. 100, n. 1-4, p. 211-216, 2002.

YAMASHITA, N.; YAMAMOTO, I.; NINAGAWA, K.; WADA, T.; YAMASHITA, Y.; NAKAO, Y. Investigation of TLD phosphors by optical excitation – Luminescence of Eu^{2+} centers in $MgSO_4$, $CaSO_4$, $SrSO_4$, $BaSO_4$. **Japanese Journal of Applied Physics**, v. 24, n. 9, p. 1174-1180, 1985.

YAMASHITA, T.; NADA, N., ONISHI, H., KITAMURA, S. Calcium Sulfate Phosphor Activated by Rare Earths. In: **Proceedings of the 2nd International Conference on Luminescence Dosimetry,** Gatlinburg, Tenn., 23-26 September 1968. Edited by J. A. Auxier, K. Becker, and E. M. Robinson. (CONF 680920). (USAEC, Oak Ridge, Tenn.) 4-17.

YOSHIMURA, E.M.; YUKIHARA, E.G. Optically stimulated luminescence: searching for new dosimetric materials. **Nuclear Instruments and Methods in Physics Research Section B: Beam Interactions with Materials and Atoms**, v. 250, p. 337-341, 2006.

YUKIHARA, E.G.; MCKEEVER, S.W.S. **Optically stimulated luminescence – Fundamentals and Applications**. Oklahama: A John Wiley and Sons, Ltd., Publication, 2011.

YUKIHARA, E.G.; MCKEEVER, S.W.S.; AKSELROD, M.S. State of art: Optically stimulated luminescence dosimetry - Frontiers of future research. **Radiation Measurement,** v. 71, p. 15-24, 2014.

ZHANG, M.; LI, X.; WANG, Z.; HU, Q.; LI, J.; LIU, W. Sol-gel synthesis and photoluminescence properties of $BaSO_4/Y_2O_3:Eu^{3+}$ core-shell submicrospheres. **Journal of Rare Earths,** v. 27, n. 6, p. 891-894, 2009.